Ordered Mesoporous Silica as Supports for Immobilization of Biocatalyst

Thesis submitted to

Cochin University of Science and Technology

in partial fulfillment of the requirements for the degree of

DOCTOR OF PHILOSOPHY

in

CHEMISTRY

by

AJITHA. S

Department of Applied Chemistry

Cochin University of Science and Technology
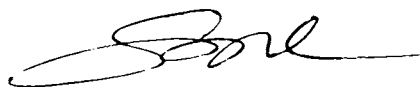
Cochin - 682022.

September 2008

Department of Applied Chemistry
Cochin University of Science and Technology
Kochi - 682 022.

Dr. S. Sugunan
Supervising Guide

Date: *06-09-2008*

Certificate

Certified that the thesis work entitled "**Ordered mesoporous silica as supports for immobilization of biocatalyst**" submitted by Ms. S. Ajitha is an authentic record of research work carried out by her under my supervision at the Department of Applied Chemistry in partial fulfillment of the requirements for the degree of Doctor of Philosophy in Chemistry of Cochin University of Science and Technology and has not been included in any other thesis previously for the award of any other degree.

Dr. S. Sugunan

DECLARATION

I hereby declare that the work entitled **"Ordered mesoporous silica as supports for immobilization of biocatalyst"** is based on the original .work done by me under the supervision of Dr. S. Sugunan (Professor) in Department of Applied Chemistry, Cochin University of Science and Technology and has not been included in any other thesis submitted previously for the award of any degree.

S. Ajitha

Acknowledgement

My deepest gratitude goes first and foremost to Prof. Dr.S.Sugunan my guide, for allowing me to do my Ph.D in the physical lab, of CUSAT. I really admire his deep knowledge in all the branches of physical chemistry and his punctuality and sincerity in any task he take up. The interesting research topic he suggested was a real challenge for me. With his constant encouragement and guidance I am happy that I could complete the work. He has, given me so much support and advice, put in me large trust, and shown me enthusiasm. I would like to thank him for providing the best possible working conditions and all facilities the moment I needed.

I thank Prof Dr.K.Girish Kumar, Head, Department of Applied Chemistry and the former Head Dr. M.R. Prathapachandra Kurup, for the timely help rendered. My Doctoral committee member Dr. S.Prathapan was very positive and encouraging and supported me in times of need. I extend a special word of thanks to all the teaching and nonteachingstaff, research scholars and students of this department for their help and support.

The interactions with Dr.B.Viswanatahan of NCCR, IIT Madras has really helped me in my research work. I thank him for the quick responses during my discussions. The acquaintance with Dr. S.Shylesh, NCL Pune, provided a turning point in my research work. I thank him for the sincere efforts he took for answering my queries.

I am really lucky to have Dr.Sanjay as my senior. Through out my entire research work he was supporting me and provided me all help including thesis writing. I express my deep gratitude to him.

I take this opportunity to thank Mr. Kashmiri and Mr.Jose of USIC, CUSAT for the technical helps. Dr. Shibu Eapen,Adarsh, Aneesh, Saji, Prem of SAIF,CUSAT,were always ready to help me with all the analytical facilities at STIC.

Novel Materials, from stone to steel to silicon, had a key role to play in the progress of civilization. Complex instruments and sophisticated theories combine to provide fundamental insights into the microscopic properties of materials, which in turn makes it possible to design new materials for specific purposes and to generate new applications for these materials. The inventions of mesoporous and nano materials and the interface of biology and chemistry will reduce the boundaries between the three branches of catalysis, namely homogenous, heterogenous and biocatalysis.

In recent years, the technique of enzyme or whole cell immobilization has revolutionized the prospects of enzyme application in industry. Immobilized enzymes enhance process robustness; allow longer duration of activity of enzymes, and re-use of the same enzymes in multiple cycles. Enzymes are key to new processes because they are environmentally friendly and reduce hazardous waste.

Conventional organic polymer supports provide essential interactions with enzymes through the rich functional groups but suffer a number of drawbacks such as, poor stability towards microbial attacks and organic solvents, disposal issues, toxicity and deactivation due to protein unfolding. The soft chemistry derived surfactant templated mesoporous materials are the appropriate class of materials for enzyme immobilization as the perfectly ordered mesoporous silica is a material that could come close to providing a homogeneous environment with a large pore system. Nature's catalyst is of nanometer scale and fixing them to nano pores of meso materials is an

interesting task. However, recent theoretical models suggest that stabilization of proteins against unfolding can be achieved by physical confinement inside relatively small cages. This stabilization effect is attributed to the fact that such confined spaces the unfolded configurations of the chain are not thermodynamically favored. Moreover the pores provide a higher density of enzyme loading and facilitate transport of substrate and product. As there are a lot of silanol groups in silica there is a chance for strong interaction between the enzyme and the support which result in enhanced stability of the immobilized form. The stability can be further enhanced by modifying the surfaces with active functional groups.

In this venture the pore size of ordered mesoporous silica SBA-15 was tuned to suit the dimension of α-amylase (alpha-1,4-glucan-4-glucanohydrolase, E.C.3.2.1.1).The surface was modified with active amine functional groups. The enzymes were fixed on the supports by adsorption and covalent binding techniques. The structural changes in the silica supports before and after adsorption were analyzed by various characterization techniques and the activity and stability measurements were carried out by following the liquefaction of starch.

Contents

Chapter 3

Natural silica for nature's catalyst ....59 - 90

Mesoporous Silica as Supports for Biocatalysts: Introduction and Literature survey

Recently, the demand for well ordered mesoporous materials has triggered major synthetic efforts in academic and industrial laboratories due to commercial interest in their use as adsorbents, catalysts, catalyst supports and adsorption of large bio-molecules owing to their high specific surface area, large specific pore volume and pore diameter. Biocatalyst technology, as a part of a broader "chemical biotechnology," is increasingly important as a tool for chemical synthesis. Its application is driven by consumer demand for new products and by industrial attempts at increasing profits via cost reduction, as well as government and regulatory pressures, new technologies and scientific discovery. Current applications of biocatalysts include the production of high fructose corn syrup, aspartame, semi-synthetic penicillins and award-winning cancer drugs. Thermostable α-amylases from Bacillus species are of great industrial importance in the production of corn syrup or dextrose. Despite these applications, biocatalysts cannot reach their potential without a concerted effort on the part of industry, non-profit and government funding agencies, as well as academic and national laboratories. One of the means of reducing the total cost in the enzyme industry is immobilization.

1.1 Mesoporous materials

Porous materials are classified into several kinds by their pore size. According to IUPAC notation a mesoporous material is a material containing pores with diameters between 2 and 50 nm., microporous materials have pore diameters of less than 2 nm and macroporous materials have pore diameters of greater than 50 nm; the mesoporous category thus lies in the middle[1]. Typical mesoporous materials include some kinds of silica and alumina that have similarly-sized fine mesopores. Mesoporous oxides of niobium, tantalum, titanium, zirconium, cerium and tin have also been reported [2]. According to the IUPAC notation, a mesoporous material can be disordered or ordered in a mesostructure [3]. The first mesoporous material, with a long range order, was synthesized in the early 90s, by a research group of the former Mobil Oil Company. Since then, research in this field has steadily grown. Technical advances in various fields, such as adsorption, separation, catalysis, drug delivery, sensors, photonics, and nanodevices, require the development of ordered porous materials with controllable structures and systematic tailoring pore architecture [4, 5]. The structural capabilities at the scale of a few nanometers can meet the demands of the growing applications emerging in processes involving large molecules, for example, biology and petroleum products. Zeolites or microporous materials, whose pore sizes are less than 1.2 nm, are far away from these demands. These motivations spark the proliferation of mesoporous materials [6-8].

1.2 Ordered mesoporous materials via nonionic-surfactant-templating approach

In materials science, building blocks play key roles which have controllable properties, as well as ordered, complex and integrated structures. For synthetic

chemistry, supramolecular assembly represents a powerful methodology in the creation of large, discrete, ordered structures. A large number of materials have been developed, particularly periodic mesoporous solids. They combine liquid-crystal packing with rigid frameworks. Exceptional properties of highly ordered mesostructures, i.e. their large surface areas and uniform pore sizes endow them with powerful properties with countless potential applications in adsorption, separation, catalysis, and photonics.

The synthesis of mesoporous molecular sieves is mainly concerned with "building mesopores". In general, two classes of materials have often been integrated as components in this mesoporous family, including mesoporous molecular sieves with open framework structures, mesoporous silicate replicas constructed by nanowire arrays. Mesoporous molecular sieves, which are obtained from the organic inorganic assembly by using soft matter, that is, organic molecules or supramolecules (e.g., amphiphilic surfactants and biomacro molecules) as templates, clearly contribute the main mesoporous family members. Surfactants are mostly used as templates. The open framework and tunable porosities endow mesopores accessible to large biomolecules, metal ions and reagents. The organic inorganic self-assembly is driven by weak noncovalent bonds such as hydrogen bonds, van der Waals forces and electrovalent bonds between the surfactants and inorganic species. Cooperative assembly between organic surfactants and inorganic precursors is generally involved, forming inorganic/organic mesostructured composites. Mesoporous molecular sieves can be obtained after the removal of surfactants. Therefore, the surfactant self-assembly is particularly essential for the formation of highly ordered mesostructures. On the basis of the current

knowledge on the surfactant self-assembly, the mesoporous materials can be rationally designed and the synthesis can be controlled.

Two most common representatives of ordered silica are MCM-41 (Mobil Composition of Matter) and SBA-15(Santa Barbara Amorphous). Both of them possess a well-order two-dimensional (2D) hexagonal (p6mm) array of mesopores. Depending on the shape of the supramolecular template, hexagonal phase MCM-41 [9], cubic phase MCM-48 [10] and lamellar phase MCM-50 [11] have been discovered. MCM-41 materials are usually synthesized in a basic medium in the presence of cationic surfactants such as cetyltrimethylammonium. Its pore diameter may be adjusted in the range from approximately 20-100 Å by changing the length of the alkyl chain of the surfactant molecule, by adding expander molecules (such as 1,2,3-trimethylbenzene) which increase the size of the hydrophobic region of the micelles, and by changing the synthesis conditions [12-14]. However, the silica walls of MCM-41 are thin (generally less than 15 Å, without additional treatment) resulting in low stability in the presence of water. Indeed, MCM-41 materials readily lose their hexagonal structure upon treatment in boiling water for short periods of time [15-16]. This lack of hydrothermal stability is a considerable drawback with respect to the use of MCM-41 kind materials in applications requiring the presence of water especially for the immobilization of enzymes.

The Santa Barbara group has contributed largely to the development of the meso ordered materials formed with non ionic Pluronics as structure-directing agents in acid medium [17]. The two-dimensional

hexagonal form SBA-15 (p6mm) and the cubic (Im_33m) form called SBA-16, as well as several other structures, were first synthesized by this group. There has been a great interest in these structures and the potential for controlling parameters such as the structure, the pore size and the wall thickness is naturally very appealing. This new class of materials offers the unique opportunity to tailor the pore size of the mesoporous host to accommodate small and large biomolecules by changing the synthesis conditions. SBA-15 materials have been synthesized in an acidic medium with the use of commercially available, low-cost bio degradable, nonionic supramolecular templates [17, 18]. Amphiphilic Pluronic surfactants, commonly used in the synthesis of SBA-15, are formed from hydrophilic poly(ethylene oxide, EO) and hydrophobic poly(propylene oxide, PO) blocks and have the following structure $EO_mPO_nEO_m$ in which n and m can be varied. SBA-15 materials prepared using $EO_{20}PO_{70}EO_{20}$ (Pluronic P123) exhibit surface areas of 690–920 m^2/g, pore volumes between 0.56 and 1.23 mL/g, pore sizes between 47 and 89Å, and unusually thick walls between 31 and 64Å [19]. Because of thicker silica wall compared to that of MCM-41, SBA-15 materials show a much higher thermal and hydrothermal stability, being stable for at least 48 h in boiling water [17,18]. Another characteristic feature of SBA-15 materials is its unique dual pore system formed by hexagonally arranged cylindrical mesopores with micropores within the walls, which provide connectivity between large pores [20-24]. The textural characteristics of SBA-15 materials can be easily changed using the same experimental approaches as the aforementioned for MCM-41 (change in surfactant structure, addition of swelling agents and variation of the synthesis conditions) [25-27]. In this

context, it was found that heat treatment during synthesis or ageing stages of SBA-15 preparation is more effective for increasing the mesopore diameter and pore volume rather than the addition of 1,3,5-trimethylbenzene [25,26]. Variation of experimental conditions used for the SBA-15 synthesis represents an easy and efficient method for controlling the textural properties that can be beneficial for certain applications, for example, a good accessibility of the pores for the reagents can be reached, providing a great enhancement in the activity and selectivity of the catalyst. The optimization of the synthesis of the SBA-15 has received a lot of attention in the past few years. However, the problem dealing with how to control good pore size of SBA-15 materials has not been solved yet. SBA-15 silica displayed significantly higher stability under various conditions (steaming, high temperature) compared with MCM-41 silica. Therefore, it is frequently used for synthesis of various advanced materials.

1.3 Mechanism of formation of SBA-15

The general idea of using block copolymers as templates is based on the fact that amphiphilic block copolymers self assemble in certain solvents to give robust, very regular superstructures that feature structural motifs on the nanometer scale (lyotropic liquid-crystalline phases). Typically, the constituting entities are spherical or cylindrical micelles or lamellar sheets with a characteristic cross-section of 5-100 nm.

The block copolymer self-assembly technique is probably the best examined mode of self-organization and is governed by the microphase separation dictated by the mutual incompatibility of the different blocks, one

being soluble and the other being insoluble in the solvent to be used ("amphiphilic" polymers). In principle, block copolymers self-assemble or microphase-separate in a variety of solvents, in particular water, but also alcohols or THF, which enables a certain width of chemistry for inorganic framework generation.

The mechanism is most likely via an $S^0H^+X^-I^+$ double layer hydrogen bonding interaction. Here I^+ are inorganic silicate precursor cations, and X^- are counter-anions. It is the cooperative interaction between inorganic and organic species at molecular scale that leads to assembly to 3D or 2D ordered arrangements. Silicate polyanions can interact with cationic surfactant molecules through coulombic forces. The polymerization of silicate species at the interface changes the charge density of inorganic layers, and in turn, the arrangement of surfactants. The matching of charge density at the surfactant/inorganic interface governs the assembly process [28].

A large number of studies have been carried out to investigate the formation and assembly of mesostructures on the basis of surfactant self-assembly. Two main pathways, that is, cooperative self-assembly and "true" liquid-crystal templating processes, seem to be effective in the synthesis of ordered mesostructures. The most popular mechanism for the formation of mesoporous solids is known as the cooperative formation mechanism which was first proposed by Stucky and coworkers.
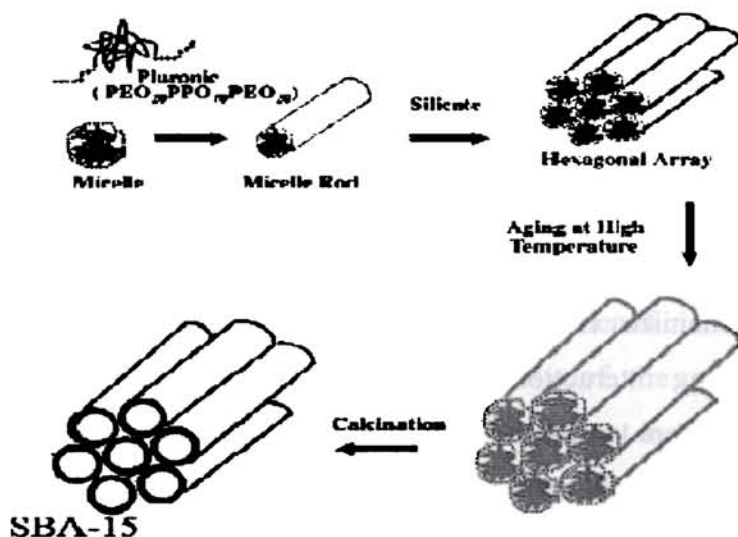
scheme showing the design and synthesis of mesoporous silica

This cooperative formation mechanism in a nonionic surfactant system was investigated by *in situ* techniques. Goldfarb and co-workers investigated the formation mechanism of mesoporous silica SBA-15, which are templated by triblock copolymer P123 ($EO_{20}PO_{70}EO_{20}$) by using direct imaging and freeze-fracture replication cryo-TEM techniques, *in situ* electron paramagnetic resonance (EPR) spectroscopy, and electron spin-echo envelope modulation (ESEEM) experiment [29,30]. They found a continuous transformation from spheroidal micelles into threadlike micelles. Bundles were then formed with dimensions that are similar to those found in the final materials. The elongation of micelles is a consequence of the reduction of polarity and water content within the micelles due to the adsorption and polymerization of silicate species. Before the hydrothermal treatment, the majority of PEO chains insert into silicate frameworks, which generate micropores after the removal of templates. Moreover, they found that the extent of the PEO chains located within the silica micropores depended on both the hydrothermal ageing temperature and the Si/P123 molar ratio. The formation

dynamics of SBA-15 was studied by Flodstrom *et al.* on the basis of time-resolved *in situ* 1H NMR and TEM investigations [31]. They observed four stages during the cooperative assembly, which are the adsorption of silicates on globular micelles, the association of globular micelles into floes, the precipitation of floes, and the micelle-micelle coalescence. Khodakov *et al.* proposed a structure with a hydrophobic PPO core and a PEO-watersilicate corona in the first stage [32]. Then the cylindrical micelles pack into large domains.

The initial liquid-crystal template mechanism first proposed by Mobil's scientists is essentially always "true", because the pathways basically include almost all possibilities [9, 10]. In this pathway, true or semi-liquid-crystal mesophases are involved in the surfactant templating assembly to synthesize ordered mesoporous solids. The condensation of inorganic precursors is improved owing to the confined growth around the surfactants and thus ceramic-like frameworks are formed. After the condensation, the organic templates can be removed by calcination, extraction, etc. The inorganic materials "cast" the mesostructures, pore sizes, and symmetries from the liquid-crystal scaffolds.

1.4   Synthesis of Mesoporous Silicate Molecular Sieves
1.4.1 Hydrothermal Method

Mesoporous silicates are generally prepared under "hydrothermal" conditions. The typical sol-gel process is involved in the "hydrothermal" synthesis. A general procedure includes several steps. First, a homogeneous solution is obtained by dissolving the surfactant(s) in a solvent. Water is the most common solvent and medium. Silicate precursors are then added into the solution where they undergo hydrolysis catalyzed by acid or base and transform to a sol of silicate oligomers. As a result of the interaction between

oligomers and surfactant micelles, cooperative assembly and aggregation give precipitation from a gel. During this step, microphase separation and continuous condensation of silicate oligomers occur. The formation of mesoporous silicates is rapid, only 3-5 min in cationic surfactant solutions, which is reflected by the precipitation and 30 min for non ionic surfactants. Hydrothermal treatment is one of the most efficient methods to improve mesoscopic regularity of products [33]. After the solution reaction, the mesostructures undergo reorganization, growth, and crystallization during hydrothermal treatment. The treating temperature is relatively low, between 80 and 150 °C, in which the range of 95-100 °C is mostly used.

1.5 Fundamental principles that govern the design and synthesis of mesoporous silica

- Amphilphilic block copolymers self assemble as lyotropic liquid crystalline phases.

- Alkoxy silane species are hydrolysed.

$$Si(OEt)_4 + nH_3O^+ \rightarrow Si(OEt)_{4-n}(OH_2^+)_n + nEtOH$$
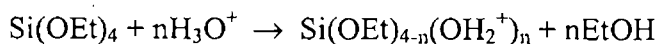
- EO moieties of the surfactant in strong acid media associating with hydronium ions.

$$REO_m + yHX \rightarrow REO_{m-y}[(EO).H_3O^+]y.....YX-$$
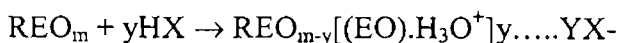
Organic inorganic self-assembly is driven by weak non covalent bonds such as H bonds, van der Waals forces and electrovalent bonds between the surfactants and inorganic species.

$$REO_{m-y}[(EO).H_3O^+]y...YX-...I+ \equiv S^0H^+X^-I^+$$
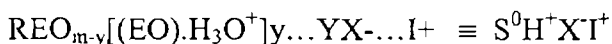
1.6 Enzymes as catalysts

Biocatalysis has a large impact in the chemical world. Uses are as divergent as chiral enzymatic transformations within an organic synthesis for a drug or for microbial desulfurization of diesel fuels. It suggests the potential and challenge of applying biocatalysis to all feedstreams. "Chemical biotechnology" is the rapidly growing application of biotechnology to chemical production [34-36]. It often goes hand-in-hand with green chemistry and the use of renewable feedstocks. Other applications of biotechnology lead to new products, new manufacturing methods and improved deleterious impacts on the environment.

The chemical industries are beginning to realize that enzymes are not only effective for catalyzing reactions of "natural" compounds within living systems, but that they can be used to catalyze reactions of "unnatural" compounds. Enzyme biocatalysts are being applied in the production of fine chemicals, pharmaceuticals and agricultural chemicals. Their attractiveness comes from high selectivity, ability for use under ambient conditions, and ease of disposal. The enzyme nitrile hydratase from a *R. rhodococcus* strain has been developed for the hydrolysis of acrylonitrile to acrylamide for use in plastics [37]. The enzyme is immobilized in whole cells and can produce acrylamide concentrations greater than 600 g/L. The biocatalytic approach has reached a production level of 100,000 tons/yr. The DSM-Toyo Soda process uses the enzymatic protease thermolysin for manufacture of aspartame, and is illustrative of two types of biocatalyst selectivity: chemical and stereoselectivity [37]. High-fructose corn syrup produced in large quantities is an enzyme-based product. The process includes three enzymatic

steps: the α-amylase catalyzed liquefaction of corn syrup, further hydrolysis of sugar oligomers by glucoamylase, and the isomerization of glucose to the glucose-fructose mixture. The hydrolysis of penicillin G or V to 6-aminopenicillinic acid (6f-APA) using penicillin acylase is an early success story for the use of enzymes in chemical manufacture. DuPont and Genencor have filed patents for processes and microorganisms to make 1,3 propanediol (1,3-PD) by fermentation in one step from various carbohydrate sources. The 1,3-PD is used in the production of the polyester polytrimethylene terephthalate. Cargill-Dow Polymers is developing a large-scale fermentation process alongside their other corn processing systems followed by chemical processing (a type of biorefinery) to generate polylactic acid for a multitude of applications including biodegradable sutures, biocompatible fibers, packaging, and functional replacements for commodity plastics such as styrene [38]. Enzyme recovery from a homogeneous catalytic process can significantly increase production costs. One method of lowering these processing requirements is to use a heterogeneous catalyst-an immobilized enzyme.

1.7 Immobilized enzymes

Immobilization means associating the biocatalysts with an insoluble matrix, so that it can be retained in proper reactor geometry for its economic reuse under stabilized conditions [39]. Since the second half of the last century, numerous efforts have been devoted to the development of insoluble immobilized enzymes for a variety of applications. The immobilized enzymes are more useful than the soluble counterparts: for instance as reusable heterogeneous biocatalysts, as stable and reusable devices for

analytical and medical applications as selective adsorbents for purification of proteins and enzymes as fundamental tools for solid-phase protein chemistry and as effective micro devices for controlled release of protein drugs [39-43]. The advantages of immobilization are,

- The enzyme can be easily removed from the product mixture

- The enzyme can be packed into columns and used over a long period

- Speedy separation of products reduce inhibition

- Thermal stability is increased allowing higher temperatures to be used.

- Higher operating temperatures increase rate of reaction

Although in 1916, Nelson and Griffin discovered that artificial carrier-bound invertase on Al $(OH)_3$ and charcoal was still catalytically active, the potential of bioimmobilization as a method of obtaining useful and reusable immobilized biocatalysts was unfortunately not recognized in the succeeding 40 years [44]. This simple fortuitous discovery has, however, been widely recognized as the cornerstone of the various enzyme-immobilization techniques currently available, because in the last half century it actually stimulated much interest and effort in exploration of insolubilized active enzymes for various studies and industrial applications that can be better met with immobilized rather than free enzymes. A systematic approach to enzyme immobilization starts in the late 1940s. From 1950s onwards much work has been devoted to the search for polymer supported materials that strongly binds the protein. Organic polymers like Eupergit C, oxirane acrylic beads, polysaccharides, carbon, polystyrenes, polyacrylates, maleic anhydride based

copolymers, polypeptides, vinyl and allyl polymers and polyamides have been commercially used as enzyme carriers [45]. Up to now, more than 5000 publications and patents have been published on enzyme immobilization techniques. Several hundred enzymes have been immobilized in different forms and approximately a dozen immobilized enzymes, for example penicillin G acylase, lipases, proteases, invertase, etc. have been used as catalysts in various large scale processes. Till 1990s organic polymeric carriers are the most widely studied supports because of the presence of rich functional groups, which provide essential interactions with the enzymes [45]. But the organic supports suffer a number of problems such as,

- Poor stability towards microbial attacks

- Poor stability to organic solvents

- Disposal issues and toxicity

- Deactivation due to protein unfolding

So the better alternatives for organic supports are the inorganic materials. Adsorption of protein over sol-gels and controlled porous glass (CPG) has been extensively studied for possible applications as biosensors and reviewed by Weetall and Avnir [46-48]. However, sol-gels are found to be unsuitable for the immobilization of proteins due to their broad pore size distribution. On the other hand, the major disadvantage of CPG materials for adsorption studies are their high cost and more importantly their surface area, which rapidly decreases with increasing pore size (30-200 nm). A large number of techniques and supports are now available for the immobilization of enzymes or cells on a variety of natural and synthetic supports. The choice

of the support as well as the technique depends on the nature of the enzyme, nature of the substrate and its ultimate application. Therefore, it will not be possible to suggest any universal means of immobilization. The most important requirements for a support material are that it must be insoluble in water, have a high capacity to bind enzyme, be chemically inert and be mechanically stable. The enzyme binding capacity is determined by the available surface area, both internal and external or the ease with which the support can be activated and the resultant density of enzyme binding sites [49]. The activity of the immobilized enzyme will also depend upon the bulk mass transfer and local diffusion properties of the system.

Template assisted synthesis of mesoporous materials with designed structure and function will provide the most suitable surface for enzyme immobilization which is to be discussed in detail later [49].

1.8 Methods of Immobilization

When immobilizing an enzyme to a surface, it is most important to choose a method of attachment that will prevent loss of enzyme activity by not changing the chemical nature or reactive groups in the binding site of the enzyme. The commonly used methods for immobilization are discussed below. Choice is governed by a number of factors some of which will not be apparent until the procedure is tried.

1.8.1 Carrier-binding

The carrier-binding method is the oldest immobilization technique for enzymes. In this method, the amount of enzyme bound to the carrier and the activity after immobilization depend on the nature of the carrier. In general,

an increase in the ratio of hydrophilic groups and in the concentration of bound enzymes, results in a higher activity of the immobilized enzymes. Some of the most commonly used carriers for enzyme immobilization are polysaccharide derivatives such as cellulose, dextran, agarose, and polyacrylamide gel. According to the binding mode of the enzyme, the carrier-binding method can be further sub-classified into: a. Physical adsorption b. Ionic binding and c. Covalent binding [50-52].

a. *Physical adsorption*

Physical adsorption of an enzyme onto a solid is probably the simplest way of preparing immobilized enzymes. The method relies on non-specific physical interaction between the enzyme protein and the surface of the matrix, brought about by mixing a concentrated solution of enzyme with the solid. A major advantage of adsorption as a general method of insolubilizing enzymes is that usually no reagents and only a minimum of activation steps are required. As a result, adsorption is cheap, easily carried out, and tends to be less disruptive to the enzymic protein than chemical means of attachment, the binding being mainly by hydrogen bonds, multiple salt linkages, and Vander Waal's forces. In this respect, the method bears the greatest similarity to the situation found in biological membranes in vivo and has been used to model such systems. A disadvantage is the weakness of the adsorptive binding forces; adsorbed enzymes are easily desorbed by temperature fluctuations and even more readily by changes in substrate concentration and ionic strength [53].

b. *Ionic binding*

The physical adsorption can be turned as ionic binding as the material for adsorption and proteins acquire charge when immersed in suitable

solvents. Depending on the pH of the medium, the biocatalyst protein can be positively or negatively charged. Such charged species can easily be coupled to ionic supports. Although ionic binding is stronger than physical adsorption; the biocatalyst is subject to leaching due to ionic strength and pH changes in the medium. It is extremely simple and the coupling is rather mild in nature [54].

c. Covalent binding

The most intensely studied insolubilization technique is the formation of covalent bonds between the enzyme and the support matrix. The functional groups of proteins suitable for covalent binding under mild conditions include (i) the alpha amino groups of the chain end and the epsilon amino groups of lysine and arginine, (ii) the alpha carboxyl group of the chain end and the beta and gamma carboxyl groups of aspartic and glutamic acids, (iii) the phenol ring of tyrosine, (iv) the thiol group of cysteine, (v) the hydroxyl groups of serine and threonine, (vi) the imidazile group of histidine, and (vii) the indole group of tryptophan. Covalent bonding should provide stable, insolubilized enzyme derivatives that do not leach enzyme into the surrounding solution [55].

1.8.2 Cross-linking

Immobilization of enzymes has been achieved by intermolecular cross-linking of the protein, either to other protein molecules or to functional groups on an insoluble support matrix. Many efforts were devoted to the development of cross-linked enzyme crystals (CLEC) suitable for biotransformations in non-aqueous media or in organic–water mixtures, because of the greater stability of the enzymes under hostile conditions.

Remarkably, it has been noticed that the performance of the CLEC obtained is highly dependent on the predetermined conformation of the enzyme molecules in the crystal lattice. Thus, selection of a highly active enzyme conformation by varying the crystallization conditions becomes crucial for the creation of highly active, stable and selective CLEC [56].

In other process of cross-linking, the individual biocatalytic units are joined to one another with the help of bi-or multi-functional reagents. In this way, very high molecular, typically insoluble aggregates are obtained. Cross-linking is a relatively simple process. The most commonly employed bifunctional reagent is glutaraldehyde [57]. In addition, di-isocyanates, (hexamethylene di-isocyanates) are often used as linking agents [58]. The disadvantages of cross-linking are that it is not suitable for packed bed operation and access to innermost catalytic sites is limited by the unfavorable conditions of diffusion. Cross-linking reactions are carried out under relatively severe conditions. These harsh conditions can change the conformation of active center of the enzyme; and so may lead to significant loss of activity.

1.8.3 Entrapping

The entrapment method of immobilization is based on the localization of an enzyme within the lattice of a polymer matrix or membrane. It is done in such a way as to retain protein while allowing penetration of substrate and products. This method is particularly common for immobilization of whole cells. Suitable matrix materials are polymers, alginate, carrageenan, pectin, agar and gelatin. Entrapment of cells in alginate gel is popular because of the

requirement for mild conditions and the simplicity of the used procedure. Several reports are available employing alginate gel [59].

This method differs from the covalent binding and cross linking in that the enzyme itself does not bind to the gel matrix or membrane. Thus the conditions necessary for continuous use of the enzyme pool are accomplished. Membrane confinement can be achieved by three methods; micro-encapsulation, liposome technique and membrane reactors. All three methods result in retention of the biocatalyst within a defined space by a semi-permeable membrane, which can be crossed by the substrate(s) and product(s) but is impermeable to the biocatalyst(s) [59].

1.9 Mesoporous materials as supports for immobilization

Silica-based materials have been widely used in chemical industries for many decades, as catalysts in petrochemical refining, synthesis of fine chemicals and pharmaceutical products and as sorbents in chromatographic and environmental applications [60,61]. However, the majority of these applications use natural or synthetic zeolites with structural repeats on the 1-2 nm scale, and pore sizes less than 1 nm. Consequently, these are not suitable hosts for bio-macromolecules such as proteins (typical molecular size of 3-30 nm). The use of zeolites in biotechnology is therefore rather limited.

Mesoporous materials have a clear advantage over microporous zeolites and zeotype molecular sieves for the transformation of large organic molecules .For example, they fulfill many of the requirements for enzyme carriers such as high specific surface areas (up to ca. 1500 m^2/g), high specific pore volumes (up to ca. 1.5 cm^3/g), well-ordered pore structures with

uniform mesopores adjustable in diameter from about 1.5 to 30 nm, sufficient functional groups for enzyme attachment hydrophilic/hydrophobic character, water insolubility, chemical and thermal stability, mechanical strength, suitable particle form, regenerability, and toxicological safety [49].

The discovery of ordered high surface area silicas with pore sizes of 5nm and above opened the way to the study of well-defined biomolecule–mesoporous silica hybrids. In particular, it has been possible to immobilize a range of small to medium size enzymes, such as proteases, lipases and peroxidases, *via* physisorption, encapsulation and tethering on the internal surfaces of the solids. Use has also been made of silicas functionalized for this purpose. In many cases the immobilized enzymes are both active and re-usable. Here we review the studies on enzymes immobilized on ordered mesoporous solids and assess the need for careful studies in real applications. In 1996 Diaz and Balkus first attempted to immobilize enzymes onto mesoporous MCM-41[62]. Since then, many research groups have established that many factors have a strong influence on the enzyme loading and on the activity of the resultant biocatalyst, including the relative sizes of the mesopore and the enzyme, surface area, pore size distribution, mesopore volume, particle size, ionic strength, isoelectric point, and surface characteristics of both the enzyme and the support.

The observation that some enzymes retain their functionality upon immobilization on ordered mesoporous supports triggered significant research activity in encapsulating enzymes as well as other bioactive components. Examples of a variety of biological molecules adsorbed onto ordered mesoporous silica and carbon materials were summarized by

Hartmann [49]. Immobilized enzymes in mesoporous materials have found applications in peptide synthesis [63], pulp bio-bleaching [64], biocatalysis [65-67] and biosensors [68-69]. Most studies have been carried out using the hexagonal MCM-41-type/SBA-15-type material because of its easy availability and good reproducibility in synthesis and modification. To create more suitable biocatalysts, biosensors, or to separate proteins by using Meso pores silicas (MPSs), it is of great importance to understand the factors that influence the immobilizing behaviour of proteins within MPSs. It has been found that two factors may greatly influence the immobilization properties of MPSs. The first is the size of the mesopore, or more specifically the mesopore size relative to the protein molecule size. Diaz and Balkus found that the amount of protein loading into mesoporous silica MCM-41 in a limited contact time decreased with increasing protein molecular weight [62]. This is expected if the pore size of the mesochannels is sufficiently large for 'comfortable' entrapment of biomolecules [66, 70]. Kisler *et al.* have demonstrated that the rate of adsorption in MCM-41 materials depends strongly on the size of the adsorbing molecule relative to the pore size for a range of biomolecules [71]. The second factor that influences the immobilizing behaviour is the surface characteristics of the MPS (meso porous silica) and proteins. The surface charges of MPS and the proteins must be complementary, because it is generally accepted that the electrostatic interaction between protein and MPS is one of the most important factors that influence adsorption and desorption [66, 67, 72]. Some researchers studied the factors that may influence the surface properties of proteins, for example, the pH [62,66] and ionic strength [65] of the protein solution. Takahashi *et al.* [73] believe that MCM-41 and SBA-15 prepared with cationic and non-ionic

surfactants, respectively, have different surface characteristics, and therefore different properties of adsorption. Lei *et al.* reported that suitable organically functionalized mesoporous hosts provide higher affinity for charged protein molecules and the more favoured microenvironment results in exceptional immobilizing efficiency [72]. Wright and coworkers have also investigated the adsorption and desorption property of SBA-15 functionalized by thiol, chloride, amine, and carboxyl groups and it has been found that the interactions of the enzyme-support depended strongly on the nature of the functional groups attached to the surface .Fan reported that the amount and size of entrance in mesoporous materials may greatly influence the bioimmobilization behaviours of MPS [74-75] and it has been revealed that for SBA-15 type MPSs, the morphology plays an important role in the immobilization ability [75]. On the other hand, some protein adsorption behaviour has not been well understood. Deere et *al.* suggested that the hydrophobic interactions dominate rather than electrostatic interactions in the desorption process of cytochrome c from commercial Kieselgel silica [76]. Lie *et al.* believed that there are electrostatic, hydrogen bond, and hydrophilic interactions between protein and MPSs functionalized by amine and carboxyl groups [72]. In the investigations of bioimmobilization within the same MPSs (*e.g.* SBA-15), their immobilization behaviour of similar proteins vary significantly according to different researchers [66,77]. Therefore, there should exists other factors that might have been ignored during former studies. Considering the large pore volume (~1.0 cm^3/g) of MPS, the previously reported specific immobilization capacity of MPS is still relatively low (<200 mg/g) Furthermore, it often takes several hours, even four days for the immobilization of proteins to reach equilibrium [65,71].

The stability of adsorbed enzymes should be discussed within two different concepts of enzyme stability: one is the intrinsic enzyme stability and the other is the operational enzyme stability. By definition, the intrinsic stability represents the stability of enzyme molecules themselves while the operational stability means the persistence of the enzyme activity during a process, *i.e.*, under conditions of use.

The enzyme leaching from host materials can seriously affect the operational stability. In most studies with adsorbed enzymes, the operational enzyme stability was discussed rather than the intrinsic enzyme stability, due to the difficulties in dissecting the intrinsic enzyme stability from the results of operational enzyme stabilities. However, several recent papers discussed the improvement of intrinsic enzyme stability by confining enzymes in mesoporous materials [78,79].This confinement can restrain enzyme unfolding or denaturation when it is located in a pore of similar dimensions or crowded by a high concentration of enzyme molecules in the same pore. The stabilization mechanism with adsorbed enzymes in mesoporous materials has been a topic of many studies, not only for practical applications, but also for scientific interests due to the resemblance of highly concentrated enzymes in mesoporous materials to the cellular environments containing high concentration of biomolecules. Many factors are known to affect the stability of adsorbed enzymes in mesoporous materials. First, the pore size of mesoporous materials affects the adsorption behaviour and enzyme leaching [61,62,73,77,]. Enzymes larger than the mesopores cannot be adsorbed within the pores. Size matching between pore and the molecular diameter of enzyme plays a key role in achieving high enzymatic stability [73,77].On the contrary, mesoporous materials with large pore size usually end up with poor enzyme

loading as well as poor enzyme stability due to quick leaching from the mesopores. The pore volume is also proven to determine the final amount of enzyme adsorption [62,77,80]. Secondly, the charge interaction is significant in determining the enzyme stability in mesoporous materials [66, 72, 80, 81]. If the net surface charge of enzymes is opposite to the charge of the mesopores, it will not only hasten the enzyme adsorption, but may also lead to a stable enzyme system due to the attractive interaction between two opposite charges, on the other hand, when enzymes and mesopores have the same charge, both enzyme adsorption and stability are poor due to the repulsion between the enzymes and the internal surface of mesopores. The charge status of enzymes and mesopores can be controlled by changing the pH of buffer solution [80,81] and functionalizing mesoporous materials with amino or carboxyl groups [72]. Finally, a hydrophobic modification is also known to affect the enzyme stability. Recent studies have shown that numerous functional groups, including amines, chlorides, thiols, carboxylic acids and phenyl may be attached successfully to the surface of mesoporous molecular sieves via tethering alkyl chains. These groups subsequently provide different interactions between the surfaces of the support and the enzyme molecule [82-85].Various nanostructures for enzyme stabilization were reviewed by Kim [86].

1.10 Significance of enzyme chosen

α-amylase (EC.3.2.1.1;1,4-glucan-glucanohydrolase; endo amylase) catalyse the hydrolysis of glycosidic linkages in starch and other related oligo- and polysaccharides in an endo fashion.. These enzymes are widespread among the higher plants, animals, and microorganisms. Some of these, particularly those of bacterial and fungal origin, are commonly used in various industries

such as starch processing, paper manufacture, and pharmacology. Amylases see a great deal of use in food and fermentation industries. Thermo stable α-amylases from Bacillus species are of great industrial importance in the production of corn syrup or dextrose. Polylactic acid synthesized from corn syrup is in turn used for a multitude of applications including biodegradable sutures, biocompatible fibers, packaging, and functional replacements for commodity plastics such as styrene [87].

1.11 Structure of α-amylase

The enzyme α-amylase catalyse the cleavage of α-1, 4-glycosidic linkages of starch components, glycogen, and various oligosaccharides. This consists of a single polypeptide chain with approximately 26 % α-helix and 22 % β-sheet and has dimensions of approximately 35×40×70 (Å)[88].
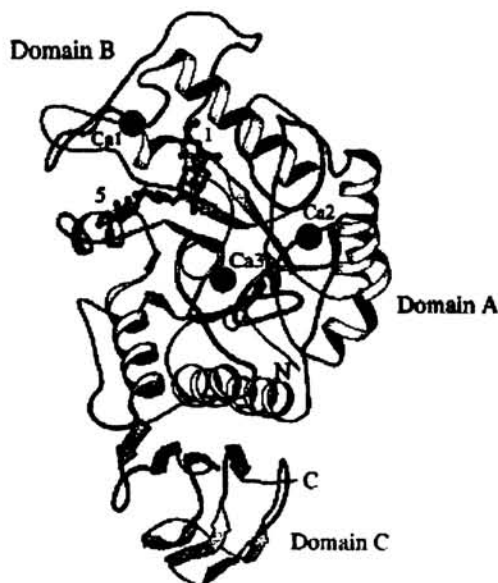
Like α-amylases extracted from other sources, the polypeptide chain folds into three distinct domains. The first domain (domain A), consisting of 291 residues (from residue 3 to 103 and 207 to 396), forms a (beta/alpha) 8-barrel structure. Important active site residues can be identified as Asp231, Glu261, and Asp328, which are all located at the C-terminal end of the central (beta/alpha) 8-barrel. Domain B overlaying the active site from one side and domain C consisting of a β-structure with a Greek-key motif

1.12 Immobilized α-amylase

In the literature there are number of reports about α-amylase immobilization on various supports using different processes .Some commonly employed organic polymers supports are polymethylmethacrylate and gamma irradiation soluble carriers (eudragit and polyethylene imine) [89,90], carbodiimide coupling paramagnetic polyacrolein beads[91] and porous polyethylene hollow fibers activated by ethanol amine or phenol [92].

Several methods have been developed for the preparation of immobilized α-amylase using inorganic materials, each having its own advantages and disadvantages. A thermo stable α-amylase was immobilized on controlled pore glass beads. The authors concluded that by the choice of a suitable pore size of the support and of a pH where the activity of the enzyme is high, the temperature need not be elevated in order to obtain a high catalytic activity [93]. α-amylase was immobilized onto the zirconium membrane by means of covalent coupling to the glutaraldehyde pretreated colloids [94]. However, the membrane could be used at a temperature below 40 ºC only to maintain its enzyme activity. Pillared clays, which possess mesopore sizes, have been extensively investigated since

the 1980s [4]. Immobilization of α-amylase on montmorillonite clay was extensively studied by Sanjay & Sugunan but the enzyme was not completely entrapped within the pore. They have proposed that when the huge enzyme, α-amylase was immobilized on acid activated montmorillonite K-10 the polypeptide backbone did not enter the interlayer space but was situated at the periphery of the clay. Intercalation occurred through the side chains of the amino acid residues [95]. Moreover in clays, the pore sizes are widely distributed, and the arrangement of pores is disordered. α-amylase was immobilized on zirconia and alumina via adsorption. From XRD, IR and N_2 adsorption studies it was confirmed that the enzyme was adsorbed on the external surface of the support [96,97].

1.13 Origin of the problem

Thermo stable α-amylases from Bacillus species are of great industrial importance in the production of corn syrup or dextrose. According to the reports of Sugunan et *al.*, complete entrapment of α-amylase onto inorganic porous clays was not possible due to inappropriate pore sizes [95]. Pandya et al. investigated adsorption on functionalized SBA-15 [98]. However, the material was of low quality as the synthesis was done at room temperature. To study the effect of pore size on protein adsorption and to compare the activity of enzymes entrapped in various pore sizes, perfectly ordered mesoporous materials with similar framework is the primary requirement. Most of the authors have compared the protein adsorption on different pore sizes of MCM-41 and SBA-15 with entirely different frame works. There are only very few reports with SBA-15 of various pore sizes. We have attempted to design the nanoporous

molecular sieve conserving the mesostucture, for the complete entrapment of the enzyme α-amylase of dimension 35×40×70 (Å).

1.14 Objectives of the present work

The present work aims at synthesizing proper materials for the immobilization of enzymes so that the stability and activity of enzymes are maintained. Cheap support rice husk silica was tried for first time as support for enzyme immobilization. As the next stage of the research the most emerging and promising support mesoporous silica were tuned to entrap the enzyme α- amylase within the pore. The materials were modified with functional groups, to enhance the stability. The major objectives can be outlined as,

- to extract amorphous silica from rice husk and to test whether it is compatible for immobilization of enzymes.

- to prepare mesoporous silca SBA-15 using amphiphilic surfactant following hydrothermal route.

- to study the influence of time and temperature of hydrothermal treatment on the pore characteristics of SBA-15.

- to characterize the materials via physico chemical techniques like SAXRD, Nitrogen adsorption isotherm, thermal analysis, FTIR spectroscopy, NMR spectroscopy, SEM and HRTEM.

- to functionalize mesoporous silica with APTES and characterize the material using FTIR,SAXRD,^{13}C NMR, ^{29}Si NMR and Nitrogen adsorption studies.

- to optimize pH, time, temperature, buffer concentration for immobilization.

- to characterize the immobilized enzymes, adsorbed and covalently bound via various physico chemical techniques like SAXRD, nitrogen adsorption isotherm, thermal analysis, FTIR spectroscopy, NMR spectroscopy.

- to estimate the efficiency of immobilized enzymes in comparison to free enzymes.

- to study the influence of pH, temperature, concentration on the activity of immobilized enzymes.

- evaluate the kinetics of enzyme catalysed reactions.

- understand the reusability of immobilized preparations in two reactor types.

- examine the storage stability of these systems.

- to study the enzyme leaching at different loadings.

References

[1]   K. S. W. Sing, D. H. Everett, R. A. W. Haul, L. Moscou, R. A. Pierotti, J. Rouquerol and T. Siemieniewska, Pure Appl. Chem.,57(1985) 603.

[2]   F.Hoffman, M.Cornelius, J.Morell, M.Froba, Angew. Chem. Int. Ed., 45(2006)3216.

[3]   M. E. Davis, Nature, 417(2002) 813.

[4]   A. Corma, Chem. Rev., 97(1997)2373.

[5]   P. T. Tanev ,T. J. Pinnavaia, Science, 267(1995) 865.

[6]   S. A. Bagshaw, E. Prouzet, T. J. Pinnavaia, Science, 269(1995)1242.

[7] G. S. Attard, J.C.Glyde, C. G. Goltner, Nature, 378 (1995)366.

[8] M. Templin, A. Franck, A. DuChesne, H. Leist, Y. M. Zhang, R. Ulrich, V. Schadler and U. Wiesner, Science, 278(1997) 1795.

[9] C.T. Kresge, M.E. Leonowicz, W.J. Roth, J.C. Vartuli, J.S. Beck, Nature, 359 (1992) 710.

[10] J.S.Beck, J.C.Vartuli, W.J.Roth, M.E.Leonowicz, C.T.Kresge, K.D.C Schmitt, T.W.Chu, .D.H.Olson, E.W.Sheppard, S.B.McCullen, J.B Higgins, J.L. Schlenker, J. Am. Chem. Soc., 114(1992) 10834.

[11] M .Dubois,T. H .Gulik-Krzywicki, B.Cabane, Langmuir,9(1993) 673.

[12] A. Sayari, Chem. Mater., 8 (1996) 1840.

[13] J.M. Kim, R. Ryoo, Bull. Korean Chem. Soc., 17 (1996) 66.

[14] R. Mokaya, J. Phys. Chem. B., 103 (1999) 10204.

[15] A. Galarneau, H. Cambon, F. Di Renzo, F. Fajula, Langmuir, 17 (2001) 8328.

[16] Y.Wang, M. Noguchi,Y.Takahashi, Y. Ohtsuka,Catal.Today, 68 (2001) 3.

[17] D. Zhao, J. Feng, Q. Huo, N. Melosh, G.H. Fredrickson, B.F. Chmelka, G.D. Stucky, Science, 279 (1998) 548.

[18] D. Zhao, Q. Huo, J. Feng, B.F. Chmelka, G.D. Stucky, J. Am. Chem. Soc., 120 (1998) 6024.

[19] T.Klimova, A.Esquivel, J.Reyes, M.Rubio,X. Bokhimi, J.Aracil, Micropor. Mesopor. Mater., 93(2006)331.

[20] R. Ryoo, C.H. Ko, M. Kruk, V. Antochshuk, M. Jaroniec, J. Phys. Chem. B., 104 (2000) 11465.

[21] M. Kruk, M. Jaroniec, C.H. Ko, R. Ryoo, Chem. Mater., 12 (2000) 1961.

[22] M. Impe'ror-Clerc, P. Davidson, A. Davidson, J. Am. Chem. Soc., 122 (2000) 11925.

[23] C.M. Yang, B. Zibrowius, W. Schmidt, F. Schuth, Chem. Mater., 15 (2003) 3739.

[24] A. Galarneau, H. Cambon, F. Di Renzo, R. Ryoo, M. Choi, F. Fajula, New J. Chem., 27 (2003) 73.

[25] A. Galarneau, H. Cambon, F. Di Renzo, F. Fajula, Langmuir, 17 (2001) 8328.

[26] Y.Wang, M. Noguchi,Y.Takahashi,Y. Ohtsuka, Catal. Today, 68 (2001) 3.

[27]   T. Yamada, H. Zhou, K. Asai, I. Honma, Mater. Lett., 56 (2002) 93.

[28]   Y. Wan,D. Zhao, Chem. Rev., 107(2007)2821.

[29]   S. Ruthstein, V.Frydman, S.Kababya,M. Landau, D.Goldfarb, J. Phys. Chem., B 107(2003) 1739.

[30]   S. Ruthstein, J .Schmidt, E. Kesselman, Y.Talmon, D.Goldfarb, J. Am. Chem. Soc., 128(2006)3366.

[31]   K. Flodstrom, H Wennerstrom, V.Alfredsson, Langmuir, 20(2004), 680.

[32]   A.Y.Khodakov, V.L.Zholobenko, M. Imperor-Clerc, D.J Durand, Phys. Chem. B., 109 (2005) 22780.

[33]   Y.Wan,Y.Shi, D.Zhao,Chem. Commun.,(2007) 897.

[34]   P. Ball, Nature, 409 (2001) 225.

[35]   K.M. Koeller, C.H. Wong, Nature, 409 (2001) 232.

[36]   A. Schmid, J.S. Dordick, B. Hauer, A. Kiener, M. Wubbolts, B. Witholt, Nature, 409 (2001) 258.

[37]   R.Padmakumar, P.Oriel, Appl. Biochem. Biotechnol., 9(1999)671.

[38]   B. Schulze, M.G. Wubbolts, Curr Opin Biotechnol., 10 (1999) 609.

[39]   Harttmeier W., Immobilized biocatalysts An Introduction, Springer – Verlag, Berlin (1988) p 1-80.

[40]   L.J. Kircka, G.H.G. Thorpe, Trends Biotechnol., 4 (1986) 258.

[41]   B.R. Dunlap: Immobilised chemicals and affinity chromatography, Plenum Press New York, (1974).

[42]   K. Martinek, V.V. Mozhaev, Adv. Enzymol., 57 (1985) 179.

[43]   C.L.L. Cristallini, M.G. Cascone, G. Polacco, D. Lupinacci, N. Barbani, Polym. Int., 44 (1997) 510.

[44]   J.M .Nelson, E.G.Griffin, J. Am.Chem. Soc., 38 (1916) 1109.

[45]   S.Pedersen, M.W Christensen Harwood, Immobilized Biocatalysts, Academic Publishers, Amsterdam, (2000).

[46]   H. H. Weetall, Appl. Biochem. Biotechnol., 41 (1993) 157.

[47]   D.Avnir, S. Braun,O.Lev, M. Ottolenghi, Chem. Mater., 6 (1994) 1605.

[48] C.B.Dave, B.Dunn, J.S.Valentine, J.I.Zink, Anal. Chem., 66 (1994) 1120A.

[49] M. Hartmann, Chem. Mater., 17 (2005) 4577.

[50] Mosbach K, Immobilised Enzymes, TIBS 1980.

[51] Ichiro Chibata, Immobilized Enzyme, Kodansha Ltd, Halsted Press, (1978).

[52] Biochemistry, 2nd edition, Voet, Donald and Judith, John Wiley & Sons Inc., (1995).

[53] Immobilized Enzymes for Industrial Reactors, Ralph Mesing, Academic Press, (1995).

[54] Z.Fujimoto, K.Takase, N. Doui, M. Momma, T. Matsumoto, H. Mizuno, J. Mol. Biol., 277 (1998) 393.

[55] F. B. Kolot, Process Biochem., 5(1981)2.

[56] R.A .Persichetti, N.L.S .lair, J.P. Griffith, M.A Navia,J. Am. Chem. soc., 117 (1998)2732.

[57] I .Chibata, T.Tosa, T.Sato,Japanese Patent No. 74,25,189, (1974).

[58] D. J. Lartigue, H. Weetall, U.S. Patent No. 3,939,041, (1976).

[59] M.Kierstan, C.Bucke, Biotechnol. Bioeng., 29(1977) 387.

[60] A. J.Dreibelbis, US Patent 4783435, (1988).

[61] A .Stein, B. J.Melde, R.C.Schroden, Adv.Mater., 12 (2000) 1403.

[62] J.F. Dýaz, K.J. Balkus Jr, J. Mol. Catal., B 2 (1996)115.

[63] G.W.Xing, X.W.Li,G.L .Tian,Y.H.Ye,Tetrahedron Lett., 56 (2000) 3517.

[64] T.Sasaki, T. Kajino,B.Li, H.Sugiyama, H.Takahashi, App. Env. Microbiol., 67 (2001) 2208.

[65] J.Deere, E. Magner, J. G. Wall, B. K. Hodnett, Biotechnol. Prog., 19 (2003) 1238.

[66] Y.J. Han, J. T Watson,G. D.Stucky, A.Butler,J. Mol. Catal. B: Enzym., 17 (2002) 1.

[67] Y.J Han, G. D Stucky, A.Butler, J. Am. Chem. Soc., 121 (1999) 9897.

[68] B. Liu, Y. Cao, D. Chen, J. Kong, J. Deng, Anal. Chim. Acta, 478 (2003) 59.

[69]   A.Heilmann, N.A.TeuscherKiesow, D.Janasek, U.J.Spohn, Nanosci. Nanotech., 3 (2003) 375.

[70]   J.Deere, E.Magner, J.G.Wall, B.K.Hodnett, J. Phys. Chem. B., 106 (2002) 7340.

[71]   J. M. Kisler, A. Dahler, G. W. Stevens, A. J. OConnor, Micropor. Mesopor. Mater., 44 (2001a) 769.

[72]   C. H. Lei, Y. S. Shin,J. Liu,E,J.Ackerman, J. Am. Chem. Soc., 124 (2002) 11242.

[73]   H .Takahashi, B.Li, T. Sasaki, C.Miyazaki,T.Kajino, S.Inagaki, Micropor. Mesopor. Mater., 44 (2001) 755.

[74]   J. Fan, C. Z Yu, T. Gao, J.Lei, , B. Z. Tian, L. M Wang, Q .Luo, B. Tu, W. Z. Zhou,D. Y Zhao., Angew. Chem., Int. Ed., 42 (2003b) 3146.

[75]   J. Lei, J.Fan,C.Z.Yu, L.Y.Zhang, S.Y. Jiang, B.Tu, D.Y.Zhao, Micropor. Mesopor. Mater.,73 (2004)121.

[76]   J.Deere, E.Magner, J. G.Wall, B. K. Hodnett, J. Phys. Chem., B 106 (2002) 7340.

[77]   H .Takahashi, B. Li, T Sasaki,C.Miyazaki,T .Kajino, S. Inagaki Chem. Mater.,12(2000)3001.

[78]   G .Ping, J.M .Yuan, M .Vallieres, H. Dong, Z .Sun, Y. Wei, F.Y.Li, S.H.Lin, J. Chem. Phys.,118 (2003) 8042.

[79]   G .Ping, J.M .Yuan,Z. Sun,Y. Wei, J. Mol. Recog.,17 (2004) 433.

[80]   A .Vinu, V. Murugesan, M. Hartmann, J. Phys. Chem. B., 108 (2004a) 7323.

[81]   A .Vinu, V. Murugesan, O.Tangermann, M. Hartmann, Chem. Mater., 16(2004b) 3056.

[82]   T. Asefa, M.J. MacLachlan, N. Coombs, G.A. Ozin, Nature, 420 (1999) 867.

[83]   A.M. Liu, K. Hidajat, S. Kawi, D.Y. Zhao, J. Chem. Soc., Chem. Commun., (2000) 1145.

[84]   P.M. Price, J.H. Clark, D.J. Macquarrie, J. Chem. Soc., Dalton Trans., (2000) 101.

[85]   A. Stein, B.J. Melde, R.C. Schroden, Adv. Mater., 12 (2000) 1403.

[86]   J.Kim,J.Krate,P.Wang, Chem. Eng. Sci.,61(2006)1017.

[87]   O. Martin, L, Averous, Polym. J., 42 (2001) 6209.

[88]   Z.Fujimoto, K. Takase, N. Doui, M. Momma, T. Matsumoto and H. Mizuno, J. Mol. Biol.,277 (1998)393.

[89]   E. Galas, S.A. Jedrzejczak, W. Pekala, M. Pietrzak, Radio-Chem. Radioanal. Lett., 43 (1980) 347.

[90]   L. Cong, R. Kaul, U. Dissing, B. Mattiasson, J.Biotechnolo., 429 (1995) 75.

[91]   A.R. Varlan, W. Sansen, A.V. loey, M. Hendrickx, Biosens. Bioelect.,11 (1996)443.

[92]   S. Miura, N. Kubota, H. Kawakita. K. Saita, K. Sugita, K. Watanabe, T. Sugo, Rad. Phy. Chem., 63 (2002) 143.

[93]   S.DeCordt, M.Hendrickx, G.Maesmans, P.Tobback, Biotechnol. Bioeng., 43 (1994)107.

[94]   J. Emneus, L. Gorton, Anal. Chim. Acta, 234 (1990) 97.

[95]   G.Sanjay, S.Sugunan, J. of Porous.Mater.,14 (2007)119.

[96]   R. Reshmi, G. Sanjay, S. Sugunan, Catal. Commun., 8 (2007) 393.

[97]   R. Reshmi, G. Sanjay, S. Sugunan, Catal. Commun., 7 (2006) 460.

[98]   P.H. Pandya, R.V. Jasra, P.N. Bhatt, Microporous Mesoporous Mater., 77(2005) 67.

The design and synthesis of inorganic porous solids with diverse compositions, structure and macroscopic morphologies are important for controlling their properties and interesting from both fundamental and technological perspectives.Complex instruments and sophisticated theories combine to provide elementary insights into the microscopic properties of materials, which in turn makes it possible to design new materials for specific purposes and to generate new applications for these materials. The variation of the synthesis conditions enables the researcher to tailor the inorganic host so that encapsulation of a variety of proteins, enzymes and other biological molecules are feasible. Modifying silica materials with functional groups enhances the properties for protein adsorption. This chapter describes the present preparation method and various experimental techniques used to tailor the porous material most suited for encapsulation of the enzyme. The adsorption capacity is dependent on the pore size of the adsorbent relative to that of the protein and a pore size slightly larger than the hydrodynamic radius is sufficient to obtain high capacities. The fixation of enzymes on inorganic materials is very useful for practical application.

2.1 Introduction

Ordered mesoporous silica is a material that could come close to providing a homogeneous surface for the adsorption of biocatalysts. Confining biocatalysts in appropriate pore sizes reduces leaching and enhances activity. This chapter gives a detailed description about the preparation of the catalytic supports, immobilization methods adopted, techniques used to characterize materials and measures used for the catalytic activity study.

2.2 Chemicals used for the preparation

The chemicals used for the preparation of catalyst support and activity studies are listed below.

Sl. No.	Chemicals	Company
1.	TEOS	Sigma Aldrich , Bangalore
2.	P123 poly(ethyleoxide)– poly(propylene oxide)– poly(ethylene oxide), Pluronic P123	Sigma Aldrich , Bangalore
3.	Rice husk	Rice Mill, Thrissur, Kerala
4	3-amino propyl triethoxy silane	Sigma Aldrich, Bangalore
5	Glutaraldehyde	Sigma Aldrich, Bangalore
6.	Conc. HCl	Merck
7.	Folin Phenol Ciocaltaue's reagent	SRL Chemicals
8	Starch	SRL Chemicals
9	Bacillus subtilis α-amylase	Sigma Aldrich, Bangalore
10	Disodium hydrogen phosphate	Merck
11	Sodium potassium tartrate	Merck
12	Potassium iodide	Merck
13	Iodine	Merck

2.3 Methods of preparation
2.3.1 Preparation of SBA-15 silica

Siliceous SBA-15 was synthesized according to the procedure reported by Zhao *et al.* [1]. In a typical synthesis procedure, 2 g of P123 (pluronic) surfactant was stirred with 20 ml of deionized water at 40 °C. The mixture was stirred till the surfactant get dissolved, followed by the slow addition of 30 g of 2M HCl solution. The stirring was then continued for 30 min and 4.5 g of TEOS was added to the solution drop wise. The mixture was stirred for another 24 h and autoclaved at 100-140 °C for 48-96 h. The solid material was then filtered, washed with water and acetone, air dried, finally calcined at 550 °C for 6-8 h.

2.3.2 Preparation of functionalized silica

Before functionalization, the silica materials prepared were dehydrated at 150 °C for 3 h to remove the physisorbed water molecules. Post synthesis modification of the mesoporous material was done by refluxing 1g of the silica sample with 2-7 mmol of 3-aminopropyltriethoxysilane in 50 mL of dry toluene [2]. The mixture was then allowed to run for 6 h at 100 °C. Finally, the material was filtered, washed with toluene, soxhlet extracted using a mixture of dichloromethane (100 mL) for 24 h and dried under vacuum.

2.3.3 Adsorption studies

Adsorption experiments were carried out by contacting 100 mg of SBA-15 phosphate buffer(0.1 M) with pH 6-8 and phthalate buffer(0.1 M) with pH 4-5 were used during the adsorption process. The adsorbent and enzyme solution were shaken at 150 rpm in a temperature controlled shaker

at 25 °C. The samples were centrifuged for 10 min at 10,000 rpm, and the supernatant was analyzed using UV spectrophotometer at 750 nm. The same procedure was repeated with functionalized materials.

2.3.4 Protein determination

The concentration of immobilized enzymes was determined from the difference between the amount of protein introduced to the coupling reaction mixture and the amount of protein present in the filtrate after immobilization. The protein amount was determined by modification of the method of Lowry *et al.* [3]

2.3.5 Activity measurements

Batch reactor: About 1 mL of free enzyme solution (0.1 g immobilized enzyme) was mixed with 20 mL buffered substrate solution (3 % w/v) at optimum pH and incubated in a water bath shaker at room temperature. After the reaction time of 20 min, an aliquot of the product was removed from the reaction mixture and analyzed colourimetrically. For starch hydrolysis, colour was developed using iodine solution and the absorbance read at 610 nm[4]. The results were compared with absorbance of standard starch solution and the amount of starch converted was calculated.

Packed bed reactor: A silica glass tube of 1.2 cm inner diameter and 25 cm length was used as the reactor. The immobilized enzyme (1 g) was packed into a bed at the middle of the reactor, which was filled with glass beads. The substrate was fed from the top of the reactor using a Cole Palmer 74900 series syringe pump and the products were collected at the bottom at 1 h intervals. Product was analyzed using the method described in the previous section. The reactor was operated at a flow rate of 4 mL/h.

2.3.6 Effect of temperature and pH

The influence of pH and temperature on activity of free and immobilized enzymes was studied by varying the pH 4-8 and temperature 30-80 °C. Stability of the enzyme preparations to various pH and temperature was estimated by calculating the activity with respect to pre incubation time.

2.3.7 Reusability & Operational stability

Reusability of the immobilized enzymes was tested in a batch reactor. The reaction was continued several times; after each reaction, the mixture was centrifuged, catalyst separated and mixed with fresh substrate solution. Around 30 continuous cycles were performed. Operational stability was tested in a packed bed reactor as described earlier. The free and immobilized enzymes were stored in 0.1 M phosphate buffer solution of optimum pH at 5 °C for a period of 30 days and the activity was tested every day in the batch mode. The results are presented as percentage of initial activity retained.

2.3.8 Determination of kinetic parameters

The kinetic parameters (Michealis constant K_m and Maximum rate V max) were calculated by measuring the rates of reaction at various substrate concentrations. The values were computed using Graph pad prism non linear regression curves.

2.3.9 Leaching studies

The leaching studies were investigated in the batch reactor. The immobilized enzyme was treated with pH buffer and shaken for 30 min. It was centrifuged and the centrifugate was estimated for protein. The influence of enzyme concentration on leaching was understood by carrying out the

reaction with enzyme amounts of 50, 100 and 150 mg per g mesoporous silica. The process was repeated continuously for 25 cycles and the influence of repeated use on leaching was analysed.

2.4 Catalysts prepared

The materials prepared for the present work with its symbols are listed below.

Sl. No.	Symbol	Material
1.	S-1	SBA-15 at 100 °C (48h)
2.	S-2	SBA-15 at 120 °C (48h)
3.	S-3	SBA-15 at 130 °C (48h)
4.	S-4	SBA-15 at 72 h (100 °C)
5.	S-5	SBA-15 at 96 h (100 °C)
6.	S-1e	Enzyme adsorbed SBA-15 at 100 °C
7.	S-2e	Enzyme adsorbed SBA-15 at 120 °C
8.	S-3e	Enzyme adsorbed SBA-15 at 130 °C
9.	S-3a	Functionalized silica (2.2 mmol)
10.	S-3b	Functionalized silica (4.4 mmol)
11.	S-3c	Functionalized silica (6.6 mmol)
12.	S-3ae	Enzyme Covalently bound silica

2.5 Catalyst characterization techniques

Several approaches can be adopted to investigate fundamental relations between the state of a catalyst and its catalytic properties. By using the appropriate combination of analysis techniques, the desired characterization on the atomic as well as bulk scale is certainly possible. Various techniques along with the information got from these are presented below.

2.5.1 Powder X-ray diffraction

One of the phenomena of interaction of X-rays with crystalline matter is its diffraction, produced by the reticular planes that form the atoms of the crystal [5]. A crystal diffracts X-ray beam passing through it to produce beams at specific angles depending on the X-ray wavelength, the crystal orientation and the structure of the crystal. In the macroscopic version of X-ray diffraction, a certain wavelength of radiation will constructively interfere when partially reflected between surfaces (i.e., the atomic planes) that produce a path difference equal to an integral number of wavelengths. This condition is described by the Bragg law,

$$n\lambda = 2 \, d_{hkl} \sin \theta_{hkl}$$

where n is an integer, λ is the wavelength of the radiation, d is the spacing between surfaces and θ is the angle between the radiation and the surfaces.

This relation demonstrates that interference effects are observable only when radiation interacts with physical dimensions that are approximately the same size as the wavelength of the radiation. Since the distances between atoms or ions are of the order of 10^{-10} m (1 Å), diffraction methods require radiation in the X-ray region of the electromagnetic spectrum, or beams of electrons or neutrons with similar wavelength. So, through X-ray spectra one can identify and analyse any crystalline matter. The degree of crystallinity or order will decide the quality of the obtained result. In order to do this, a diffractometer is needed. Basically, an X-ray diffractometer consists of X-ray generator, a goniometer and sample holder and an X-ray detector, such as photographic film or a movable proportional counter. The most usually employed instrument to generate X-rays is X-ray tubes, which generate

X-rays by bombarding a metal target with high energy (10-100 keV) electrons that knock out core electrons. Thus, an electron in an outer shell fills the hole in the inner shell and emits an X-ray photon. Two common targets are Mo and Cu, which have strong K_α X-ray emissions at 0.71073 and 1.5418 Å, respectively. Apart from the main line, other accompanying lines appear which have to be eliminated in order to facilitate the interpretation of the spectra. These are partially suppressed by using crystal monochromator.

Perhaps the most routine use of diffraction data is for phase identification [6, 7]. Each crystalline powder gives a unique diffraction diagram, which is the basis for a qualitative analysis by X-ray diffraction. The X-ray diffraction pattern of a crystalline phase is a characteristic fingerprint, which enables the determination of phase purity and of the degree of crystallinity. Identification is practically always accompanied by the systematic comparison of the obtained spectrum with a standard one (a pattern), taken from any X-ray powder data file catalogues, published by the American Society for Testing Materials (JCPDS).

Structural details of porous materials on a scale covering from approximately 1 to 100 nm may be determined from measurements of the small angle scattering (SAS) of both X-rays (SAXS) and neutrons (SANS) Conventional mesoporous materials like MCM-41, MCM-48 or SBA-15 are amorphous. Nevertheless reflexes are observed in X-ray powder patterns at low 2θ angles (0.5 < 2 θ < 10 °). These reflexes are due to the long-range order induced by the very regular arrangement of the pores. Because *d*-spacings are rather big for the mesopores, the reflexes appear at low angles. Unit cell parameter (a_o) of a hexagonal lattice can be calculated from,

$a_o = 2d_{100}/\sqrt{3}$ and a cubic lattice can be determined by the following equation: $a_o = d_{211} \times \sqrt{6}$. The unit cell dimension determined by XRD is also used to calculate the frame wall thickness (FWT) of the channels of the mesoporous materials. Wall thickness is calculated as unit cell parameter (a_o)- pore diameter (from surface area measurements).

Powder XRD of the immobilized enzyme and the supports were taken on a *Panalytical Xpert PRO MPD* model with Ni filtered Cu Kα radiation (λ-1.5406 Å) within the 2θ range 0-10 ° at a speed of 1°/min.

2.5.2 Adsorption Isotherms

Gas adsorption is a prominent method to obtain a comprehensive characterization of porous materials with respect to the specific surface area, pore size distribution and porosity. This requires, however, a detailed understanding of the fundamental processes associated with the sorption and phase behaviour of fluids in porous materials and their influence on the shape of sorption isotherms, which serves as a basis for surface and pore size analysis. Pore width, pore shape and the effective adsorption potential are the factors that determine the pore filling. In case of so-called micropores (pore width < 2 nm, according to IUPAC classification) the pore filling occurs in a continuous way, whereas in case of mesopores (pore widths in the range from 2-50 nm) pore filling occurs by pore condensation, which reflects a first order gas-liquid phase transition.

Nitrogen physisorption is a commonly applied technique to characterize porous and nonporous materials. [8-10]. Properties like surface area, pore size, pore volume, and pore size distribution can be obtained by careful

analysis of the measured data. The amount of adsorbed/desorbed nitrogen is measured as a function of the applied pressure, giving rise to the adsorption/ desorption isotherm. The shape of the isotherm depends on the porous texture of the measured solid. According to the IUPAC classification six types of isotherms can be distinguished as shown in Figure 2.1.
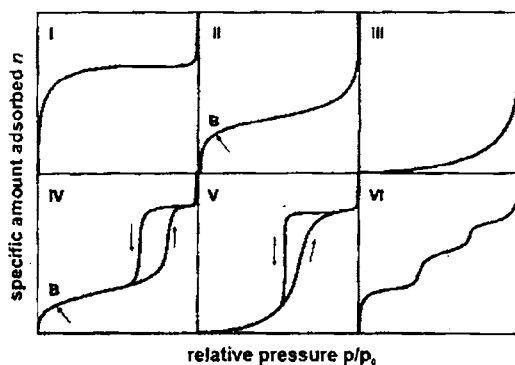
Fig.2.1 Isotherm types according to IUPAC definition. Very general assignment: type I– microporous material, type II – macro- or non-porous material, type III – macro- or non-porous material with weak adsorbate-solid interactions, type IV – mesoporous material, type V– mesoporous material with weak adsorbate – solid interactions, type VI – stepwise adsorption at very weak adsorbate-solid interactions.
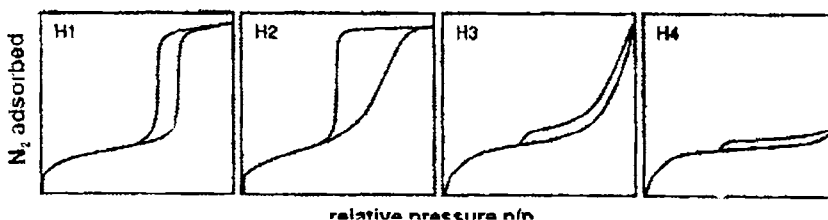
Fig.2.2 Hysteresis types according to IUPAC definition. H1- typical for type IV isotherms, H2- characteristic for "ink-bottle" pores, H3 and H4 - slit pores

Hysteresis types according to IUPAC definition is given in Figure 2.2

The standard for the determination of specific surface area of silica materials is the BET method. This method was established by Brunauer, Emmet and Teller [11]. The model, on which it is based, assumes that the heat of adsorption on the bare surface is different from the heats of adsorption of all successive layers.

The BET equation extends the Langmuir isotherm to multilayer adsorption,

$$P/V_{ads}(P_o - P) = 1/V_m C + (C-1) P/CV_m P_o) \quad ....(2.1)$$

$$S_{BET} = V_m A_m N_a/V_{mol} \quad ....(2.2)$$

where V_{ads} is the volume at STP occupied by molecules at pressure P and C is an empirical constant that is related to the difference between the heats of adsorption on the bare surface (*E*ı) and on the following layers (*E*ʟ).

The BET plot is linear as long as only multilayer adsorption occurs. From the slope and the intercept, *Vm* and *C* can be calculated. According to equation 2.2, the specific BET surface area (*S*ʙᴇᴛ) can be calculated by measuring *Vm* and knowing the area of a single adsorbate molecule on the surface (0.162 nm^2 for N_2). *N*ᴀ is the Avogadro constant. When data points in the pressure range of capillary condensation are included in the BET analysis, the plot is not linear. The obtained specific surface areas are too large. To avoid that, data points in the relative pressure range of $0.02 < p/p_o < 0.2$ were used in this work.

In the t plot method the measured adsorbed volumes are plotted against the statistical layer thickness t [12]. The t plot allows the examination of three properties of an adsorbent (a) to detect the onset of capillary condensation,

denoted by deviation from linearity in the higher regions of the plot; (b) to detect the micro porosity from an estimate of the amount of micro pores, from the intercept of the extrapolated plot on the ordinate, (c) to compute the V_m from the multi layer region of the isotherm. This method of isotherm data analysis was introduced by de Boer. The statistical thickness is specific for the combination of an adsorptive capacity, the temperature, and the surface of a solid material. In this work statistical thickness was calculated with the semi-empirical formula of Harkins and Jura. The specific pore volume is calculated from the intercept of the straight line that is drawn through the second linear region in the t plot. From the slope of this line a value for the external surface area could be calculated.

Pore diameter distributions were calculated by the BJH method developed by Barret, Joyner and Halenda [12]. In this approach the filled pores are taken as a starting point. The emptying of the filled pores with decreasing relative pressure is incrementally evaluated to obtain a pore diameter distribution. For each increment the pore diameter of pores emptied is calculated according to the Kelvin equation (equation 2.3).

$$\frac{P}{P_0} = \exp\left(-\frac{2\gamma V^{l}}{r_k RT}\right) \qquad \text{.....................................(2.3)}$$

The Kelvin equation(P/P_0 is the relative vapor pressure over a curved surface, γ is the surface tension, V^{l} is the molar volume of the liquid, and r_k is the radius of curvature) expresses mathematically that adsorption on a curved surface is more favorable than on a flat surface. According to equation 2.3, the vapor pressure over a concave surface is lower than over a flat surface.

This causes the filling of the mesopores at relative pressures, which are characteristic for the pore diameter This process is often called capillary condensation because the environment of the adsorbate in filled mesopores is comparable to a liquid state environment .Since the assumptions of Kelvin equation (equation 2.1) are not completely fulfilled in small mesopores, the real pore diameter may vary a little from the calculated value. But in a relative sense the BJH distributions are correct.

Nitrogen adsorption measurements were performed at liquid nitrogen temperature with a of *Micromeritics Tristar 3000* surface area and porosity analyzer. Prior to the measurements the samples were degassed for 1h at 90 °C followed by 4h at 300 °C. Functionalized materials were degassed at 60 °C for 4h. Immobilized enzymes were degassed at room temperature overnight.

2.5.3 High-Resolution Solid-State NMR: Magic Angle Spinning and Cross Polarization

NMR Spectroscopy is one of the most powerful techniques for structural investigations. So far most applications are focused on molecules dissolved in liquids, where NMR is an indispensable tool for the synthetic chemist, materials chemist or structural biologist alike. This was recognized by awarding the 1991 Nobel prize in chemistry to Richard Ernst, Zürich, for his eminent contributions to the advancement of this technique. New materials for future technologies, however, often function in the solid state as highly viscous systems such as gels, or as molecules attached to surfaces.

Solid state NMR spectroscopy is a kind of nuclear magnetic spectroscopy characterized by the presence of anisotropic interactions

(directionally dependent). The dominant structure dependant interactions which contribute to the shape and position of NMR lines of solids are [13-15]

a. Dipolar interactions

b. Chemical shift interactions

c. Quadrapolar interactions for nuclei with $I > 1/2$

These interactions are closely related to the structural environment of the nucleus under investigation, they are the main source of structural information from solid state NMR. However the above interactions are responsible for considerable line broadening in NMR spectra of solids that may lead to serious problems in attaining sufficient spectral resolution. The reason for the line broadening is that all the above interactions are anisotropic, i.e. depend on their orientations relative to the direction of magnetic field B_o. Therefore the shape and position measured by NMR lines depend strongly on the orientation of the nuclear environment, which defines the direction of the internal interactions. In liquids, the direction dependency is averaged by fast thermal motion of the molecules and sharp lines are usually observed. The spectra of polycrystalline samples are characterized by broad super positioning of resonances arising from different orientations of crystallites weighed by statistical probability with which each orientation may occur. The super position of wide distribution of interactions of different strengths and their random orientation usually give rise to broad signals without characteristic shape.

Various spin interactions result in the appearance of broad powder patterns. Thus for the measurement of well resolved NMR spectra of powder

with individual resonance lines for inequivalent nuclei, special techniques have to be applied to remove or at least to reduce substantially the line broadening effects. The most important techniques are: 1) Dipolar decoupling (2) Magic angle spin and (3) Double oriented rotation (DOR).

2.5.3.1 *Magic Angle Spinning*

We know from the previous section that the line broadening in spin-1/2 solids mainly comes from the following anisotropic internal interactions like, 1) direct dipolar interactions 2) electron shielding interactions such as chemical shift and 3) quadrupole interaction of its electric quadrupole moment with the electric field gradient. The effect of MAS on each of them is discussed below. The procedure of this technique consists of rotating the solid specimen about an axis inclined at the angle 54.7 ° to the direction of magnetic field of the NMR magnet. Sufficiently rapid rotation about this particular axis removes most broadening interactions from the NMR spectra and gets the liquid like high resolved NMR spectra. Magic angle spinning may be used on its own, and may also be combined with other line narrowing techniques. For example it may be combined with multiple pulse sequence to obtain high resolution NMR spectra, especially of hydrogen and fluorine nuclei, in solids: it may be combined with cross polarization and high power heteronuclear decoupling methods to obtain the high resolution spectra from ^{13}C, ^{29}Si and other nuclei of low abundance. Of most importance in this dissertation is cross polarised magic angle spinning [15].

2.5.3.2 *Cross Polarisation*

Shorter transverse relaxation times and residual anisotropic broadening that is not fully averaged by rotation (homonuclear dipole-dipole coupling)

lead to significantly broader lines in solid-state MASNMR spectra compared to the same substance in solution. Typically, lines are by a factor of 10-100 broader. This does not only mean that MASNMR spectra still have significantly lower resolution than solution spectra, they also have poor signal-to-noise ratio. The signal-to-noise ratio roughly scales with the inverse of the linewidth, as the integral intensity of the whole line is constant. For heteronuclei with spin 1/2 (^{13}C, ^{15}N, ^{31}P), the situation is worsened by the fact, that longitudinal relaxation times T_1 are longer in the solid state than in solution. This means that the experiment cannot be repeated as fast as in solution and a smaller number of accumulations are possible in a given time. Taken together, these effects would render ^{13}C solid-state NMR useless, if there were no technique for enhancing the signal. In fact, this situation applied until the early 1970 s.

The signal can be enhanced by a double resonance technique that is called cross polarization. Unlike the nuclear overhauser effect (NOE) enhancement, cross polarization (CP) is not dependent on a certain balance of relaxation times. Furthermore, CP also solves the problem of slow signal accumulation caused by the long longitudinal relaxation times T_1 of heteronuclei in the solid state. The polarization required for the experiment comes from the protons. Thermal equilibrium polarization of the protons is restored with the longitudinal relaxation time of the protons, which is much faster than the one of heteronuclei.

The CP experiment is often combined with the MAS technique (CP/MAS NMR) and with proton decoupling during detection. For decoupling, the full radiofrequency power is used, while during cross

polarization usually less power is applied to establish the Hartmann-Hahn match. The CP/MAS NMR experiment is the standard experiment in solid state NMR of nuclei with spin 1/2 other than protons. For quadrupole nuclei ($I > 1/2$), CP becomes more complicated and less efficient. Moreover, quadrupole nuclei usually have much shorter T_1, as the nuclear quadrupole interaction contributes to relaxation [16].

The measurements were done on a *Bruker DRX 500* NMR spectrometer using CP/MAS pulse sequence with number of scans (10,000-17000).

2.5.4 UV Absorption Spectroscopy

The instrument used in ultraviolet-visible spectroscopy is called a UV/vis spectrophotometer. It measures the intensity of light passing through a sample (I), and compares it to the intensity of light before it passes through the sample (Io). The ratio I / Io is called the transmittance, and is usually expressed as a percentage (%T). The absorbance, A, is based on the transmittance:

$$A = - log \, (\%T)$$

A spectrophotometer can be either single beam or double beam. In a single beam instrument, all of the light passes through the sample cell. I_o must be measured by removing the sample. In a double-beam instrument, the light is split into two beams before it reaches the sample. One beam is used as the reference; the other beam passes through the sample. Some double-beam instruments have two detectors (photodiodes), and the sample and reference beam are measured at the same time. In other instruments, the two beams pass through a beam chopper, which blocks one beam at a time. The detector alternates between measuring the sample beam and the reference beam.

Samples for UV/Vis spectrophotometry are most often liquids, although the absorbance of gases and even of solids can also be measured. Samples are typically placed in a transparent cell, known as a cuvette. Cuvettes are typically rectangular in shape, commonly with an internal width of 1 cm. (This width becomes the path length, L, in the Beer-Lambert law)

2.5.5 Fourier Transform-Infrared spectroscopy

Infrared spectroscopy is a very useful technique for characterization of materials, providing information of structure of molecules [17]. IR spectrum of a compound is the superposition of absorption bands of specific functional groups.

The advantages of infrared spectroscopy include wide applicability, nondestructiveness, measurement under ambient atmosphere and the capability of providing detailed structural information. Besides these intrinsic advantages the more recent infrared spectroscopy by Fourier transform (FTIR) has additional merits such as: higher sensitivity, higher precision (improved frequency resolution and reproducibility), quickness of measurement and extensive data processing capability. IR spectra originate in transitions between two vibrational levels of a molecule in the electronic ground state and are usually observed as absorption spectra in the infrared region. For a molecule to present infrared absorption bands it is needed that it has a permanent dipole moment. When a molecule with at least one permanent dipole vibrates, this permanent dipole also vibrates and can interact with the oscillating electric field of incident infrared radiation. In order for this normal mode of vibration of the molecule to be infrared active, that is, to give rise to an observable infrared band, there

must be a change in the dipole moment of the molecule during the course of the vibration. Thus, if the vibrational frequency of the molecule, as determined by the force constant and reduced mass, equals the frequency of the electromagnetic radiation, then adsorption can take place. As the frequency of the electric field of the infrared radiation approaches the frequency of the oscillating bond dipole and the two oscillate at the same frequency and phase, the chemical bond can absorb the infrared photon and increase its vibrational quantum number or increase its vibrational state to a higher level. As an approximation, larger the strength of the bond the higher the frequency of the fundamental vibration. In the same way, the higher the masses of the atoms attached to the bond the lower the wavenumber of the fundamental vibration. As a general guide, the greater the number of groups of a particular type, more polar the bond, the more intense the band. The infrared spectrum can be divided into two regions, one called the functional group region and the other the fingerprint region. The functional group region is generally considered to range from 4000 to 1500 cm^{-1} and all frequencies below 1500 cm^{-1} are considered characteristic of the fingerprint region. The fingerprint region involves molecular vibrations, usually bending motions that are characteristic of the entire molecule or large fragments of the molecule and these are used for identification. The functional group region tends to include motions, generally stretching vibrations, which are more localized and characteristic of the typical functional groups, found in organic molecules. While these bands are not very useful in confirming identity, they do provide some very useful information about the nature of the components

that make up the molecule. Basically an IR spectrometer is composed of source, the monochromator and the receptor.

The infrared induced vibrations of the samples were recorded using *JASCO FTIR* spectrometer by means of KBr pellet procedure. Spectra were taken in the transmission mode and the samples were evacuated before making the pellet and the spectra were taken under atmospheric pressure and temperature 293 K.Changes in the absorption bands were investigated in the 400-4000 cm^{-1} region. The resolution and acquisition applied were 4cm^{-1} and 60 scans respectively.

2.5.6 Scanning Electron Microscopy

The scanning electron microscope (SEM) is a type of electron microscope capable of producing high-resolution images of a sample surface by analyzing electrons emitted from a specimen. The interaction of a beam of electrons with the specimen results in the generation of secondary electrons, back scattered electrons, auger electrons, characteristic X-rays and photons of various energies.Secondary electrons and back scattered electrons can form images as well as supply atomic information about the sample. In SEM analysis finely powdered sample was applied on to a double sided carbon tape placed on a metal stub. The stub was then inverted in such a manner that the free side of the carbon tapes gently picked up a small amount of the sample, thereby creating a thin coating. It was then sputtered with a thin layer of gold to obtain better contrast and provide improved cohesion [18]. During SEM inspection, a beam of electrons is focused on a spot volume of the specimen, resulting in the transfer of energy to the spot. These bombarding electrons, also referred to as primary electrons, dislodge electrons from the specimen itself. The dislodged electrons,

also known as secondary electrons, are attracted and collected by a positively biased grid or detector, and then translated into a signal. To produce the SEM image, the electron beam is swept across the area being inspected, producing many such signals. These signals are then amplified, analyzed, and translated into images of the topography being inspected. Finally, the image is shown on a cathode ray tube.

The scanning electron microscopy of the samples were carried out in *JEOL JSM 840 A (Oxford make) model 16211* SEM analyzer with a resolution of 1.3 eV. The samples were dusted on a double sided carbon tape, placed on a metal stub and coated with a layer of gold to minimize charge effects.

2.5.7 Transmission electron microscopy

Transmission electron microscopy (TEM) is an imaging technique whereby a beam of electrons is transmitted through a specimen, then an image is formed, magnified and directed to appear either on a fluorescent screen or layer of photographic film or to be detected by a sensor such as a CCD camera (charge couple device) [19]. The transmission electron microscope is an optical analogue to the conventional light microscope. It is based on the fact that electrons can be ascribed a wavelength but at the same time interact with magnetic fields as a point charge. A beam of electrons is applied instead of light, and the glass lenses are replaced by magnetic lenses. The lateral resolution of the best microscopes is down to atomic resolution. Like SEM, a TEM uses an electron gun to produce the primary beam of electrons that will be focused by lenses and apertures into a very thin, coherent beam. This beam is then controlled to strike the specimen.

[5] H. Lipson, H. Steeple, Interpretation of X-ray Powder Diffraction Patterns, Macmillan, London (1970) 261.

[6] C. Suryanarayana, M.G. Norton, X-ray Diffraction-A Practical approach, Plenum Press, Newyork (1998).

[7] G. Bergeret, Hand book of Heterogeneous Catalysis eds. Ertl G., Knozinger H., Weitkamp. J, 2 (1997) 464.

[8] S.J. Gregg, K.S.W. Sing, Adsorption, Surface Area and Porosity, Academic Press, London (1982).

[9] P.A. Webb, C. Orr, Analytical Methods in Fine Particle Technology, Micromeritics (1997).

[10] K.S.W. Sing, D.H. Everett, R.A.W. Haul, L. Moscou, R.A. Pierotti, J. Rouquerol, T. Siemieniewska, Pure Appl. Chem., 57 (1985) 603.

[11] S. Brunauer, P.H. Emmett, E. Teller, J. Am. Chem. Soc., 60 (1938) 309.

[12] M. Kruk, M. Jaroniec, A. Sayari, Langmuir, 13 (1997) 6267.

[13] E.P. Barrett, L.G. Joyner, P.P. Halenda, J. Am. Chem. Soc.,73(1951) 373.

[14] M. Mehring, Principles of High Resolution NMR in solids, Springer-Verlag, Berlin (1983) 1.

[15] G. Engelhardt, Solid state NMR in Handbook of Heterogenous Catalysis (Ed. Ertl. G., Knozinger H., Weitkamp.J) 2, Wiley VCH, (1999) 525.

[16] Akitt, J.W, Mann, B.E, 'NMR and Chemistry', Stanley Thornes: Cheltenham, UK, (2000)273

[17] J.W. Neimantsverdriet, Spectroscopy in catalysis- An introduction, VCH Verlagsgesellschaft, D-69451, Weinheim, Germany (1995).

[18] I.E. Wachs, Characterisation of Catalytic Materials, Butterworth-Heinemann: Manning (1992).

[19] B. Fultz, J. Howe, Transmission Electron Microscopy and Diffractometry of Materials, Springer, 2nd edn. (2002).

[20] H.H. Willlared, L.L. Merrit Jr., J.A. Dean, F.A. Settle Jr., Instrumental Methods of Analysis, 7th edn., CBS Publishers, New Delhi (1986).

Natural Silica for Nature's Catalyst

High grade amorphous silica obtained from rice husk an agricultural waste, under controlled burning conditions is highly reactive due to its ultra fine size and high surface area. The porous silica so obtained was used for immobilization using two procedures, adsorption and covalent binding. An industrially important enzyme α- amylase was chosen for immobilization. Covalent binding was carried out by a two-step process through alkyl amine and glutraldehyde. The plenty of silanol groups on rice husk silica gave a high loading of organo functionalities which were comparable to meso porous silica. The materials were characterized using CHN, DRIFT, TG, N_2 adsorption, SEM and NMR analysis. The efficiency of immobilized enzymes for starch hydrolysis was tested in a batch reactor. The kinetic parameters were determined using the non linear regression curves. The immobilized enzymes could be reused 6 cycles without much loss in activity. The immobilized enzyme was stable for 1 hour at $60^{\circ}C$ in a batch reactor. Valuable silica powder from a cheap source can be efficiently used for immobilization.

3.1 Introduction

One of the chief principles of green chemistry is to use raw materials and feed stock that are renewable rather than depleting. At present, nanoscale silica materials are prepared using several methods, including vapor-phase reaction, sol–gel and thermal decomposition technique [1–5]. However, their high cost of preparation has limited their wide application. In contrast, rice husk is an agricultural byproduct whose major constituents is organic materials and hydrated silicon. The silicon atoms in the rice husk have been naturally and uniformly dispersed by molecular units, very fine particle size, with very high purity and surface area, silica powder can be prepared under controlled conditions. This process has the benefit of not only producing valuable silica powder but also of reducing disposal and pollution problems. On the other side, chemical analysis shows that rice husk contain up to 90-99% silica. It is, therefore, not unusual that this cheap source of silica may be of interest for numerous industrial uses, including the large-scale synthesis of SiO_2, $SiCl_3$, SiN,SiC, zeolites [6-10]. More over these silica samples are highly porous materials which have larger internal surface area. A major contribution for the increase of specific surface area is that the organic matter has been broken up during the thermal decomposition of rice husk, thus leaving a highly porous structure [11-12].

The biocatalytic properties of enzymes with heterogeneity are the main advantage of immobilization that makes it possible to use them in packed bed reactors [13-15]. The newer technological developments in the field of immobilized biocatalysts can offer the possibility of a wider and more economical exploitation of biocatalysts in industry, waste treatment,

medicine, and in the development of bioprocess monitoring devices like the biosensor. Over the last few decades, intense research in the area of enzyme technology has provided many approaches that facilitate their practical applications. By fixing the enzymes to solid support they mimic the natural mode of occurrence in living cells. Thus as compared to free enzymes in solution immobilized enzymes are more robust and more resistant to environmental changes.

Amylases catalyze the hydrolysis of glycosidic linkages in starch and other related oligo- and polysaccharides. These enzymes are widespread among the higher plants, animals, and microorganisms. Some of these, particularly those of bacterial and fungal origin, are commonly used in various industries such as starch processing, paper manufacture and pharmacology. Apart from being a major constituent of foodstuffs, starch is very important as a raw material for the production of sweeteners, thickening and binding agents and adhesives [15-18]. Bacterial amylase has been covalently bound to silica carriers using glutaraldehyde or titanium chloride at pH 4.8 [19]. The presence of both calcium chloride at 0.05M and ethanol at 12% (w/v) were found to improve enzyme stability. Storage activity was retained for more than 6 months when the immobilized enzyme was kept in 0.015M acetate buffer at pH 4.8 and 4°C. Immobilization of α-amylase on ultra-fine silica particles using both physical adsorption and covalent cross-linking (using glutaraldehyde as the cross-linking reagent) were found to provide similar immobilized activities [20]. The covalently bound enzyme was then used for hydrolysis studies and it was reported that the immobilized enzyme could be reused with its activity retained. The thermostability of

bacterial α-amylases was found to improve after the enzyme was immobilized on silica and plastic carriers. $CaCl_2$ was found to be important for storage stability of the immobilized enzyme [21]

In the last decade,the most widely studied material for enzyme immobilization is mesoporous silica .The cost of preparation of such silica and the decrease in activity of enzyme due to mass transfer limitations when entrapped in nanopores is a draw back of such mesoporous matrices. Immobilization using porous naturally occurring silica is not much explored area. To overcome the problem of leaching of adsorbed enzymes, we studied the immobilization of α amylase by covalently binding enzyme molecules on rice husk silica after surface functionalization with 3-aminopropyltri ethoxysilane and glutaraldehyde.

Many authors have discussed the advantages of covalent binding on different silicas. The chief principle of immobilization is that the total cost should not exceed the cost of enzymes or a cheaper method should be followed. In this venture we could find that simple adsorption using cheap, thermally stable rice husk silica itself can enhance the thermal stability and pH stability of α-amylase. But leaching could be prevented to large extent only by chemical modification of rice husk silica. The low loading of enzyme due to reduced surface area was one disadvantage.

3.2 Experimental
3.2.1 Materials

Rice husk was obtained from a (Rice Mill, Thrissur, Kerala) Bacillus subtilis α-amylase, 3-amino propyl tri ethoxy silane (3-APTES) and glutaraldehyde were

purchased from Sigma-Aldrich chemicals Pvt Ltd., Bangalore. All other chemicals were of the highest purity commercially available.

3.2.2 Preparation of rice husk silica

The rice husk was first washed with distilled water to remove adhering materials and dried at 60°C. It was leached with 10% solution of HCl in distilled water at its boiling point for 3 h. The digested husk was then washed with distilled water and dried in an oven at 110 °C for 12h. Pure amorphous white silica (RS) was obtained by burning the rice husk at 600°C in a muffle furnace for 6h [22].

3.2.3 Functionalization of rice husk silica

The surface of pure silica was amino functionalized by reacting 1g of solid with 50 ml of 5 % solution of 3-APTES in toluene (v/v) at 393 K for 48 h with stirring under N_2 gas. Products were separated by filtration, washed with dry toluene and methanol. It was also washed with dichloro methane by soxhlet extraction for 18 h and dried at ambient temperature. Silica sample after amino functionalization is notated as RS-S. Following this 1g of amino functionalized silica sample was reacted with 25 ml of a 2.5 % solution of glutaraldehyde in phosphate buffer (pH = 6.62) for 1h at room temperature. The product was washed exhaustively with distilled water till all excess glutaraldehyde was removed which was tested by Tollen's reagent method and then dried at room temperature. Sample after aldehyde functionalization are designated as RS-G.

3.2.4 Synthesis of mesoporous silica from rice husk silica

1.5 g of rice husk silica was mixed with 50 ml 1 M NaOH aqueous solution. The mixture was refluxed for 1.5h at its boiling point and was filtered to remove the undissolved residues to get pure sodium silicate. 3 g P123 was stirred with 180 mL 2M HCl for 12 h and 9.6 mL sodium silicate was added dropwise. The

contents were transferred to an autoclave, kept at 100 °C for 6-12 h. Filtered, dried and calcined at high temperature of 600 °C. The sample is designated as MRS

3.2.5 Immobilization on pure and functionalized silica

α-amylase was immobilized on above functionalized silica and nonfunctionalized silica surface by contacting 1 g of solid with 10 mL of 0.1 % solution of enzyme at room temperature for 1.5 h with continuous but moderate shaking of the reaction mixture. The enzyme silica complex was separated by filtration and washed thoroughly with phosphate buffer till excess enzyme was removed. Concentration of enzyme protein was determined by spectrophotometric method using BSA as standard. The protein loaded on solid supports was determined by measuring the concentration of the enzyme in the original enzyme before and after adsorption. Samples after adsorption of enzymes are designated as RSE and after covalent binding are designated as RSGE.

3.3 Characterisation

Silica samples were characterized before and after enzyme loading. Powder X-ray diffraction pattern at low and wide was collected using *Rigaka d-Max* Ni filtered Cu Kα radiation. Nitrogen sorption isotherms were measured at liquid temperature (77 K) using *Micromeritics Tristar 3000* system. Silica samples were degassed at 383 K for 4 h prior to analysis. BET surface area was calculated using adsorption data in the BET region and the pore size distribution of the samples was determined by the BJH method. Elemental analysis, percentage of carbon, hydrogen and nitrogen of samples was done using *Perkin Elmer CHNS elemental analyzer, model 2400*. DRIFT was done using *JASCO FTIR* spectrometer. The spectrum was recorded at room temperature with a resolution of 4 cm^{-1} after 60 scans using a KBr spectrum as background.

3.4   Results and Discussion

3.4.1 X-ray Diffraction Patterns

Fig 3.1 shows X-ray diffraction analysis on rice husk after calcination at 600°C. The sample is X-ray amorphous although a broad diffraction peak around $2\theta \sim 22$ °is typical of silica. These results agree with those obtained in other studies [22, 23]. Hamad et *al.* mentioned that cristabolite was detected at 800°C when rice husk was burnt in air. At 1150°C both cristobalite and tridymite were present [24]. Silica modified with template and the one modified with functional group did not show any change in the XRD pattern. The XRD profiles of covalently bound and adsorbed samples showed a slight distortion and a reduction in the peak height. After immobilization of α-amylase there was no shift in the 2θ values and hence the d spacing. This means that the sorption of α-amylase was entirely external.
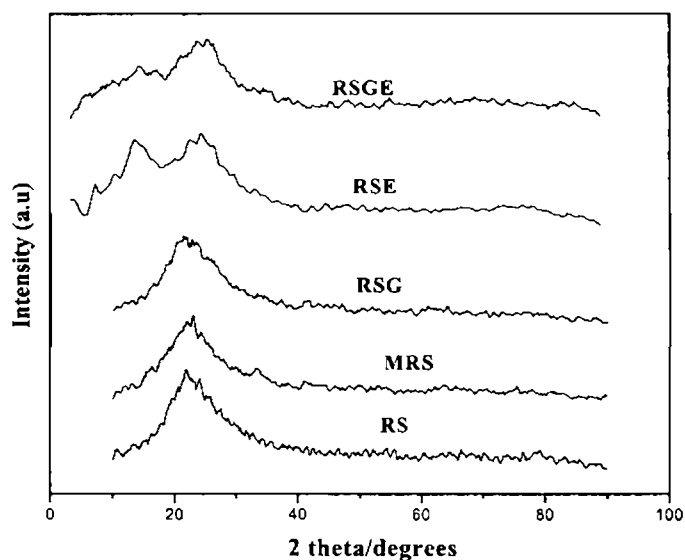

Fig. 3.1   X-ray diffraction pattern of a) RS b) MRS c) RSG c) RSE and d) RSGE.

The low angle XRD patterns of rice husk silica and modified forms are given in Fig. 3.2. Like mesoporous silica both didn't not show any well defined peak at low values, which indicated that the porous structure was a disordered one in rice husk silica and modified forms or the structural ordering (mesophase)was not attained with our experimental conditions. Few authors have reported the synthesis of mesoporous silica from rice husk [25-26].
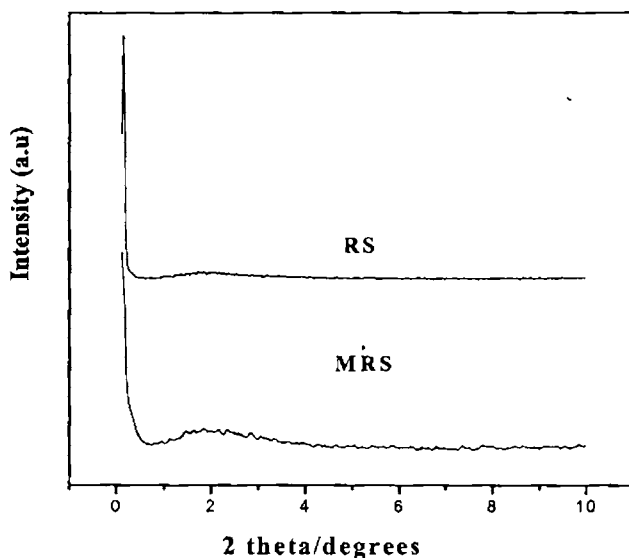

Fig. 3.2 Low angle X-ray diffraction pattern of a) RS and b) MRS.

3.4.2 C H N Analysis

As expected, calcined silica has no C and N. However, on APTS loading, % of C, H and N is observed to increase. On further binding of glutaraldehyde to amino functionalised silica, % of C and H are expected to increase whereas overall % N is expected to decrease. C, H, N data given in Table 3.1 show similar trend. The observed % of N decrease on binding with

glutaraldehyde is expected as glutaraldehyde does not have any nitrogen in it. A similar observation was reported by Pandya et al [27].

Table 3.1 CHN Analysis

Sample	Elemental Analysis (%)		
	C	**H**	**N**
RS-S	5.60	2.09	1.72
RS-G	8.84	2.80	1.28

3.4.3 Adsorption Isotherms

Surface area as well as pore volume decrease upon functionalization and immobilization (Table 3.2). Activation of silica with aminopropyl silane and glutaraldehyde reduced the pore volume, suggesting that the binding of silane and glutaraldehyde was inside the irregular pores. The enzyme bound samples also showed marked difference in surface area indicating successful immobilization of enzymes. The surface area of MRS was low compared to rice husk silica. But the average pore width increased from 85 to 155 Å.

Table 3.2 BET surface area and Pore Volume measurements

Catalyst	BET Surface area (m^2/g)	Pore Volume (cm^3/g)	Average Pore Width (Å)
RS	247	0.62	85
RS-E	172	0.41	70
RS-S	63	0.09	59
RS-SE	18	0.003	31
MRS	122	0.69	155

Fig.3.3 shows adsorption isotherm which resembles Type IV of Brunaur's classification [6]. At low values of P/P_0 the isotherm is similar to Type II, but then adsorption increases rapidly at P/P_0 above 0.5, where pore condensation takes place. These results indicate that the silica from rice husk was a porous material. Adsorption isotherms corresponding to pressure range P/P_0 0 to 0.3 reflected the monolayer formation of nitrogen gas adsorbed on the walls of the mesopores and was used for calculation of BET surface area of the samples. A small inflection observed in the isotherms around $P/P_0=0.5$ shows the capillary condensation within mesopores. There was no sharpness in the inflection step which indicated the non uniformity of mesopore. The low P/P_0 value indicated the narrow pore size [11-12].
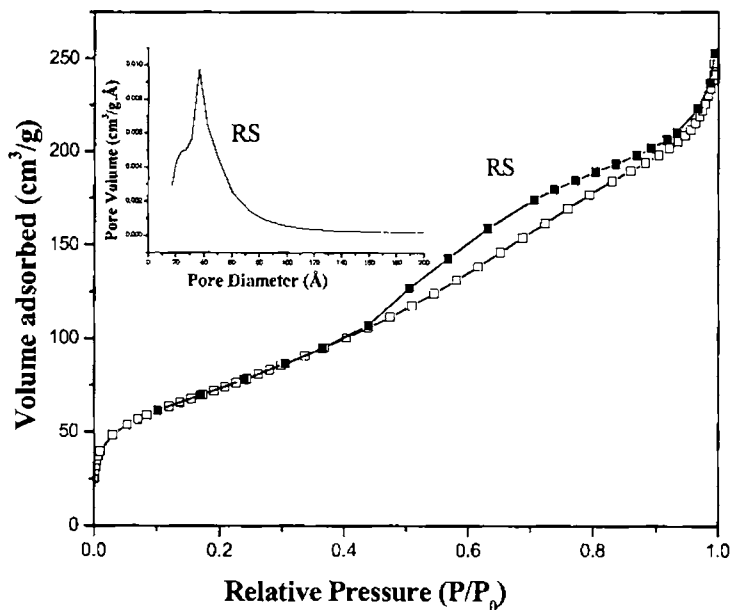

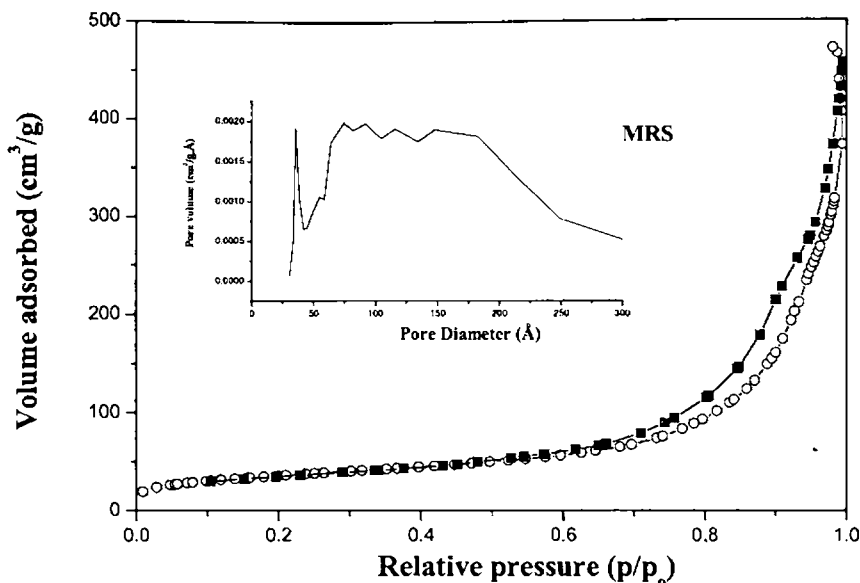**Fig. 3.3** Nitrogen adsorption isotherm of RS with the pore size distribution

Fig.3.4 Nitrogen adsorption isotherm of MRS with the pore size distribution

Pore size distribution of calcined rice husk silica is also given in inset of Fig. 3.3. A double peak was observed having maxima at about 25 to 40 Å. α-amylase whose size is much larger could not penetrate into the pore but most of the molecules were attached on the external surface itself. The adsorption isotherm along with the pore size distribution after template modification is given in Fig. 3.4. The figure clearly showed that even though the pore size increased, the pore size distribution was very broad, which indicated the non uniformity of the pores.
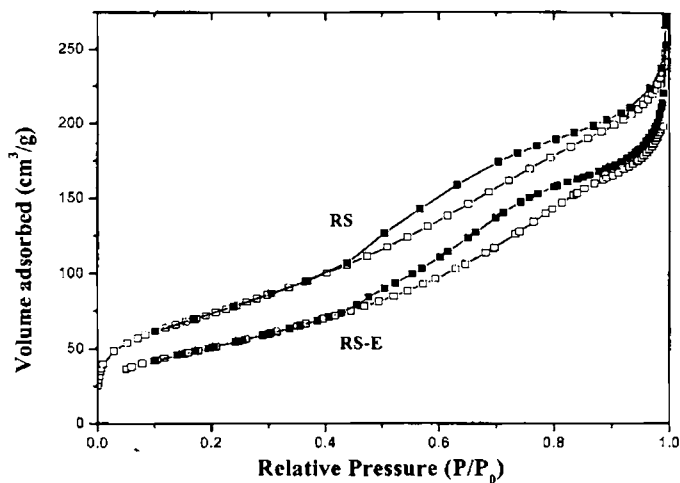
Fig. 3.5 Nitrogen adsorption isotherm of pure rice husk silica and enzyme adsorbed silica sample

After adsorption of enzymes the volume of nitrogen adsorbed decreased but the hysteresis had no change in shape or shift in P/P_0 as the enzymes being too large to enter the pores (Fig. 3.5)
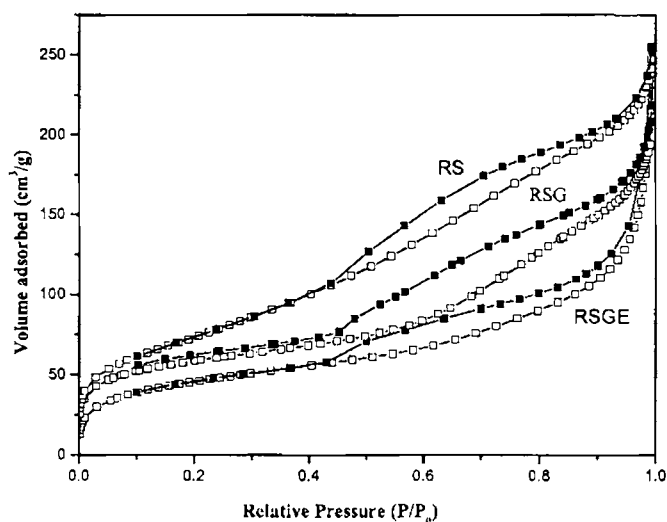

Fig.3.6 Nitrogen adsorption isotherms of RS-Rice husk silica, RSG-Glturaldehyde bound to silane modified silica (functionalized silica) RSGE-enzyme bound functionalized rice husk silica.

Nitrogen adsorption isotherms of functionalized samples are shown in Fig. 3.6. The P/P_0 value decreased from 0.43 to 0.39 indicating the occupancy of functional groups within the pore. Reduction in volume of nitrogen adsorbed after enzyme binding was a clear indication of immobilization. (Fig.3.6).

3.4.4 Thermogravimetry

Fig. 3.7 represent TG curves for various samples. The TGA plot of acid treated rice husk shows a sharp peak at 300-550°C. The weight decrease is attributed to the removal of combustible, volatile organic matter lignin and cellulose [12].The figure also shows the TGA profiles for pure silica, functionalized and the immobilized samples. The thermo gram (RS) reflected the purity and thermal stability of rice husk silica. The first stage of weight loss from 40 to 120°C could be associated with desorption of the adsorbed water as well as water generated by the condensation of part of free silanols. In the functionalized sample a strong peak at 300-500 °C is due to the decomposition of attached functional groups [28]. The loading of enzymes on calcined silica and functionalized was evident from the weight loss extending over a large range of temperature.
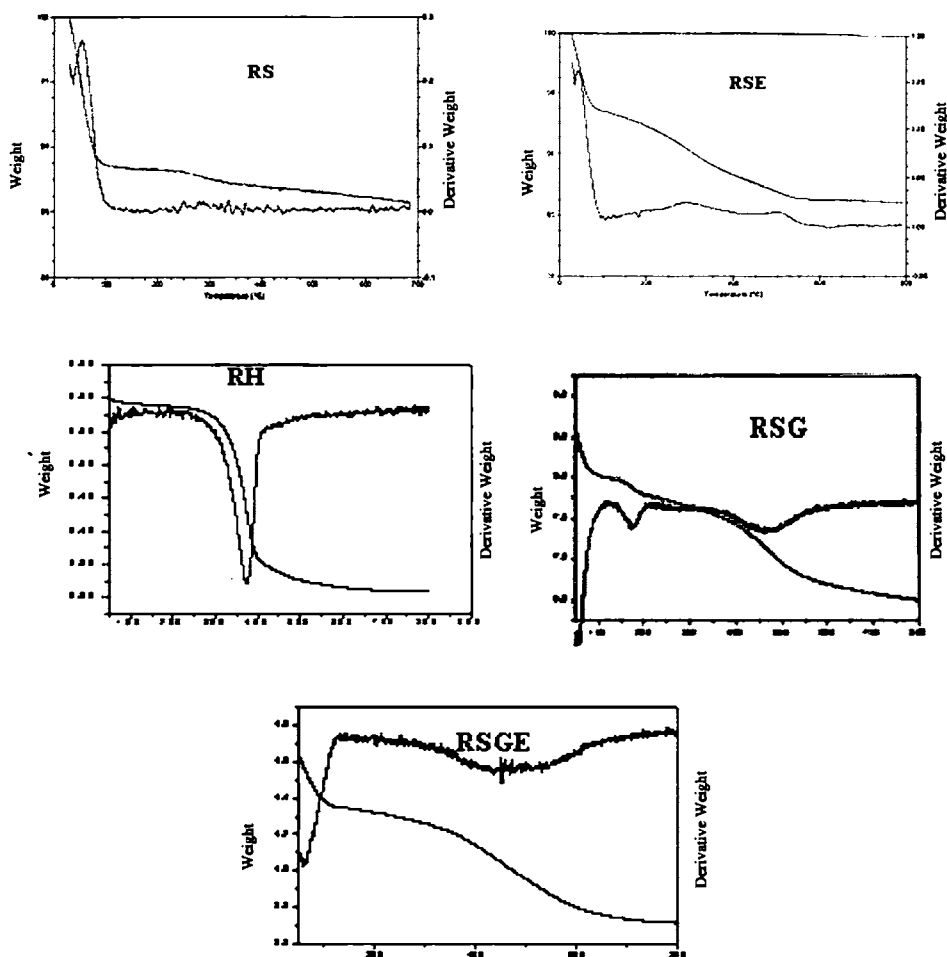
Fig. 3.7 Thermograms of pure rice husk silica (RS), enzyme adsorbed silica (RSE), ricehusk (RH) ,functionalizedsilica (RSG),enzyme covalently bound silica (RSGE)

3.4.5 Scanning electron microscope

SEM reflects the porosity of the material (Fig.3.8). The organic materials in rice husk consisting of cellulose, hemicelluloses and lignin, thermally decompose when acid leached rice husk was calcined leaving irregular pores ranging from 20 to 85 Å. After modification with the template

the morphology and particle size changed considerably. After immobilization neither the morphology nor the particle size changed. Hence the SEM of immobilized samples is not included in the figure.
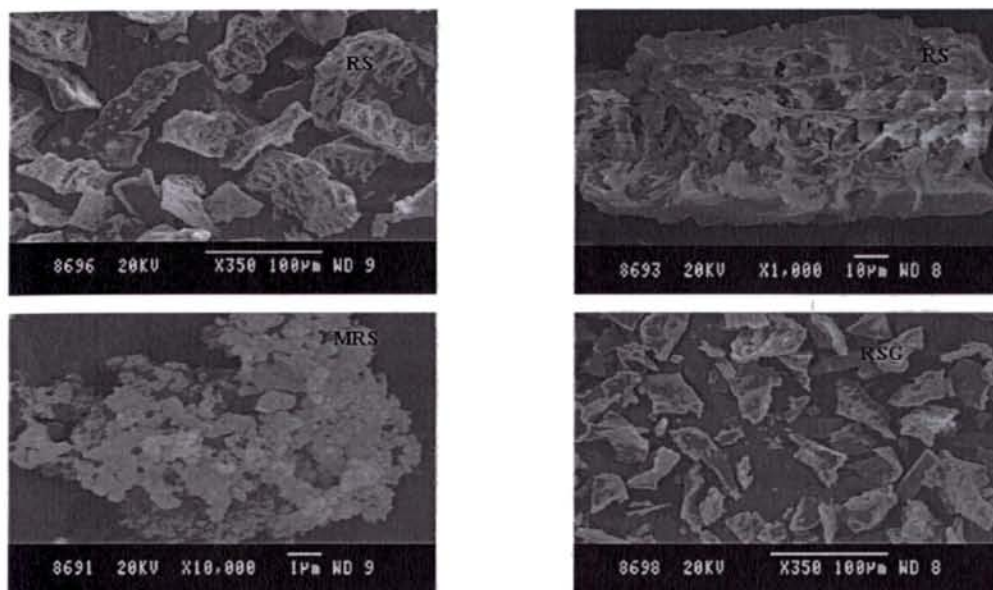

Fig.3.8 Scanning electron micrographs of rice husk silica (RS), template modified rice husk silica (MRS) and functionalized rice husk silica (RSG)

3.4.6 FTIR spectroscopy

Whereas, the FTIR spectrum of sample RS in Fig. 3.9 showed a typical amorphous silica spectrum with intense asymmetric, symmetric stretching and bending vibration for Si-O-Si bonds at wave numbers 1103, 800, and 468 cm^{-1} respectively [20].After adsorption of enzyme due to lower loading there was no change in the spectra and it is not shown. After functionalization the presence of aminopropyl groups was confirmed by the appearance of C–H asymmetric stretching, at 2927 and 2857 cm^{-1} respectively.
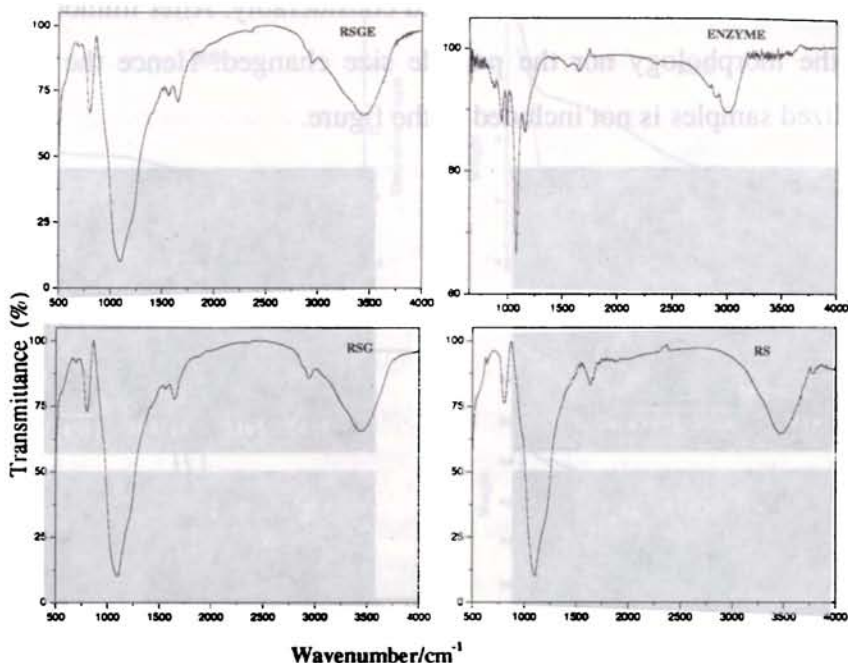
Fig.3.9 FTIR spectra of rice husk silica (RS), pure enzyme functionalized (RSG) and enzyme bound samples(RSGE)

3.4.7 Diffused reflectance spectroscopy DRIFT

DRIFT spectrum of sample RS in Fig. 3.10 showed a typical amorphous silica spectrum with intense asymmetric, symmetric stretching and bending vibration for Si-O-Si bonds at wave numbers 1094, 810, and 470 cm^{-1} respectively [20]. An intense peak at 3640 cm^{-1} confirmed the presence of silanol group. Whereas, spectra of the adsorbed amylase on rice husk silica confirm that the adsorption of the enzyme did not result in denaturation of enzyme. After immobilization the Amide I and Amide II peaks appear at 1638 cm^{-1} ,and 1518 cm^{-1} respectively. The Amide III band at 1252 cm^{-1} merges as a broad peak of the Si-O-Si asymmetric band[29].
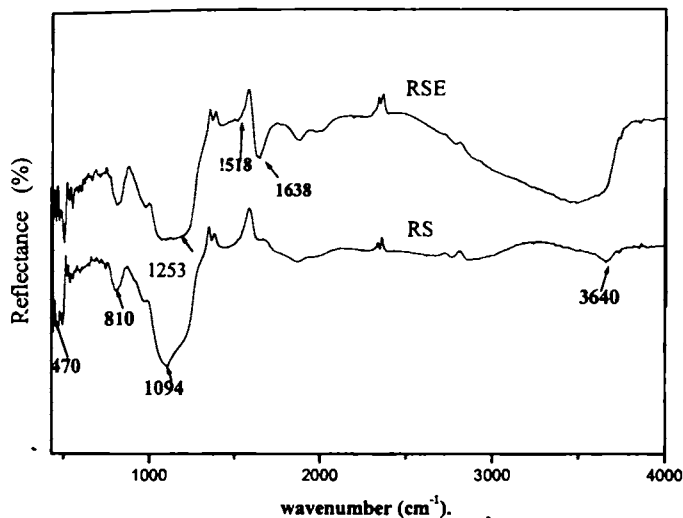
Fig.3.10 DRIFT spectra of silica from rice husk before and after immobilization
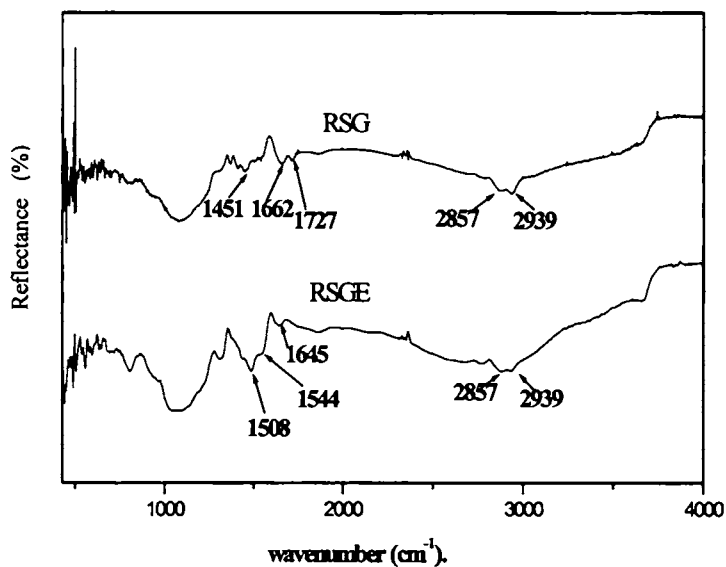

Fig. 3.11. DRI FT spectra of b) RS-S and c) RS-G

Fig. 3.11 gives the DRIFT spectra of the functionalized and immobilized samples.The insertion of aldehydic group was confirmed by the C=O strectching

at 1727 cm^{-1}. The C-N stretching vibration is normally observed in the wavenumber range 1000-1200 cm^{-1}. However, this peak was not resolved due to the overlay with the IR absorptions of Si-O-Si in the range 1000-1130 cm^{-1}. The C–H asymmetric stretching and C-H symmetric stretching occurs at 2939 and 2857 cm^{-1} respectively. After immobilization the Amide I and Amide II peaks appear at 1645 cm^{-1} and 1508 cm^{-1} respectively [29].

3.4.8 ^{29}Si MAS spectroscopy

Fig. 3.12 shows the typical ^{29}Si CP/MAS NMR spectra for the silica obtained from rice husk before and after immobilization. The peak at 100.4 could be assigned to the Q^3 site .The intense Q^3 sites are associated with the isolated Si-OH groups (i.e., free and hydrogen-bonded) [30, 31] After immobilization the peaks were broadened indicating the participation of free silanol groups for enzyme attachment.
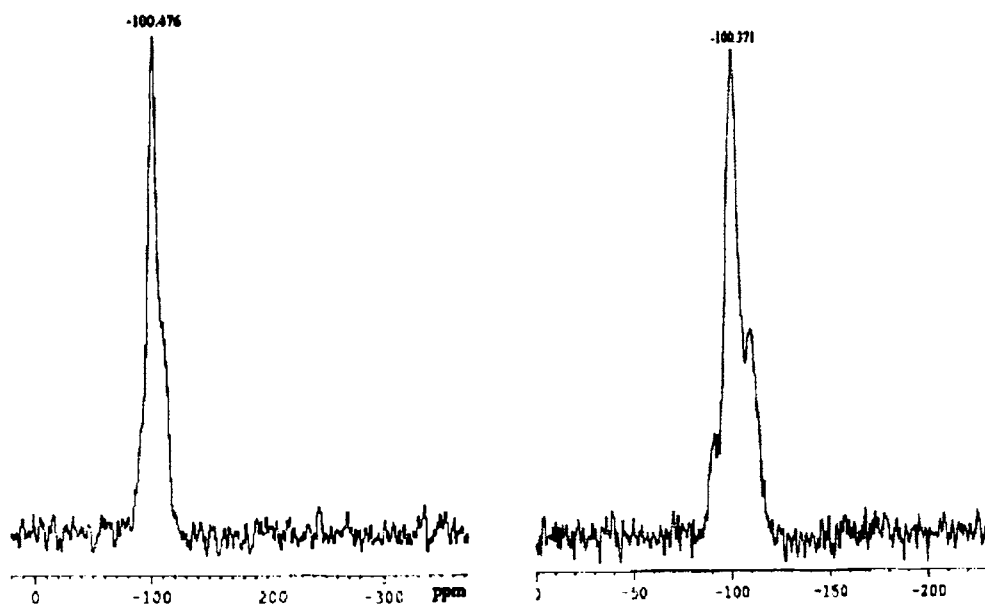

Fig. 3.12 ^{29} Si NMR of rice husk silica and enzyme adsorbed sample

As shown in Fig. 3.13 two lines at -59.2 and -67.1 ppm were observed upon incorporation of functional groups. The additional peak could be assigned to the T^3 (SiR(OSi)$_3$), and T^2 (Si(OH)R(OSi)$_2$) sites, respectively. The results suggested that the surface silanol groups, which were associated with Q^3 and Q^2 structural units of the rice husk silica were reduced in intensity indicating the consumption of these during functionalization [32]. On enzyme immobilization the T^2 and T^3 peaks were broadened due to hydrophobic interactions of aldehydic groups with the guest molecules having long hydrophobic groups. The shift in resonance of T^2 from 57.4 to 58.6 ppm was a clear indication of strong bonding with enzyme molecules. The T^3 peak also shifts from 65.1 to 66.2 after immobilization.
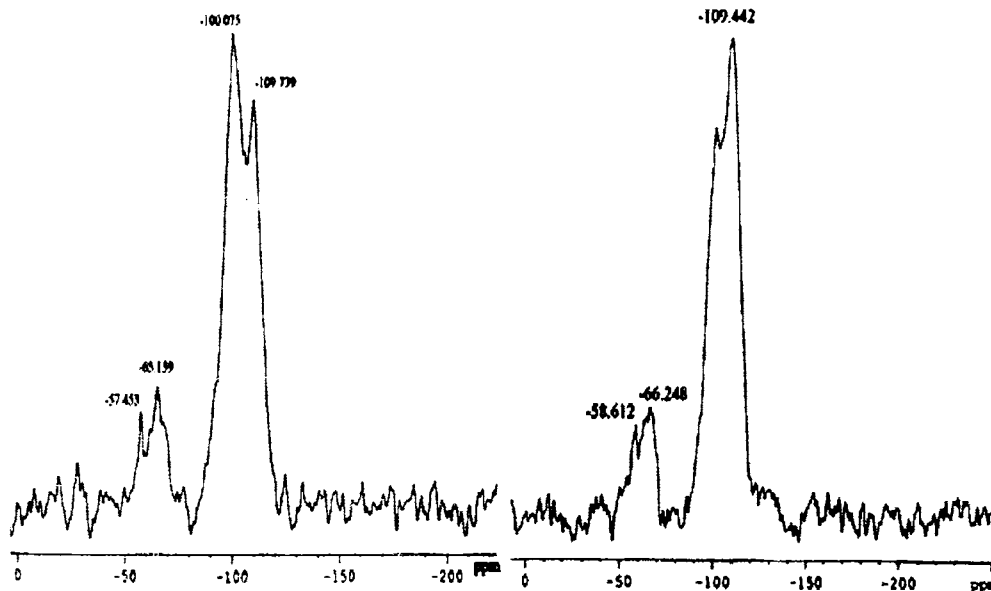

Fig. 3.13 ^{29}Si NMR of functionalized and enzyme binded sample

3.4.9 Optimization of immobilization parameters

By varying the pH, temperature, buffer concentration, and time the optimum conditions for immobilization were found out. The optimization of immobilization parameters are summarized in Fig. 3.14

- The optimum pH for adsorption and covalent binding was found to be 6. At pH 6 the enzyme is almost having zero charge (iso electric point is 5.6) and as the intermolecular repulsion is least the monomolecular layer of enzymes are stable and here the nature of the force which holds the enzyme to the surface is hydrophobic in nature.

- At higher temperature enzyme inactivation is favored. Both the enzymes exhibited similar activity at 303 and 313K. So room temperature was opted as the immobilization temperature.

- The activity of the immobilized enzymes did not vary much with buffer concentration. The optimum buffer concentration taken was 0.1 M.

- Varying the time for immobilization and measuring the activity found that longer period (optimum time was 90 min) deactivated the enzyme. Usually immobilization is done by continuously shaking the enzyme with the support in a water bath. This shaking for longer duration disrupts the three dimensional structure of protein and hence was deactivated.
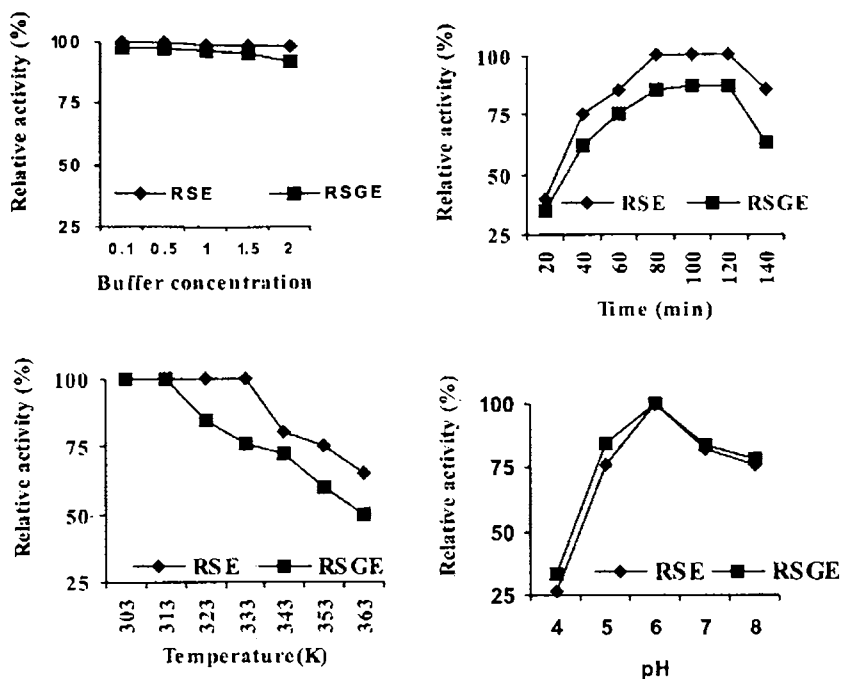
Fig.3.14 Optimization of immobilization parameters.

3.4.10 Activity and stability studies

a. Variation of activity with pH

The variation of activity with pH for free and immobilized α - amylase is depicted in Fig. 3.15. Commonly, there was a decrease of enzyme activity after immobilization. This was attributed to the minor modification in the enzyme three-dimensional structure that may lead to the distortion of amino acid residues involved in catalysis, the presence of random immobilization which hindered the analytic approach to the active site of the enzyme, and the limitations imposed by the slow mass transfer of substrate or product to/from the active site of the enzyme. The free enzyme was active over a range of pH 5-8, the immobilized enzyme both adsorbed and covalently bound were active in the similar range. This indicated that the native confirmation was

not altered much from the free enzyme after immobilization. pH stability experiments confirmed that the optimum pH for immobilized enzymes is 6.
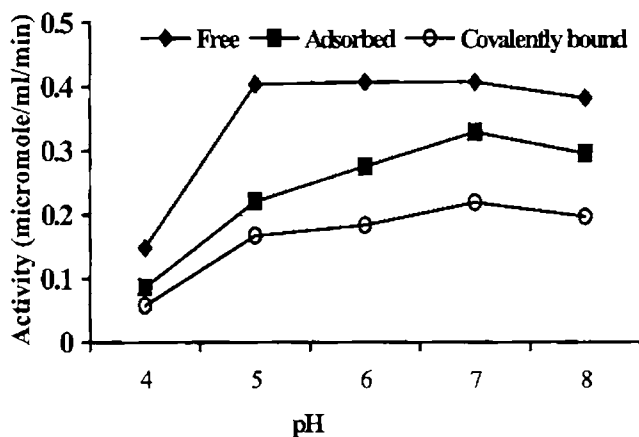

Fig. 3.15 Variation of activity with pH

b. Variation of activity with substrate concentration

The velocity of an enzyme reaction is influenced by the concentration of its substrate. In free and immobilized state α-amylase follows Michaelis Menten kinetics. In Fig. 3.16 the activity is plotted as a function of the substrate concentration for free and immobilized enzyme. The solid line was modeled by non linear regression of the Michaelis Menten equation using graph pad soft ware. The kinetic parameters obtained from these plots are summarized in Table 3.3. Conformational changes of the enzyme, diffusion limitation effects and partition effects are the main factors that affect the kinetic parameters V_{max} and K_m after immobilization.
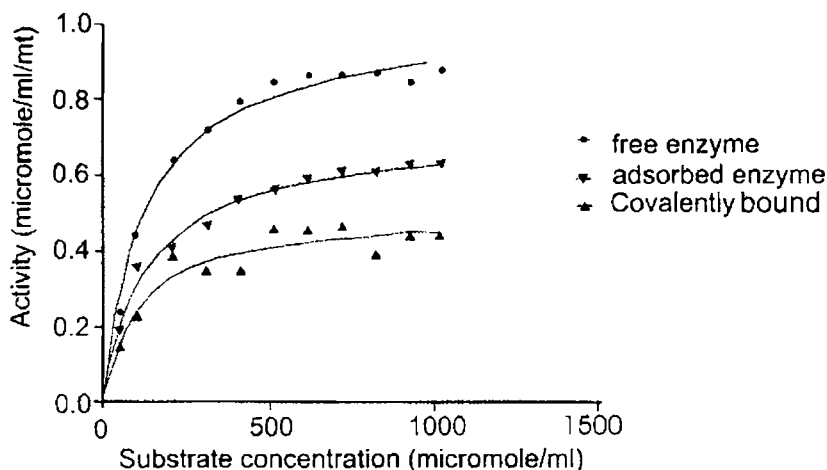
**Fig. 3.16** Michaelis–Menten plot for free and immobilized enzymes.

The quantity K_m is a measure of the stability of the ES complex or, in other words, affinity of the enzyme for its substrate; it is inversely proportional to the affinity. As seen in the table the K_m of adsorbed enzyme is slightly decreased, or there is more affinity towards the substrate even after immobilization. The substrate starch is hydrophilic in nature and has a better affinity towards the silanols on the surface of rice husk silica [33]. As usual; the maximum reaction rate catalyzed by the immobilized α-amylase was clearly lower than that of the free enzyme. The decrease in V_{max} is the result of the structural changes of the enzyme upon immobilization and the difficulty in diffusion of the substrate to reach the active site of the enzyme. While in covalently bound amylase the K_m value was increased indicating a lesser affinity for the substrate. The hydrophilic starch molecules had lesser affinity for amino propyl modified hydrophobic surface. The decrease in V_{max} was due to steric hindrances imposed by the support on the macro molecular substrate or due to chemical modification [34]. In a batch reactor the efficiency of immobilization was 68 and 56 % for adsorbed and covalently bound amylase.

Table 3.3 Kinetic Parameters of enzymes immobilized on rice husk silica

Catalyst	Michealis constant Km (μmoles/mL)	V max (μ moles/mL/mt)	Effectiveness factor (η)
Free enzyme	130.9	1.02	
Adsorbed enzyme	124.3	0.69	0.68
Covalently bound enzyme	166.2	0.57	0.56

c. **Variation of activity with temperature**

Temperature plays an important role in determining activity of enzyme. After immobilization, the optimum temperature was raised. The increase in optimum temperature was a direct outcome of immobilization; due to change of confirmation of the enzyme. The adsorbed α-amylase demonstrated a higher optimum temperature compared to the covalently bound form Fig.3.17
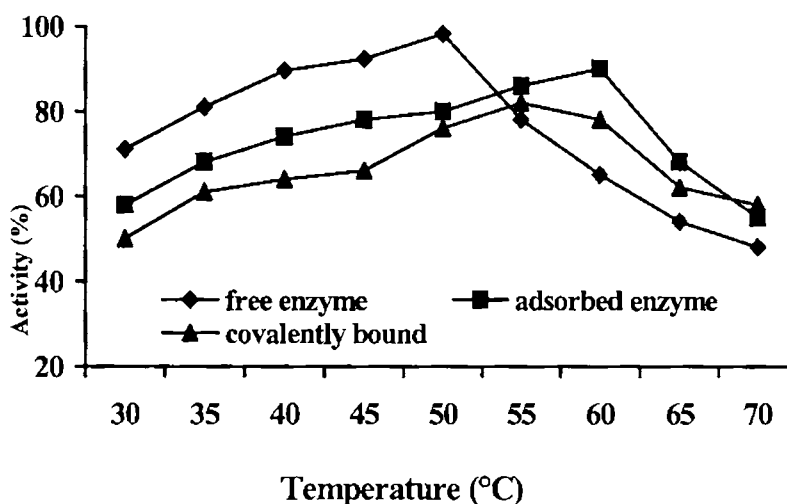
Fig.3.17 Variation of activity with temperature

d. Reusability and Operational stability.

Easy separation of the catalyst from the product mixture followed by reuse is one of the most important advantages of heterogeneous catalysis. Reusability was tested in a batch reactor and operational stability in a packed bed reactor at room temperature by loading 50 mg enzyme per gm of support. Results are represented in Fig. 3.18 and 3.19. The adsorbed and covalently bound enzyme could be recycled 6 times without loss in activity.

Nearly 75% of initial activity was retained after 24 cycles. Another major objective was application to continuous process whereby the reactor can be operated continuously without break. In the continuous operation, the activity of adsorbed and covalently bound enzyme was reduced to 75 and 80 % respectively after 96 h.
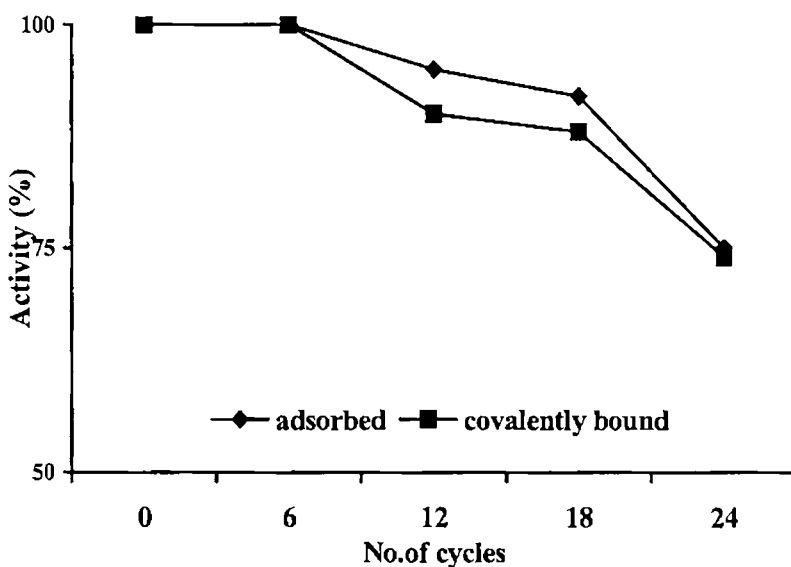

Fig. 3.18 Reusability of adsorbed and covalently bound amylase in a packed bed reactor.
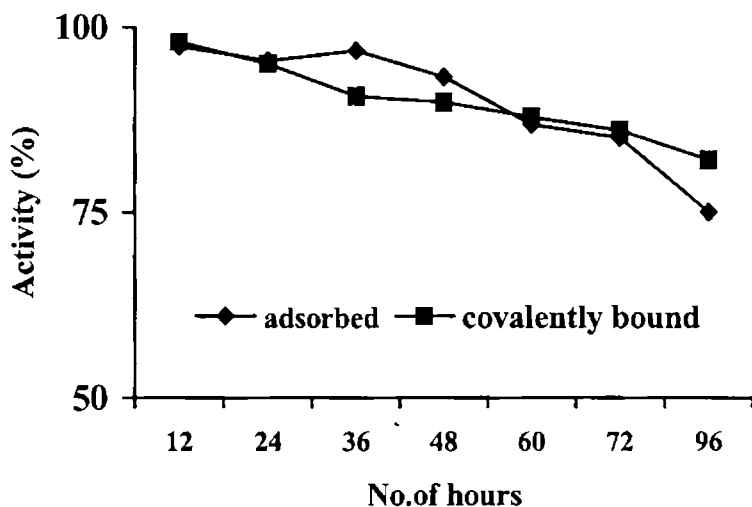
Fig.3.19 Operational stability of adsorbed and covalently bound α-amylase in a packed bed reactor.

e. Leaching Studies

Fig. 3.20 shows the amount of enzyme retained with respect to number of working cycles. There was a possibility for leaching of the enzyme that will disrupt the heterogeneous nature of the reaction. The type of immobilization is an important parameter in understanding leaching effects. At the end of 16 cycles about 65% adsorbed and 45% covalently bound enzyme leached out. During adsorption irregular pores with low dimension do not allow the enzyme molecules to penetrate inside the pores. So the degree of leaching is greater. An enhanced hydrophobic interaction along with the electrostatic interactions and hydrogen bonding has strengthened the enzyme binding in covalently immobilized form.
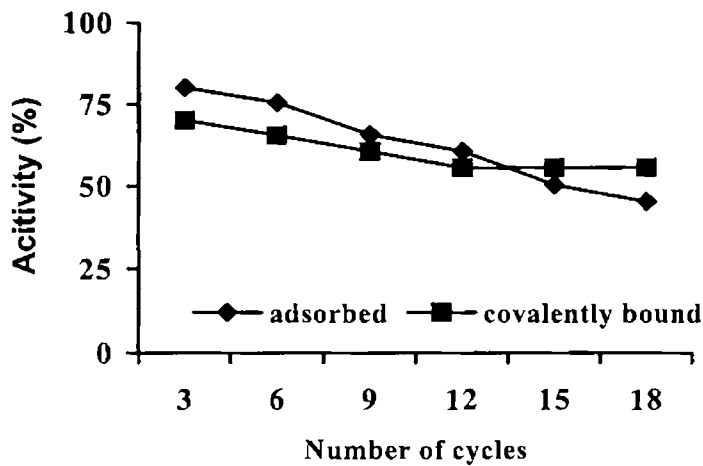
Fig 3.20 Enzyme reatined after continous use by loading 50mg enzyme/ gm silica

f.   Storage stability

The stability of the biocatalyst at room temperature in the solid form but wetted by buffer, was checked for five simultaneous days. The activity was not altered much for the first two days but decreased to 45% at the end of the third day. Immobilized enzyme can be stored in solid form at room temperature by adsorbing on silica from rice husk. Multipoint attachments to well hydrated surface reduced denaturation. There are plenty of silanol groups on the surface of rice husk silica which accounted for enhanced stability of enzyme immobilized on silica.

When stored in 0.1M buffer of optimum pH, the free α- amylase lost all its activity within 10 days (Fig. 3.20). The adsorbed form could retain 80% activity even after 24 days. Covalently bound form could retain 72% activity after the same period. This decrease in activity was explained as the time-dependent natural loss in enzyme activity. The long-term stability

of the immobilized enzyme increased to a great extent. The decrease in activity of the free α-amylase might be due to its susceptible autolysis during the storage time. The stability of the adsorbed enzyme is due to protein surface interactions on a silanol rich surface.
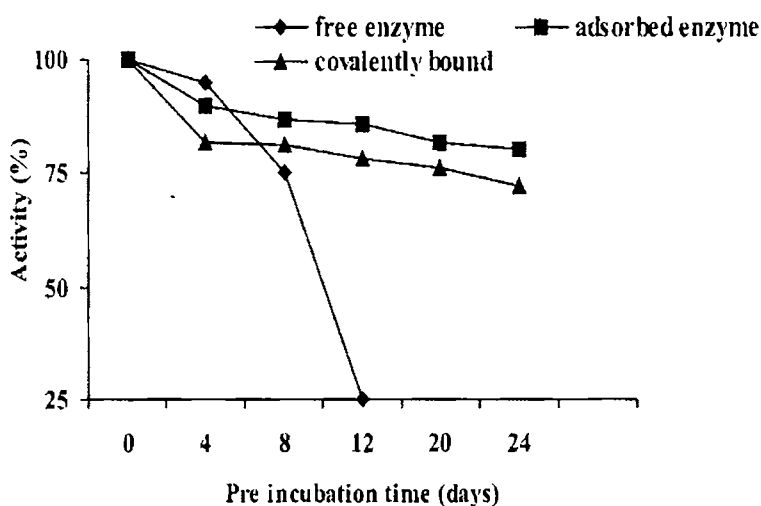
Fig. 3.21 Storage stability studies in 0.1 M buffer at optimum pH, for free, adsorbed and covalently bound form.

g. Thermal stability

The thermal stability of an immobilized enzyme can be enhanced, diminished or unchanged relative to the native, water soluble enzyme. Thermal stability experiments were performed with free and immobilized enzymes, which were incubated in the absence of substrate at higher temperatures i.e. 333K in a batch reactor (Fig.3.21). The activity of free enzyme reduced to 25% in 60 min while both the immobilized forms retained more than 70% activity in the same period. On the basis of these results, we

confirmed that the immobilization matrix increased the stability of enzyme against thermal denaturation.
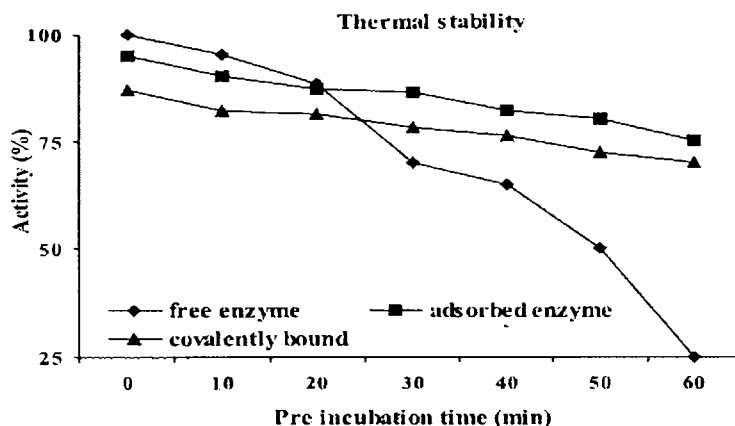
Fig. 3.22 Variation of activity of free, adsorbed and covalently bound α-amylase at 60°C in a batch reactor.

3.5 Conclusions

- Pure silica with plenty of silanol groups can be extracted from a cheap source rice husk by a simple, less time consuming, acid leaching process.

- Enzyme immobilization on external surface of silica was confirmed from XRD, FTIR, DRIFT, TG, MAS[29]SiNMR and adsorption isotherm.

- Synthesis of template assisted mesoporous material from rice husk requires more optimization.

- The surface of silica was functionalized with aldehyde functional group for the firm binding of enzymes.

- Both adsorbed and covalently bound α - amylase exhibited activity but lower than free enzyme.

- Loss of activity in batch reactor is an outcome of resistance to mass transfer due to improper diffusion of substrate from bulk to the enzyme surface.

- Storage stability improved after immobilization.

- Leaching of bound enzymes was a problem at higher loading.

- Reusability was enhanced both in batch and packed bed reactors.

References

[1]   M. Tomozawa, D.L. Kim, V. Lou, J. Non Cryst. Solids, 296 (2001) 102.

[2]   P.A. Tanner, B. Yan, H. Zhang, J. Mater. Sci., 35 (2000) 4325.

[3]   G. Wu, J. Wang, J. Shen, T. Yang, Q. Zhang, B. Zhou, Z.Deng , F.Bin, D. Zhou, F.Zhang, J.Non Cryst. Solids, 275 (2000) 169.

[4]   Z. Deng, F. Bin, D. Zhou, F. Zhang, J. Non Cryst. Solids, 275 (2000) 169.

[5]   S. Sadasivan, D.H. Rasmussen, F.P. Chen, R.K. Kannabiran, Colloids and Surf. A., 132(1998)45.

[6]   A. Karera, S. Nargis, S. Patel, M. Patel, J. Sci. Ind. Res., 45 (1986) 441.

[7]   J. James, M.S. Rao, Thermochim. Acta., 97 (1985) 329.

[8]   Y. Nakata, M. Suzuki, J. Ceram. Soc. Jpn., 97 (1989) 830.

[9]   R.V. Krishnarao, Y.R. Mahajan, T.J. Kumar, J. Eur. Ceram. Soc., 18 (1998) 147.

[10]   S.B. Hanna, N.A.L. Mansour, A.S. Taha, H.M.A. Abd-Allah, Br. Ceram.Trans., 84 (1985) 18.

[11]   T.H.Liou, Mater. Sci. Eng. A, 364 (2004) 313.

[12]   T.H.Liou,Carbon, 42 (2004) 785.

[13]   M.D Trevan, Immobilised enzymes, Wiley, London, 1980.

[14]   W.Hartmeier, Immobilised Biocatalysts, Springer, 1988.

[15]   N .Gerbsch, N.Buchholz, Microbiol Rev., 16(1995)259.

[16] N.E. Lloyd, W.J. Nelson, Starch: Chemistry and Technology, Academic Press, Orlando, 1984, pp. 611.

[17] V. Ivanova, E. Dobreva, Process Biochem., 29 (1994) 607.

[18] H. Guzman-Maldonado, O. Paredes-Lopez, Crit. Rev. Food Sci. Nutr., 35 (1995) 373.

[19] G.I. Kvesitadze, M.S.H. Dvali, Biotechnol. Bioeng., 14 (1982) 1765.

[20] A. Kondo, T. Urabe, K. Higashitani, J. Ferment. Bioeng., 77 (1994) 700.

[21] M.G. Roig, A. Slade, J.F. Kennedy, Biomater. Artif. Cells Immob. Biotechnol., 21 (1993) 487.

[22] T.Radhika, S.Sugunan, J. Mol. Catal. A: Chem., 250(2006)169.

[23] A.Proctor, J. Am. Oil Chem. Soc., 67 (1990) 576.

[24] M.A Hamad, I.A Khattab, Thermochim. Acta, 48 (1981) 343.

[25] N. Grisdanurak, S. Chiarakorn, J. Wittayakun, Microchim. Acta, 159 (2007) 217.

[26] K. Tungkananurak, S. Kerdsiri, D. Jadsadapattarakul,D.T. Burns, Korean J. Chem. Eng., 20 (2003) 950.

[27] P.H.Pandya, R.V.Jasra, B.L Newalker, P.N.Bhatt, Microporous Mesoporous Mater., 77(2005) 67.

[28] Z. Luan, Jay A Fournier, Jan B. Wooten, Donald E. Miser, Microporous Mesoporous Mater., 83 (2005) 150.

[29] A. Vinu, V. Murugesan, M. Hartmann, J. Phys. Chem. B., 108(2004) 7323.

[30] A.S. M. Chong, X.S. Zhao, Angeline T. Kustedjo, S.Z. Qiao, Microporous Mesoporous Mater., 72 (2004) 33.

[31] J. H.Y. Xu, H. M. Q.Zhang, D.G. Evans, X. Duan, J. Colloid Interface Sci., 298 (2006) 780.

[32] S. Shylesh, A.P. Singh, J. Catal., 244 (2006) 52.

[33] D.Park. S. Haam, K.Jang, I.SAhn,W.S Kim, Process Biochem., 41 (2006)770.

[34] M.D,Busto,K.E.G.Tramontin,N.Ortege, M.P.Mateos, Biosour. Techno., 97 (2006) 1477.

Tuning of SBA- 15 for Immobilization of α- amylase

Precise knowledge of structure and dynamics of advanced materials is essential to tailor them for specific functions. The observation that some enzymes retain their functionality upon immobilization on ordered mesoporous supports triggered significant research activity in encapsulating enzymes as well as other bioactive components. More importantly, the characteristics of the tailor able physical (e.g., pore size and volume) and chemical (e.g., hydrophilicity and other functionalities) structures of the nanopores could provide a unique system for the stabilization of proteins against denaturation. The nanoporous matrices may also function like rigid matrix artificial chaperones to provide designable assistance in protein folding processes. The controlled biocompatible nanoporous materials containing catalytic single protein may provide an excellent and unique system for studying and establishing the effect of such a conformational change on the bioactivity of the protein molecule because the conformational change depends on available space around the protein molecule. Size matching between pore and the molecular diameter of enzymes plays a key role in achieving high enzymatic stability. We have characterized the materials and confirmed that the material is compatible for the encapsulation of biocatalyst α-amylase. Further we have also monitored how textural properties of mesoporous silica change with incorporation of enzymes.

4.1 Introduction

Porous materials have attracted the attention of chemists and material scientists due to commercial interest in their application in chemical separations and heterogeneous catalysis as well as scientific interest in the challenges posed by their synthesis, processing and characterization. Application of basic scientific principles to the key technological issues involved has been difficult; however, much more progress has been achieved in tailoring porous materials through manipulation of processing parameters than through understanding of the chemical and physical mechanisms that influence porosity. As a result, the tailoring of porous materials has proceeded largely in an empirical fashion rather than by design. SBA-15 has proved to be very promising for the size selective adsorption of large biomolecules because pore diameters are in the range required for these enzymes and the silica frame work is well suited for the development of bonded, selective sorption phases [1-9]. Variation of experimental conditions used for the SBA-15 synthesis represents an easy and efficient method for controlling the SBA-15 textural properties that can be beneficial for certain applications, for example, a good accessibility of the pores for the reagents can be reached providing a great enhancement in the activity and selectivity of the catalyst.

Generally, tailoring the pore sizes of mesoporous silicas can be achieved either by using surfactants with various chain lengths or by adding swelling agents, such as 1,3,5-trimethylbenzene(TMB) amines and decane, which dissolve in the hydrophobic region of the micelles, thus increasing their size, or hydrothermal treating under different temperatures [10].

Moreover, the pore size of mesoporous materials can be adjusted by post-synthesis silylation [11].

However, the problem dealing with how to control good pore size of SBA-15 materials without loss in ordered structure has not been studied thoroughly. Post Hydrothermal Treatment (PHT) is one of the most efficient methods to improve mesoscopic regularity of products [10]. The mesopore sizes of SBA-15 can be easily tuned from 4 to 11 nm by increasing the hydrothermal temperature from 70 to 130 °C and by prolonging the hydrothermal time from 6 h to 4 days, respectively [12].

Tuning the pore with an ordered structure to suit the hydrodynamic radius of the enzyme was our aim. In the present work we have synthesized SBA-15 with various pore diameters by varying the synthesis temperature from 35 to 40 °C during silica condensation and hydrothermal synthesis at temperatures 100 to 130 °C (PHT) till the pore size suited to the dimension of the α-amylase 35×40×70 (Å) obtained from Bacillus subtilis. An attempt was also made to enlarge the pore size at a lower temperature 100°C by increasing the ageing time from 48-96 h [13]. The post synthesis heat treatment at various temperatures and time of synthesized silica resulted in SBA-15 silica with various pore sizes of well ordered structure.

4.2 Characterization
4.2.1 Small angle X-ray powder diffraction

Mesoporous oxides, such as SBA-15 have much larger pore dimensions which are uniform and adjustable, and generally do not possess three dimensional (3D) crystallinity at atomic level. Since the

materials are not crystalline at the atomic level, no reflections at higher angles were observed. Due to the long range order induced by the regular arrangement of pores, reflexes are observed at very low angle [14]. The XRD pattern of silica sample at room temperature was not well resolved and a single peak at a higher 2θ, 1.13 appeared.

The small angle XRD diffraction patterns of samples autoclaved at different temperatures (100-130 °C) are presented in Fig. 4.1.

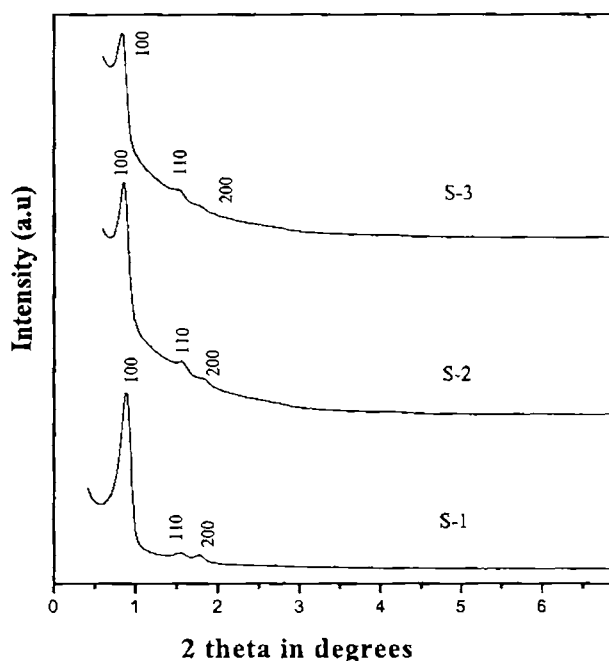**Fig. 4.1.**Low angle XRD patterns of SBA-15 silica after post synthesis heat treatment at various temperatures

The intensity of the d_{100} reflection for the small-angle XRD pattern S-1 (autoclaved at 100 °C) exhibited three well-resolved peaks characteristic of SBA-15 namely, a very intense peak at about 0.89 (2θ) and two distinct weak peaks between 1.53 and 1.78 (2θ). This implied the

relevance of autoclaving at high temperature for an ordered structure. These XRD signals were indexable as (100), (110) and (200) a reflection associated with p6mm hexagonal symmetry which was characteristic of SBA-15 materials [14]. The high-intensity (100) peak had a d-spacing of 100.4 Å and the remaining peaks had d values 57.36 Å (110) and 49.37 Å (200) peak respectively consistent with a 2D hexagonal arrangement of the pores with a unit-cell parameter 'a'=115.9 Å. The diffractions due to 100,110 and 200 planes were clearly evident in all the other samples. When the temperature was increased from 100-130°C the 2θ value shifted to lower values indicating an increase of pore size. It was evident that increasing the aging temperature increased the pore size of the SBA-15 materials and decreased the fraction of microporosity present in the pores [15, 16]. The d spacing shifted to higher values and the unit cell parameter also changed with an increase in temperature. For the SBA-15 samples prepared at varying temperatures the unit cell parameter increased from 11.5 to 12.6 nm. A similar trend was seen when the ageing time of hydrothermal treatment was varied at a constant temperature. The d_{100} values and the unit cell parameters calculated are shown in Table 4.1.

But further increasing the temperature to 140 °C ruptured the ordered nature of the material and the pore structure collapsed. Sample S-2 (ageing temp.120°C) exhibited the correct pore size and the low angle XRD showed that the material possessed ordered pore structure maintaining all the planes. PHT after reaction of an acidic homogeneous mixture of a triblock copolymer and TEOS worked more efficiently for

increasing the pore diameter and volume of SBA-15 than the addition of TMB before reaction [17].

Table 4.1 XRD results of SBA-15 synthesized at different temperatures and time.

Sample	d (100)nm	a(100)nm	2θ
S-1	100.4	115.9	0.89
S-2	105.9	122.3	0.75
S-3	109.8	126.9	0.73
S-4	115.25	133.08	0.76
S-5	117.86	136.10	0.74

The patterns obtained at various ageing time after synthesis at 40°C and hydrothermal treatment at 100 °C (48h-96 h) is given in Fig. 4.2. With the increase of time, the pore diameter was found to increase which was indicated by the shift of 2θ to lower values but the ordered structure was lost when kept for long hours like 96 h. The reduction in intensity of 100 and the disappearance of 110 and 200 planes in low angle XRD at 72 h and 96 h clearly showed the degradation of ordering. This lead to the conclusion that a low quality SBA-15 material was formed when the ageing was continued for long hours. So a better quality SBA-15 material with optimum pore diameter suitable for the enzyme chosen was obtained by the synthesis at 40°C and hydrothermal treatment at 120°C for 48 h.
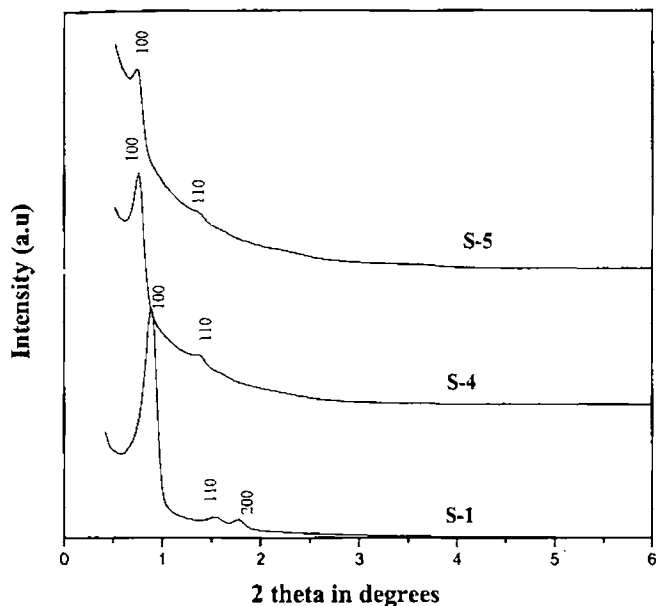
Fig.4.2. Low angle XRD patterns of SBA-15 silica samples after post synthesis treatment at various time intervals

Presence of all the above peaks for immobilized samples confirmed that the hexagonal structure was retained after enzyme incorporation. But with the adsorption of enzyme, the intensity of the low angle (100) and high angle peaks (110 and 200) decreased for all the samples with different pore dimensions as compared to the parent SBA-15 as shown in Fig. 4.3. This indicated that the incorporation of enzyme in the frame work slightly decreases the ordered nature of SBA-15, and the decrease was probably due to the larger contrast in density between the silica walls and the empty pores relative to that between the silica walls and the pores filled with α-amylase molecules [18-23]. The slight change in d spacing after immobilization in the samples S-2 and S-3 was due to the slight disordering in the pore channels or the strain arising due to the confined enzyme molecules as shown in Fig. 4.4 and Fig. 4.5.
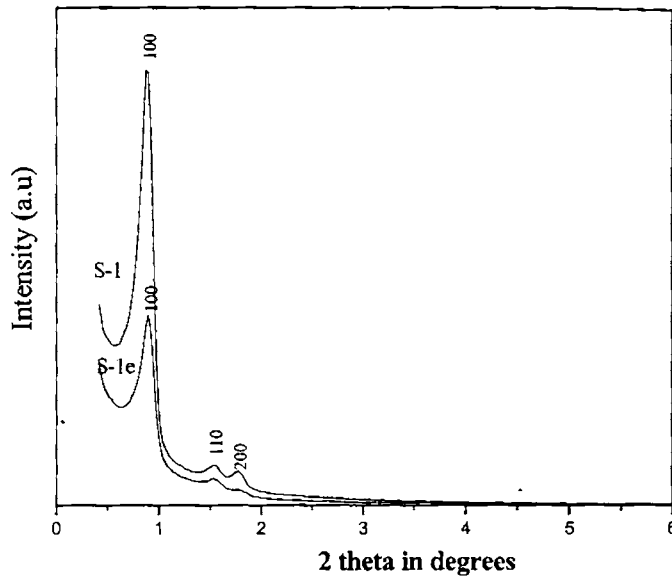
Fig. 4.3. Low angle XRD of silica samples before and after immobilization on S-1
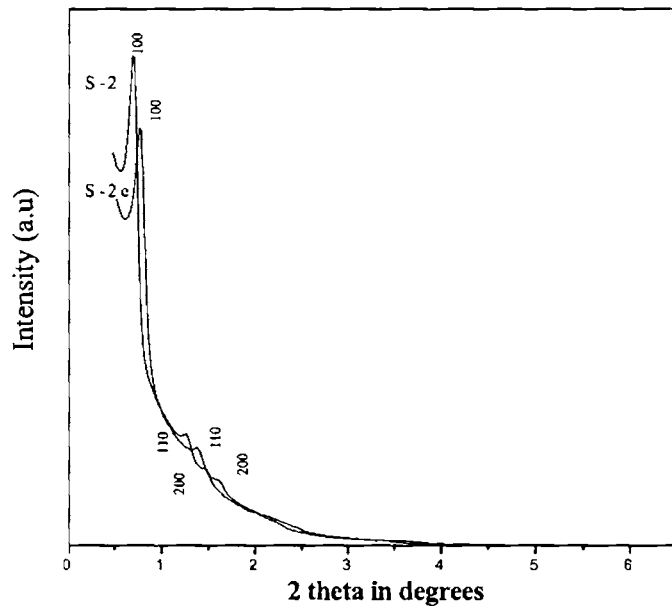

Fig. 4.4 Low angle XRD of silica samples before and after immobilization on S-2

2 theta in degrees
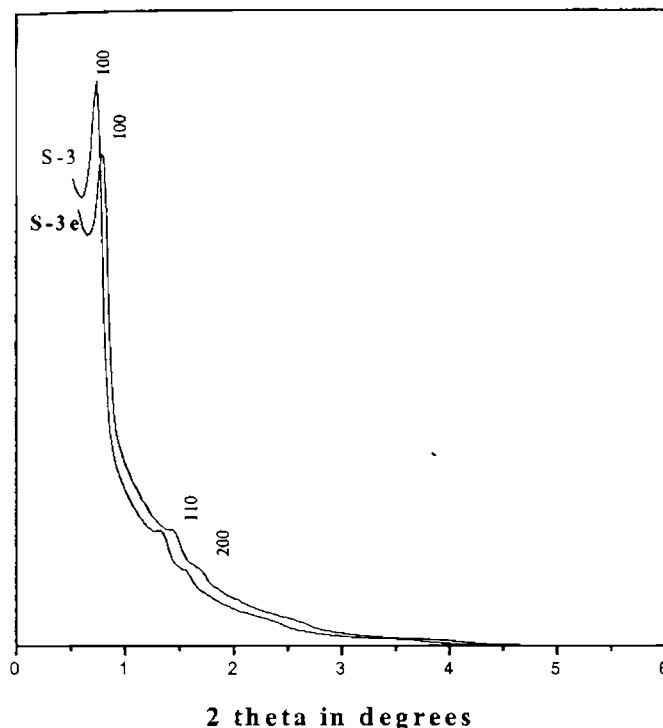
Fig 4.5 Low angle XRD of silica samples before and after immobilization on S-3

4.2.2 Nitrogen physisorption
a. Isotherms

Fig. 4.6 shows the nitrogen adsorption-desorption isotherms for the different SBA-15 silica samples treated hydrothermally at various temperatures. It was observed that all the nitrogen adsorption/desorption isotherms were of Type IV in nature as per IUPAC classification and exhibited H1-type broad hysteresis loop which was characteristic of large-pore mesoporous materials with uniform cylindrical channels. These results could be attributed to capillary condensation taking place within a narrow range of tubular pores. The sharpness of the adsorption and desorption branches (located at a relative pressure from 0.6 to 0.8)

indicated a narrow mesopore size distribution, and was characteristic of good quality of SBA-15.
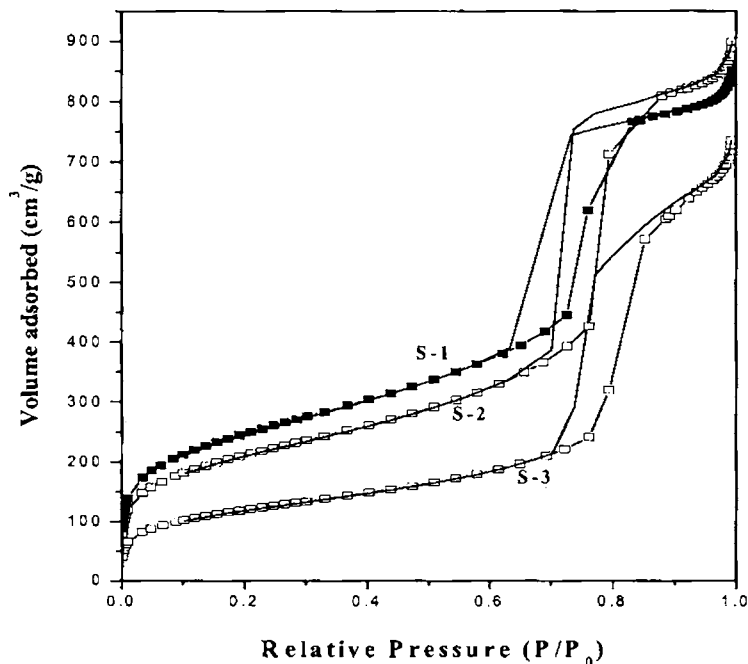
Fig. 4.6 Nitrogen adsorption isotherms of samples synthesized at various temperatures.

The P/P_0 value of the inflection point could be correlated to the mesopore diameter, small pores are filled at low pressures and larger pores at higher pressures. The sharpness and height of the capillary condensation step indicated pore size uniformity and the deviations from sharpness and well-defined pore filling step demonstrated increase in pore size heterogeneity. The sample S-2 exhibited perfectly ordered structure. The shift in P/P_0 values with increase of temperature was due to the increase in pore diameter which was in accordance with the Kelvin equation as mentioned in the earlier chapter. In S-1 the P/P_0 was 0.62 which shifts to 0.69 and 0.71 at higher temperatures.
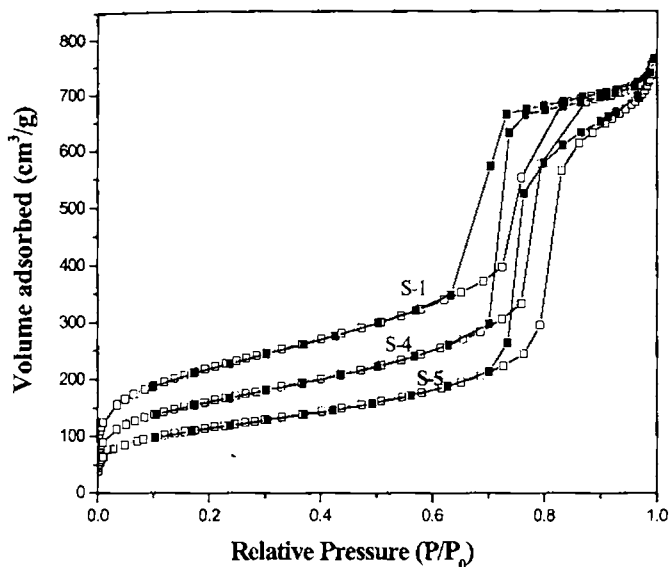
Fig. 4.7 Nitrogen adsorption isotherms of samples at various ageing time

The important textural parameters such as BET surface area, pore volume, wall thickness and average pore diameter are compiled in Table 4.2.

Table 4.2 Textural parameters of SBA-15 at different temperatures and time

Sample	Ageing time (hydrothermal) (h)	Ageing temp (hydrothermal) (°C)	BET surface area (m²/g)	Pore diameter (Å)	Pore Volume (cm³/g)	Wall Thickness (Å)
S room	-	-	424	36	0.31	55
S-1	48	100	856	63	1.35	52
S-2	48	120	734	74	1.41	48
S-3	48	130	515	84	1.14	42
S-4	72	100	666	73	1.39	51
S-5	96	100	402	81	1.18	49

A similar result was obtained when the samples were synthesized hydro thermally at 100°C and aged at different time intervals. The isotherms for SBA.15 samples at different ageing time is shown in Fig.4.7.

Higher temperatures or longer ageing time result in larger pore sizes and thinner silica walls [24-28]. The large pore size and silica wall thickness may be due to the relatively long hydrophilic EO blocks of the copolymer. The block copolymer consists of a hydrophilic block (EO) and a hydrophobic block (PO). The micelle of this triblock copolymer in the acidic solution consists of a core and a shell formed by the hydrophobic and hydrophilic parts of the block copolymer, respectively. The micelle core radius depends upon the temperature of the aqueous solution [28-30]. In acid solution the hydrophilic EO moieties are expected to interact with the protonated silica by the ($S^0H+X-I+$) mechanism and thus be closely associated with the inorganic wall. Increasing the temperature results in increased hydrophobicity of the EO block moiety and therefore decreases, on average the lengths of the EO segments that are associated with the silica wall. This tends to increase the hydrophobic volumes of the surfactant aggregates resulting in the increased pore sizes in SBA-15 materials prepared at higher temperatures [31].

The N_2 adsorption-desorption isotherms of the immobilized enzymes are shown in Fig. 4.8. The very good adsorption property of S-2 was evident from the sharp shift in P/P_0 value in the isotherms. Upon immobilizing the enzyme the sharpness of condensation step was found to deviate considerably indicating the heterogeneity in pore size. The P/P_o values were suddenly lowered indicating pore blockage. The good adsorption property of mesoporous silica when the pore size is adequate was reported by several authors [20]. It was observed that the amount of nitrogen adsorbed was decreasing systematically with increasing enzyme loading and this was of course due to immobilization of the biomolecules inside the pore channels of the SBA-15 support. In the sample S-1e it was evident that due to lower pore

size the enzyme cannot enter the pore channels and hence the p/p$_o$ values were not altered. The reduction in volume of N$_2$ adsorbed was due to external adsorption of enzyme molecules.
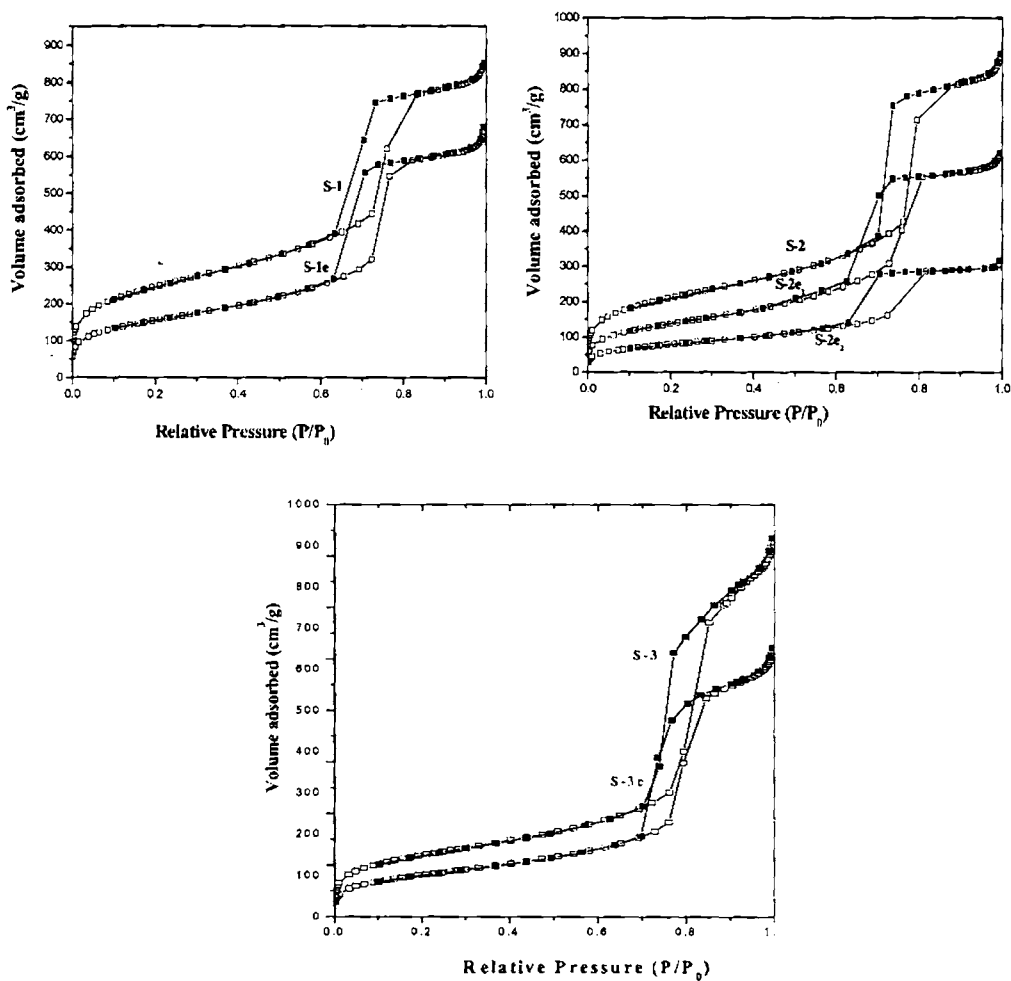

Fig 4.8 Nitrogen adsorption isotherms before and after immobilization on various silica samples of different pore sizes.

In the sample S-3 there was no shift in P/P_0 and it was evident from the adsorption studies that this sample exhibited poor adsorption property because of the lower surface area and coiling of SBA-15 rods being subjected to higher temperature (130°C) during hydrothermal synthesis.

b. Pore size Distribution and Pore Volume

Ordered materials are associated with well-defined pore geometry and narrow pore size distribution (PSD), whereas disordered materials exhibit pores with a wide distribution of different shapes and widths. The simultaneous filling of many mesopores with the same diameter causes a narrow capillary condensation step. Hence a narrow PSD is a characteristic feature of well ordered porous materials [1]. The PSD is based on the BJH method. The thickness of the wall was calculated from the pore size determined from gas adsorption experiments and unit cell parameters determined from XRD.

The effect of ageing temperature and time on the pore size distribution of SBA-15 samples is shown in Fig. 4.9 and 4.10. All the graphs indicated the tight distribution, which was the most important parameter in order to develop SBA-15 with ordered structure. Pore diameter values from pore size distribution were in agreement with the average pore diameter from the desorption branch of adsorption desorption isotherm. A regular increase in pore diameter with increase in temperature was clear from the distribution plots. The narrow, pore size distribution of sample S-2 confirmed the ordered SBA-15 with pore diameter 74 Å which was optimum for the immobilization of α -amylase (35×40×70Å). The pore size distributions at 100 and 130 °C were not as narrow as S-2. The one at 100 °C having a pore size of 63 Å does not allow the complete penetration of amylase molecule and most of the internal surface area remained

unoccupied. The sample at 130 °C allowed the easy penetration of enzyme but a possibility of enzyme leaching cannot be ruled out.

The observed increase of pore diameter corresponds to a well-known property of nonionic surfactants: the increase of micelle size with temperature. A rise of temperature brings about a partial dehydration of the PEO units and decreases the volume of the hydrophilic corona (and so decreases the surface of the hydrophilic part of the micelle). The corresponding decrease of the surface/volume ratio of the micelle is the driving force for an increase of the aggregation number and the volume of each micelle, leading to an increase of pore size.

The rapid uptake of protein by the adsorbents when the pore size is adequate (S-2 and S-3) is an important characteristic for practical application [1].
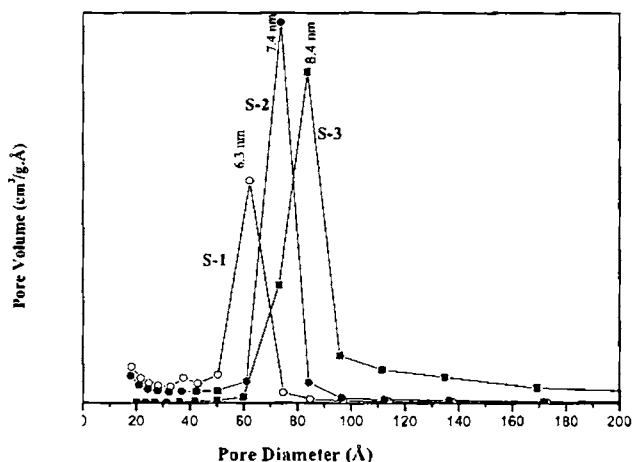

Fig. 4.9 Effect of ageing temperature on the pore size distribution
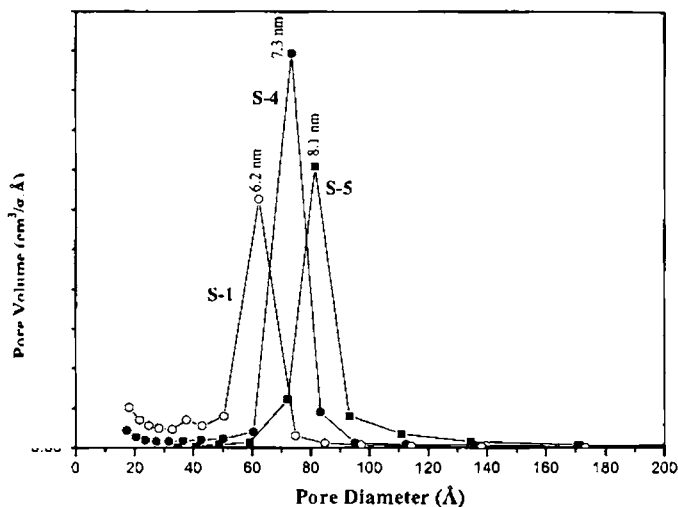
Fig. 4.10 Effect of aging time on the pore size distribution

It is well known that SBA-15 materials have hexagonal arrangement of mesopores interconnected by smaller micropores. The present study was attempted to reduce the micropores via hydrothermal treatment at higher temperatures. The reduction of micropores facilitates the proper orientation of biomolecules inside the well defined mesopores. The pore size distribution of the samples at different temperatures and time indicated a very low concentration of micropores.

The pore size distribution after immobilization is given in Fig. 4.11. The pore size distributions after immobilization are not as narrow before immobilization. This clearly indicates that the ordered structure of the pores is disrupted with large biomolecules. Nevertheless the difference between pore sizes without and with enzyme is hardly significant, and it does not justify the presence of the protein inside the pore channels.
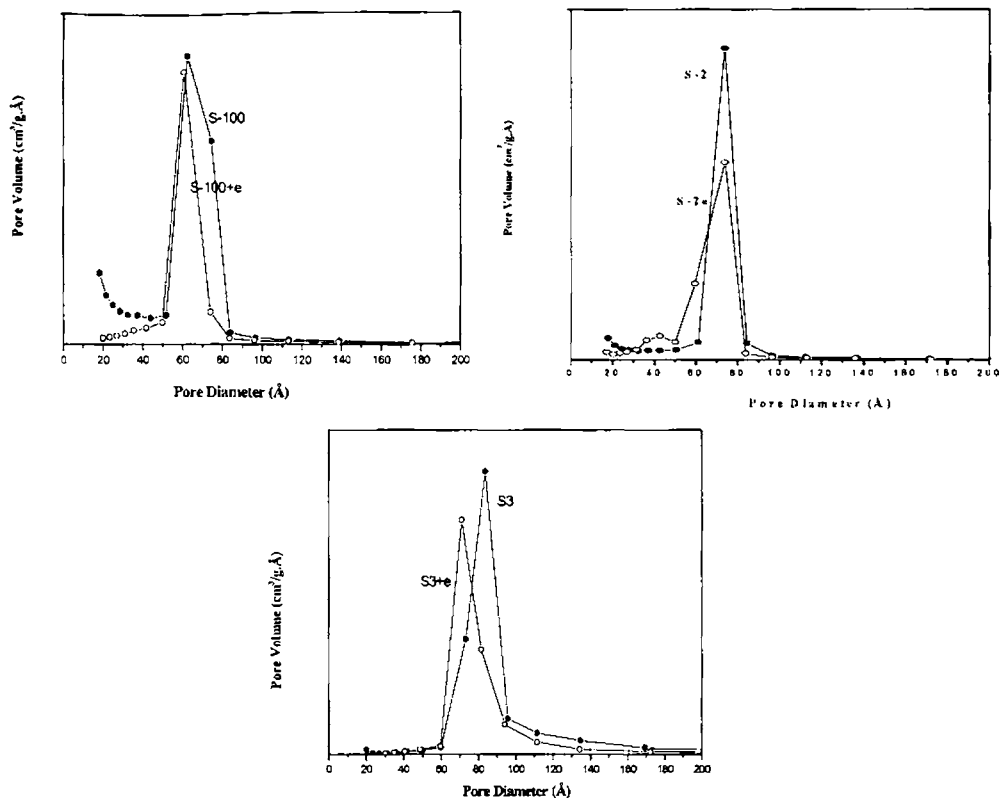
Fig 4.11 Pore size distributions of silica before and after immobilization

All the textural characteristics of enzyme immobilized SBA-15 samples revealed the slight decrease in the ordered nature of the hexagonal structure of SBA-15. Similar observation was made in XRD analysis. The drastic lowering of specific pore volume is tentatively attributed to the tight packing of α-amylase molecules in the pores of these materials. The changes in surface area, pore volume, and pore diameter of free silicas and immobilized forms are summarized in Table .4.3

Table 4.3 The change in the textural properties before and after immobilization.

Sample code	BET surface area m^2/g	Total pore volume cm^3/g	Pore diameter from PSD (Å)
S1	856	1.35	63
S1e equ	544	1.19	60
S2	734	1.41	74
S2e equ	277	0.49	62
S3	515	1.14	84
S3e equ	355	0.98	70

c. BET Surface area

The surface area decreased gradually with increasing temperature and time as shown in Table 4.3. The surface area varied from 856 to 515 (m^2/g) as temperature changed from 100-130 °C. A similar observation was reported by Galarneau et *al.* [32]. For the equilibrium adsorption of enzymes on S-2, there was a large decrease in surface area from 734 to 277 (m^2/g). High intake of enzymes by S-2 (surface area reduces by 62 %) might be due to the fine tuning of pore diameter and other textural properties. It confirmed the adsorption of enzyme molecules on the internal and external surfaces. In S-1 even though the surface area was high the intake was low since the pore diameter was very low the internal surface could not be occupied by the enzyme (surface area reduces by 36 %). In S-3 the reduction in surface area was low (33 %). This was because at higher temperatures even though the pore diameter was optimum, a drop in the number of surface hydroxyl groups, low surface area and the slight coiling of the SBA-15 rods might have reduced the intake of enzyme molecules.

d. *t*-plot Analysis

The *t*-plot analysis consists of plotting the volume of the porous materials, V, as a function of the previously calculated thickness of the monolayer *t* (for the

same p/p$_o$). As long as the multilayer of adsorbate is formed unhindered on the solid surface, V is a straight line passing through the origin. SBA-15 frame work has been classified as an array of mesopore micropore network instead of an array of uniform mesoporous network. The existence of ultramicroporosity which disappears with hydrothermal treatment (T > 80 °C) and of secondary porosity bridges between pores which appears with temperature can be expected to be a general feature for all MPS synthesized using surfactants with oligomeric ethylene oxide chains as the hydrophilic part.
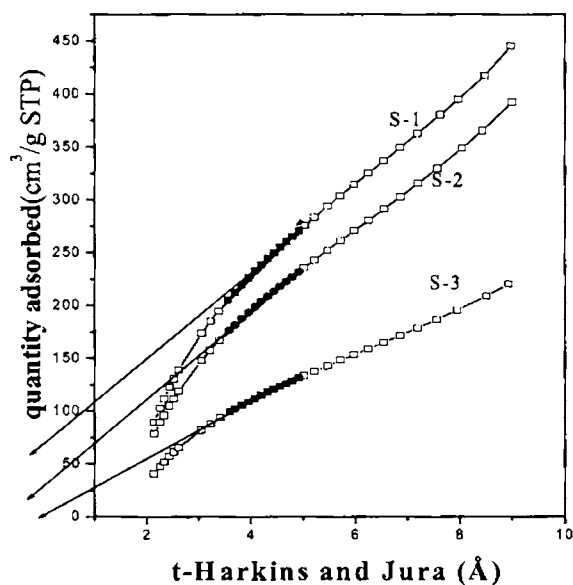
Fig 4.12 *t* plot analysis showing the reduction in microporosity with increase in temperature.

The ratio of micro-/mesoporosity in SBA-15 materials can be easily tuned by changing preparation conditions. An increase in the synthesis temperature and the temperature of the following hydrothermal treatment of the silicate-surfactant mesophase has a negative influence on micropore area and wall thickness. In this case the increase of synthesis temperature to 40 °C

and the hydrothermal treatment at high temperatures at 100, 120 and 130 °C has reduced the microporosity.

The reduction of microporsity in samples at higher temperature was confirmed by the fact that the linear region of the *t*-plot could be extrapolated to a very low intercept as shown in Fig. 4.12.In particular, the pore sizes strongly depend on the synthesis temperature because the hydrogen bonds between inorganic species and surfactants under neutral conditions are sensitive to temperature. The reduction in microporosity was due to the penetration of the hydrophilic PEO blocks in to the silica walls [19].At high-temperature SBA-15 synthesis, the degree of hydration around the EO blocks decreases, in turn causing a redistribution of the EO blocks to the core region of the micelles, leading to materials devoid of micropores. The micropore volumes of the samples are derived from the *y*-axis intercept of the extrapolated linear region in these plots.

e. Ordered meso structure

The calculated WS_p/V_p values for different samples along with micropore volume and micropore area from *t*-plot are compiled in Table 4.4. The factor WS_p/V_p is theoretically expected to be 4 for cylindrical and 4.2 for hexagonal pores [32-36].

Table 4.4 Illustrates reduction in micropore area/ volume with increasing ageing temperature

Sample	Micropore area/m^2g^{-1}	Micropore vol/cm^3/g	(WS_p/V_p)/nm
S-1	113	0.05	3.6
S-2	90	0.04	3.5
S-3	41	0.02	3.6

It is the geometric relation between the specific pore volume and the pore size of an infinite array of cylindrical pores arranged in a hexagonal pattern. S_p and V_p are the surface area and pore volume of mesopores. W is the mesopore diameter. The values are in close agreement with the theoretical values. But the values show deviation from earlier reports (which are 5-10 for SBA-15 type materials).

### 4.2.3 Scanning electron microscopy

Scanning electron microscopy (SEM) allows the visualization of materials at very high magnifications. Depending on the instrument and materials properties, it is capable of providing resolutions down to the nanometer scale and is used to obtain images which reflect the morphology of the sample. The structure and morphology of the siliceous SBA-15 and enzyme loaded-SBA-15 samples were analysed by scanning electron microscopy (Fig. 4.13). The morphology of the SBA-15 was said to be controlled by condensation rate of silica species (pH and silica source), stirring rate, micelle shape, and concentration of inorganic species present [37-39]. In particular, it was evident that the macroscopic mesoporous SBA-15 morphology was crucially dependent on the local curvature energy that was present at the interface of the inorganic silica and amphiphilic block copolymer species. When synthesis time was increased the rods grow into long fibres. Large fibrous structures 20-30 μm in length and 3–5 μm in diameter were observed when the synthesis time was enhanced (S-4 & S-5). The fibrous structure is an agglomerate of long fibers that were constituted from small rod-like sub-particles 1–2 μm in length and 0.5 μm in diameter. Similar SEM images were reported by other authors [1,28].It is also reported that long fibers were obtained using stirring, while the rod like particles of SBA-15 can be obtained in the absence of stirring.
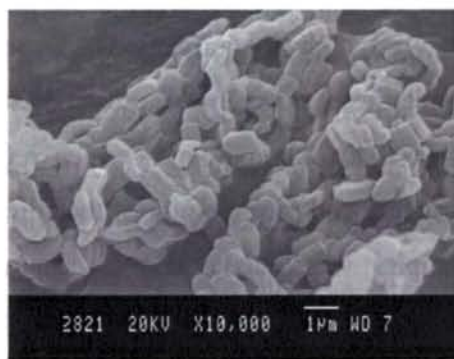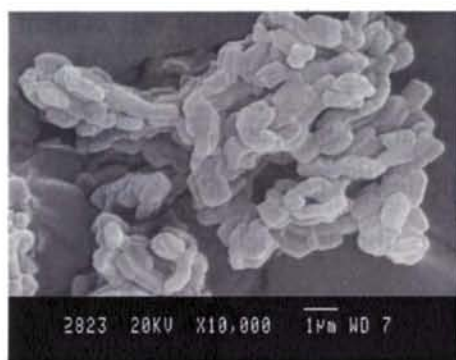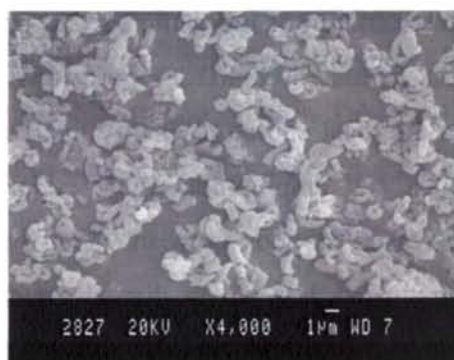
S-1

S-2
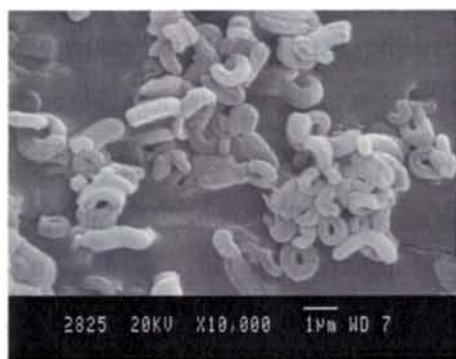
S-3

S-4

S-5

S-2e

Fig.4.13 Scanning electromicrographs of SBA-15 samples

From the SEM images at different temperatures but the ageing time being constant it was evident that the morphology of the samples were alike and the slight differences was due to the variation in the stirring speed during the synthesis. Raising the temperature to 130 °C during the hydrothermal treatment induced a slight coiling of rods (S-3) which might inhibit the smooth entrapment of large biomolecules. Hence the synthesis at 130 °C was less favourable for protein adsorption. After adsorption a similar morphology was observed indicating that the overall structure was maintained even after immobilization.

4.2.4 High resolution Transmission Electron Microscopy

The Fig. 4.14 are the HRTEM micrographs of the SBA-15 samples. The images were recorded along two different crystallographic directions,with the incident electron beam parallel and perpendicular to the direction of main channels of SBA-15, respectively. The TEM images show well-ordered hexagonal arrays of mesopores with one dimensional channel, indicating the 2-D hexagonal mesostructure characteristic of SBA-15 materials [40-42]. All the pore channels were highly uniform, regular and ordered. The pores of the rod-like sub-particles ran parallel to the long axis of the rod. It was clear that the pores of different sub-particles were not, in general, connected. Comparing the pore sizes of the samples S-1, S-2 and S-3 the increase in pore size with temperature was evident. The result was in agreement with the data from pore size distribution. The pore size at 100 °C was 5-6 nm and it increased to 8-8.5 nm with an increase in temperature. The decrease in pore wall thickness was also evident from the images and agreed with the data earlier calculated.
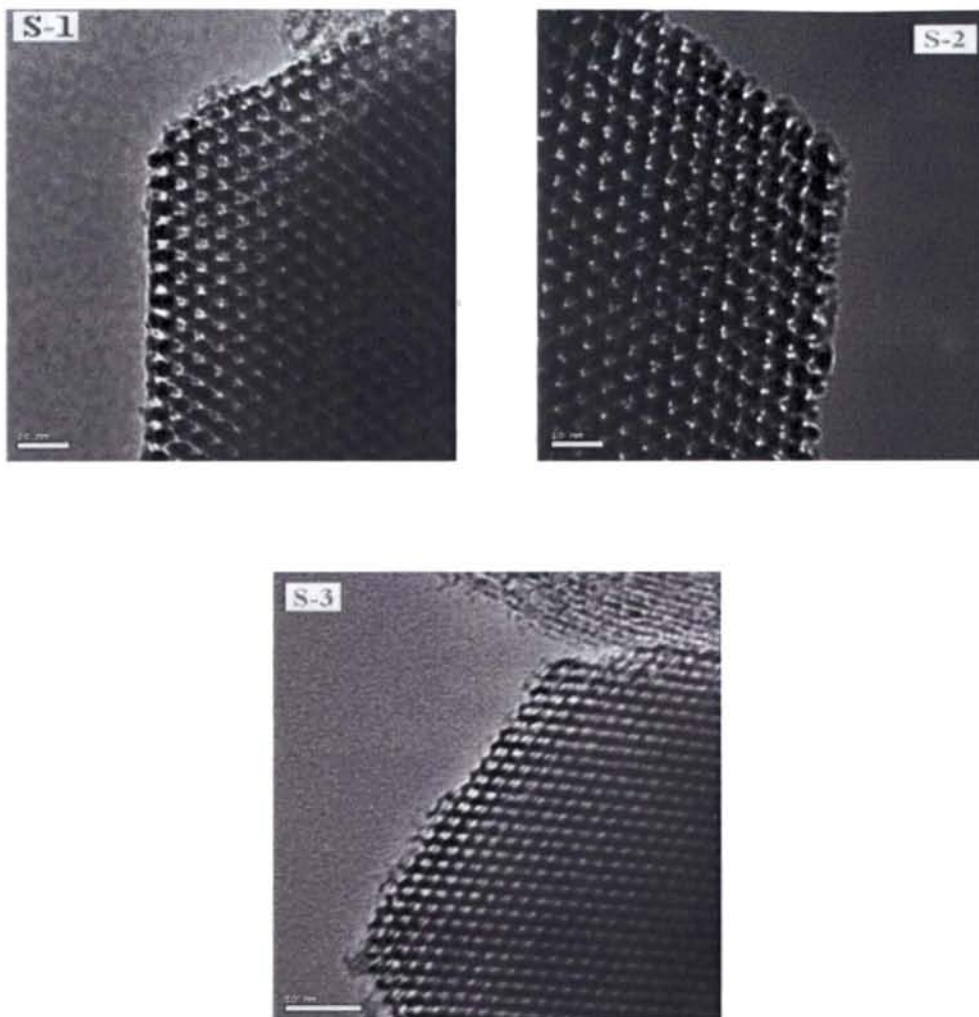
Fig. 4.14 HRTEM of samples of various pore sizes taken along the parallel channels

Fig 4.15 HRTEM of samples of various pore sizes taken vertical to the parallel channels

4.2.5 Thermal analysis

Thermograms of silica samples are given in Fig. 4.16. The major loss at 300-500°C in the uncalcined sample is due to the removal of surfactant P123. In calcined silica there was no major weight loss at higher temperatures, which indicates that the silica is free from surfactants. The weight loss below

120 °C was due to physically adsorbed water or other gases .The weight loss curves of all adsorbed silica samples confirmed the loading of enzymes.
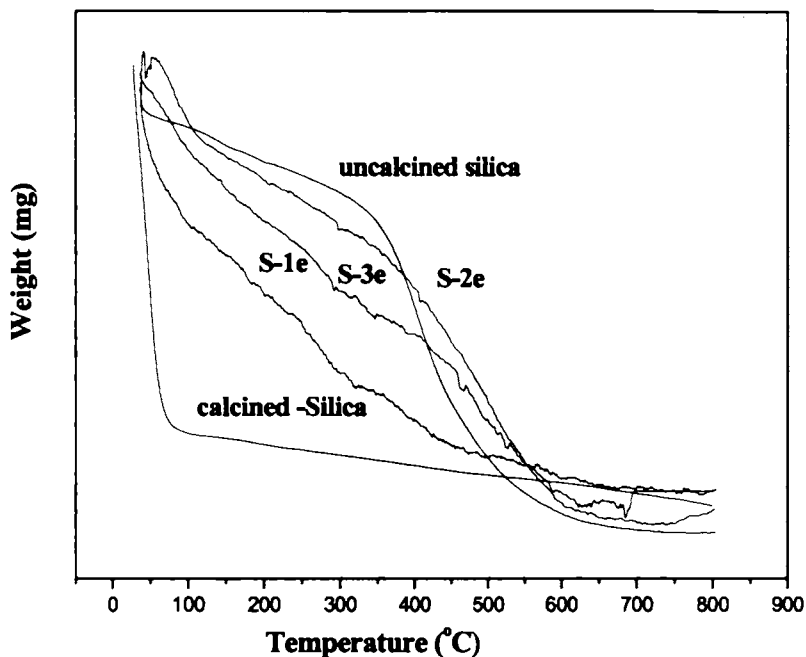
Fig.4.16 TG curves of silica before and after calcination, and enzyme adsorbed samples on various silica.

4.2.6 ^{29}Si MAS spectroscopy

^{29}Si NMR spectra of pure and enzyme adsorbed sample are shown in Fig. 4.17 .The broad peak at 100.95 ppm indicated the presence free silanol groups .After enzyme adsorption the peak slightly broadened indicating the interaction of enzyme molecules with the silanol groups.

S-2

100.95

100.95

S-2e

109.34

50   0   -50   -100   -150   -200   ppm
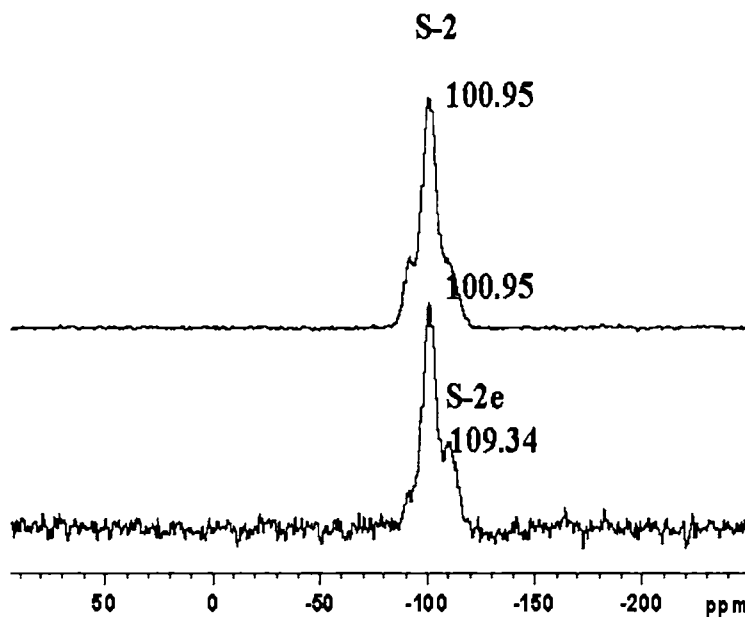
Fig. 4.17 [29] Si NMR spectroscopy of pure and enzyme adsorbed silica
sample.

4.3   Conclusions

Different physico chemical characterization techniques have been effectively employed for the proper understanding of the synthesis of SBA-15 with different pore sizes got by varying the synthesis time and temperature. The material was tuned for the immobilization of enzyme α-amylase.

- Hydrothermal synthesis at various temperatures could tailor the pore size of mesoporous materials with ordered structure.

- Varying the ageing time from 48-96 h under hydrothermal conditions also gave SBA-15 materials with large pore sizes but with less order.

- The SBA-15 silica obtained at 120 °C was optimum to immobilize α- amylase whose hydrodynamic radius is 35×40×70 (Å).

- The XRD results indicated the shift in d spacing after immobilization.

- The Nitrogen adsorption isotherms were Type IV with sharp H1 hysteresis which confirmed the ordered mesoscopic pore structure of synthesized materials.

- The narrow pore size distribution also confirmed the ordered structure of mesoporous materials.

- The t plot analysis confirms that the micro porosity is reduced with the rise in temperature.

- The shift in P/P_0 of adsorption isotherms, large reduction in pore volume and surface area with immobilization on sample S-2 confirmed that the enzyme molecules occupy both internal and external surfaces of mesoporous silica.

- The SEM reflects that a very good control of experimental conditions is required to control the morphology.

- The HRTEM indicates the increase in pore size with the increase of temperature. The 1D channel structure is clearly seen in the TEM pictures.

- Thermograms give evidence of enzyme immobilization.

References

[1]   A.Katiyar, S.Yadav, G .Panagiotis, P.Smirniotis, N.G.Pinto,J. Chromatogr. A, 1122 (2006) 13.

[2]   A. Katiyar, L. Ji, P. Smirniotis, N. Pinto, J. Chromatogr. A,1069 (2005) 119.

[3]   J. Zhao, F. Gao, Y. Fu, W. Jin, P. Yang, D. Zhao, Chem. Commun., (2002) 752.

[4]   A. Vinu, V. Murugesan, M. Hartmann, J. Phys. Chem. B., 108 (2004) 7323.

[5]   H.H.P. Yiu, C.H. Botting, N.P. Botting, P.A. Wright, Phys. Chem. Chem. Phys., 3 (2001) 2983.

[6]   L. Washmon-Kriel, V.L. Jimenez, K.J. Balkus Jr., J. Mol. Catal. B: Enzym., 10 (2000) 453.

[7]   J. Lei, J. Fan, C. Yu, L. Zhang, S. Jiang, B. Tu, D. Zhao, Microporous Mesoporous Mater., 73 (2004) 121.

[8]   J.F. Diaz, K.F. Balkus Jr., J. Mol. Catal. B Enzym., 2 (1996) 115.

[9]   L. Han, J.T. Watson, G.D. Stucky, A. Butler, J. Mol. Catal. B: Enzym., 17 (2002) 1.

[10]   J .Patarin, , B.Lebeau, R. Zana, Curr. Opin. Colloid Interface Sci., 7(2002) 107.

[11]   H. H. P.Yiu, P.A.Wright, J. Mater. Chem., 15(2005) 3690.

[12]   Q. S. Huo, D.I.Margolese,G. D .Stucky, Chem.Mater., 8(1996)1147.

[13]   P.F. Fulvio, S. Pikus , M. Jaroniec, J. Mater. Chem.,15 (2005) 5049.

[14]   D. Zhao, Q. Huo, J. Feng, B.F. Chmelka, G.D. Stucky, J. Am. Chem. Soc., 120 (1998) 6024.

[15]   Y. Wan, Y.Shia ,D.Zhao, Chem. Commun.,(2007) 897.

[16]   A.Galarneau, H. Cambon, F. Di Renzo, R. Ryoo, M. Choi, F. Fajula,. New J.Chem., 27 (2003)73.

[17]   M .Thommesa, R. Ko¨hn, M.Fro¨ba ,Appl. Surf. Sci., 196 (2002) 239.

[18]   A. Vinu, M.Hartmann, In *Proceedings 14th International Zeolite Conference*; Cape Town, (2004) 2987.

[19] A Vinu. V. Murugesan.O.Tangermann, M. Hartmann, Chem. Mater., 16(2004) 3056.

[20] B.Marler, U.Oberhagemann, S Vortmann,H Gies, Microporous Mesoporous Mater., 6(1996)375.

[21] W.Hammond, E. Prouzet, S. D Mahanti, T. J. Pinnavaia, Microporous Mesoporous Mater., 27(1999)19.

[22] A. Vinu,,M. Miyahara, and K.Ariga, J. Phys. Chem. B., 109(2005) 6436.

[23] D. Zhao, J. Feng, Q. Huo, N. Melosh, G.H. Fredrickson, B.F. Chmelka, G.D. Stucky, Science, 279 (1998) 548.

[24] A.Sousa, E.M.B.Sousa , J. Non-Cryst. Solids, 352(2006) 3451.

[25] L.B. Fagundes , T.G.F. Sousa , A. Sousa , V.V. Silva , E.M.B. Sousa, J. Non-Cryst. Solids, 352 (2006) 3496.

[26] A.Galarneau, H.Cambon, F.D. Renzo, F. Fajula, New J.Chem., 27 (2003) 73.

[27] M. Krut, M. Jaroniec, C.H.Ko, R.Ryo, Chem. Mater., 12 (2000)1961.

[28] Katarina Flodstrom, Viveka Alfredsson, Microporous Mesoporous Mater., 59 (2003)167.

[29] K. Mortensen, J.S. Pedersen, Macromolecules, 26 (1993) 805.

[30] K. Mortensen, W. Brown, Macromolecules, 26, (1993) 4128.

[31] G. Wanka, H. Hoffmann, W. Ulbricht, Macromolecules, 27(1994) 4145.

[32] A.Galarneau, H.Cambon, F.D. Renzo, F. Fajula, Langmuir, 17(2001) 8328.

[33] R. Ryoo,C.H. Ko,M. Kruk,V. Antochshuk, M.Jaroniec, J. Phys. Chem. B., 104, (2000)11465.

[34] H.J. Shin, R. Ryoo, M. Kruk, M. Jaroniec, Chem. Commun., (2001) 349.

[35] M. Krut, M. Jaroniec, C.H.Ko, R.Ryoo, Chem. Mater., 12(2000)1961.

[36] S. S Kim, W.Zhang, T. J. Pinnavaia, Science, 282(1998)1302.

[37] H.P. Lin,C.Y Mou, Science, 273(1996)765.

[38] H .Yang,G.Vouk, N.Coombs, I.Sokolov,G. A.Ozin,J. Mater. Chem., 8(1998) 743.

[39] P .Tanev, Y.Liang, T. J Pinnavaia, J. Am. Chem. Soc., 119(1997) 8616.

[40]   A.S.M. Chong, X.S. Zhao, A.T. Kustedjo, S.Z. Qiao, Micropor. Mesopor. Mater., 72 (2004)33.

[41]   Y. Ma, L. Qi, J. Ma, Y. Wu, O. Liu, H. Cheng, Colloids Surf. A., 229 (2003) 1.

[42]   W.H. Zhang, L.Zhang, J. Xiu, Z. Shen, Y. Li, P.Ying, C. Li, Microporous Mesoporous Mater., 89 (2006)179.

Functionalized Nano Porous Materials for Enzyme Immobilization

*O*f special interest are the silica-based organic-inorganic hybrids because they combine the attractive properties of a mechanically and thermally stable inorganic backbone that can be quite easily prepared with a tailor-made structure by means of the versatile sol-gel technique, with a specific chemical reactivity that can be tuned by the choice of appropriate organofunctional groups. The silanol groups react with the organosilane to form a layer of covalently coupled surface functional groups. Surface functionalization is one of the key steps toward the utilization of mesoporous materials in different applications. Surface modification using (3-aminopropyl) triethoxysilane (APTES), producing a terminal amine group (-NH$_2$), has been found to be useful for covalent coupling of protein to the surface of the silica materials. This chapter deals with the characterization of functionalized material and enzyme bound material using FTIR, ^{13}C NMR, ^{29}Si NMR, CHN, Nitrogen adsorption studies, Low angle XRD and TG/DTG. The application of the material as a stable support for the immobilization of α- amylase was studied in detail.

5.1 Introduction

Surface modification using organic functional groups has been found to be useful for the immobilization and encapsulation of enzymes to the surface of the silica materials [1-3]. Due to the lack of strong binding force between enzyme molecules and the supports, one serious problem with the adsorption approach is enzyme leaching, resulting in poor enzyme loading and stability. It was not until extra large pore mesoporous solids, such as SBA-15 (pore size up to 8–10 nm), were prepared that immobilization of more molecules of biological interest really came into range. At the same time, routes to the organic functionalization of mesoporous solids were developed, giving a family of large pore molecular sieves with great chemical versatility with pore sizes suitable for the uptake of many molecules of biological interest, and with well defined and readily characterized structural features, these materials are attractive for a range of applications in biotechnology, including purification environmental applications and enzymatic catalysis for fine chemicals. In particular, applications in the separation of proteins and in immobilizing enzymes are the most widely studied.

For modifying the mesoporous materials through covalent linkage between functional groups and silica framework, two major methods, grafting (post synthesis) and co-condensation (direct incorporation), have been traditionally explored [4-11]. In addition, novel mesoporous materials having functional groups in framework wall, periodic mesoporous organosilicates, have been also paid much attention in recent days. Post-synthetic grafting is a method more commonly used in performing surface modification by covalently linking organosilane species with surface silanol groups using an

appropriate solvent under reflux conditions [12]. Grafting method, which consists of silanol groups react with the organosilane to form a layer of covalently, coupled surface functional groups (Scheme5.1).
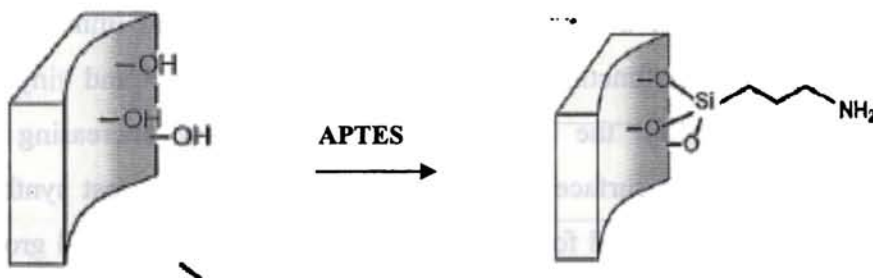
Scheme-5.1showing the functionalization of surface silanols on mesoporous silica

Compared with post synthesis grafting methods, which use a two-step synthesis procedure the direct method allows preparation of nanoporous organic-inorganic hybrid materials in a limited time. However the resultant materials usually show less structural ordering and the organosilane precursor must be chosen carefully to avoid phase separations and Si–C bond cleavages during both synthesis and the surfactant removal process. On the other hand, the post synthesis methods have the following advantages: (i) The structure of the resultant mesoporous materials is ordered after, the grafting reactions; (ii) the functional groups can be chosen according to the requirements; and (iii) the obtained materials show higher hydrothermal stability. Even though the literature displays a wide spectrum of organo-tethered mesoporous materials with active functionalities, thiol (–SH) and amine (–NH$_2$) terminated mesoporous materials receive more attention than the other active pendant groups (–Cl, –OH, (–PPh$_3$)$_3$) for the immobilization of enzymes [13-17]. In efforts to overcome the problems of leaching of enzymes without

the subsequent deactivation it has been found that organic modification of the silica surface can strengthen the binding of the enzyme on the surface via covalent bonding. Lei et al. reported that suitable organically functionalized mesoporous host provided higher affinity for charged protein molecules and more favored microenvironment that resulted in exceptional immobilizing efficiency [18]. Other functional groups such as alkyl, phenyl and vinyl can be added to modify the enzyme's environment by increasing the hydrophobicity of the surface [19-22]. In the present study, post synthesis grafting methods were used for the functionalization of aminopropyl groups, because it is known that the co-condensation of TEOS and 3-APTS groups can cause severe damage to the mesopore structural ordering for a synthesis in an acidic route [21-23]. We have concentrated on the largest pore mesoporous solid, S-3 of pore size 84Å for silanization, because after silanization it should permit easier access of reactant molecules to the active sites of modified silica. The concentrations of APTS were varied so that the mesostructure was intact even after modification. The amine moiety is an important functionality for many applications such as enzyme immobilization on porous solid supports. The distribution and concentration of functional groups are influenced by reactivity of the organosilane and their accessibility to surface silanols, which are limited by diffusion and steric factors.

5.2 Characterisation of functionalized materials
5.2.1 Low angle X-ray Powder Diffraction

It was checked by XRD measurements that the mesoporous architecture remained intact after grafting. For this purpose three different concentrations of APTES solutions were used varying from 2 – 7 mmol.
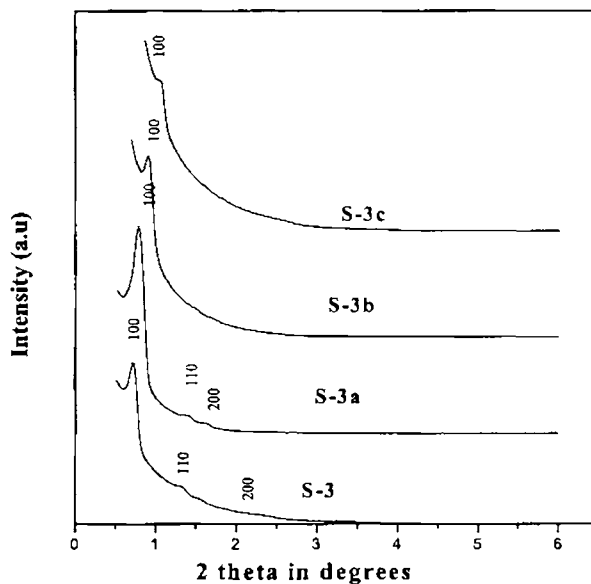
Fig.5.1 XRD patterns indicating the loss of ordered structure with the increase in concentration of APTES. S-3(pure SBA-15 with pore size 84Å) S-3a (2.2mmol of APTES) S-3b (4.4mmol of APTES) S-3c (6.6mmol of APTES)

The optimum concentration at which the ordered structure was maintained was chosen for further studies. The small-angle X-ray diffraction (XRD) patterns of SBA-15 of pore size 84 Å (S-3), NH_2-SBA-15 at various APTES concentrations are given in Fig. 5.1.

The XRD pattern of pristine SBA-15 showed three (*hkl*) reflections of (100), (110) and (200) in the 2θ range of 0.7-2 ° indexed to two-dimensional (2D) hexagonal *p6mm* symmetry, indicating a highly ordered hexagonal structure. However, the decrease in intensity of the d_{100}, d_{110}, d_{200} peaks after post synthesis modifications with increasing concentrations of APTES demonstrated the partial structural collapse of the mesoporous materials or the flexibility induced in the silica framework due to the strain generated

from the functionalized groups [20].With an increasing concentration of APTES the width of the d_{100} peak of all the samples narrowed, possibly related to the decrease in the homogeneous distribution of the pore structure brought about by the attachment of aminopropyl groups inside the mesopore channels. The Table5.1 below shows how the d spacing with respect to d_{100} and unit cell parameter changes with increasing concentration of APTES. The decrease in the crystallinity was more likely due to the inherent disorder introduced by the modification process rather than due to the collapse in the pore structure of the mesoporous silica. The conservation of pore structure is evident from the nitrogen desorption studies.

Table 5.1 d spacing with respect to d_{100} and unit cell parameter changes with increasing concentration of APTES

Sample	d_{100} (nm)	a $_{100}$ (nm)	2θ
S-3	119.8	138.3	0.73
S-3a	110.7	127.9	0.79
S-3b	110.1	127.1	0.80
S-3c	108.1	124.8	0.81

The structure collapse of the ordered phases was due to contrast matching between the inorganic framework and the organic ligands [21].

5.2.2 Nitrogen adsorption studies

Effect of grafting on the physicochemical properties of mesoporous silica samples is summarized in Table 5.2. Both specific surface area and pore volume were found to decrease upon modification. The specific surface area of SBA-15 with pore size 84 Å was 515 m^2/g which reduced to 213m^2/g after surface modification with 6.6mmol concentration of APTES. The

decrease in surface area for the modified mesoporous materials showed the anchoring of 3-APTES inside the mesopore channels with subsequent significant reduction of its textural qualities. The reduction in surface area was 31, 26 and 20 (%) respectively for SBA-15 modified with different concentrations of APTES.

Table 5.2. Textural parameters of functionalized SBA-15 with different concentrations of APTES and enzyme immobilization

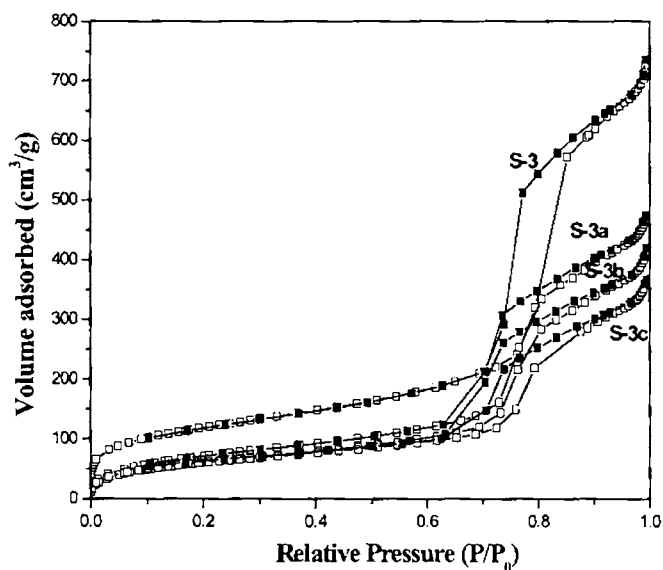| Sample	BET surface area/m^2/g	Total pore volume/cm^3/g	Pore diameter from PSD /Å
S-3	515	1.14	84
S-3a	250	0.73	74
S-3b	218	0.64	72
S-3c	213	0.56	72
S-3ae	175	0.53	74

Fig.5.2 Adsorption isotherms of functionalized samples at various APTES concentration

All the functionalized samples exhibited type 1V isotherms and a distinct hysterisis loop according to the IUPAC nomenclature with an almost parallel adsorption and desorption (classification type H1) Fig. 5.2. The sudden sharp increase of adsorption path, characteristic of ordered porous materials was less with the increase of concentration of APTES. After functionalization with different APTES concentrations, the increase in loading of organic moieties was evident from the volume of nitrogen adsorbed. The sharpness in the N_2 condensation step for 2.2mmol of APTES points to the uniformity of the mesopore structure [2]. However, there is a notable shift of the hysteresis position toward low relative pressures and decreasing trend in overall nitrogen adsorption volume as the loading of aminopropyl groups increases. The P/P_0 values were shifted to lower values indicating the reduction in pore size due to the uniform coating of the functional groups.
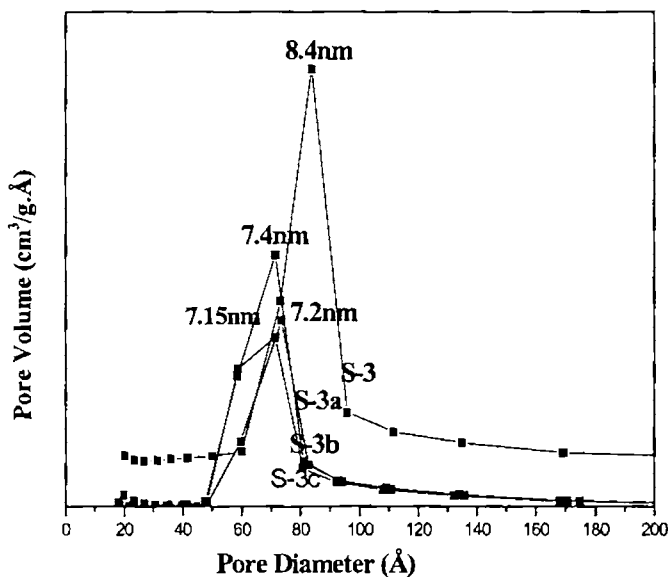
Fig. 5.3 Pore size distribution of pure and functionalied samples

Moreover, the width of the hysteresis loop did not change significantly after aminopropyl functionalization and showing the preservation of pore arrangement after the modification.

The pore sizes were reduced from 8.4 nm to 7.4-7.1 nm for different APTES concentrations as shown in Fig. 5.3. The reduction of pore size with broadening in PSD indicated the uniform functionalization well within the pore. We can find in the literature that the ~ 6 Å long APTES chain has reduced the pore opening by ~10-12 Å[23].Similar results were obtained in our experiments.
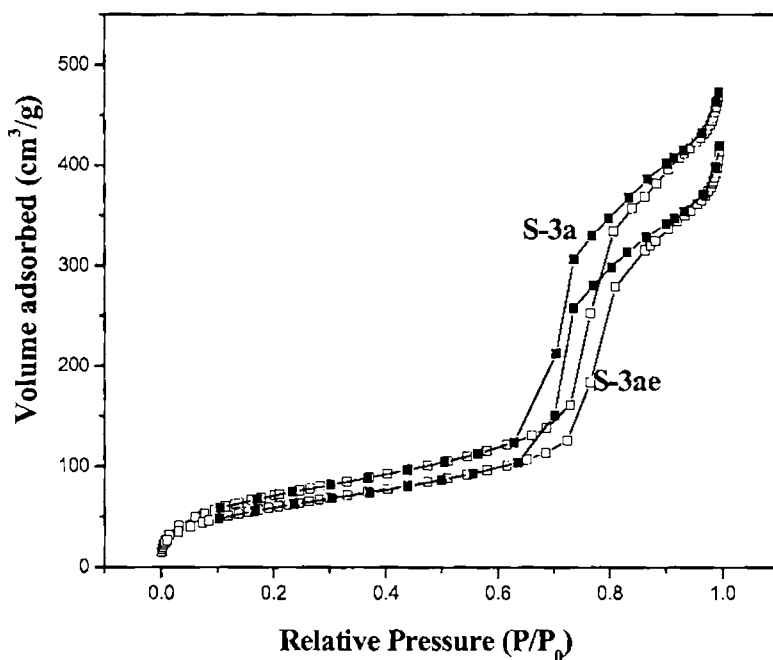
Fig. 5.4 Adsorption isotherms of functionalized sample before and after immobilization.

Fig. 5.4 indicate the nitrogen adsorption isotherm of most ordered functionalized sample (S-3a) before and after adsorption. There was no shift in p/p_o as the enzyme could not be entrapped within the pore but the reduction in the height of adsorption isotherm confirmed the binding of enzyme with the functionalized material.

Fig.5.5 Pore size distribution before and after immobilization

However, the reduction in surface area was rather less pronounced after immobilization of enzymes. The pore volume of the modified SBA-15 after immobilization was reduced from 0.73 to 0.53 which corresponded to 27 % pore occupation. This quantity was very low when compared to simple adsorption as discussed earlier. This might be due the steric hindrance offered

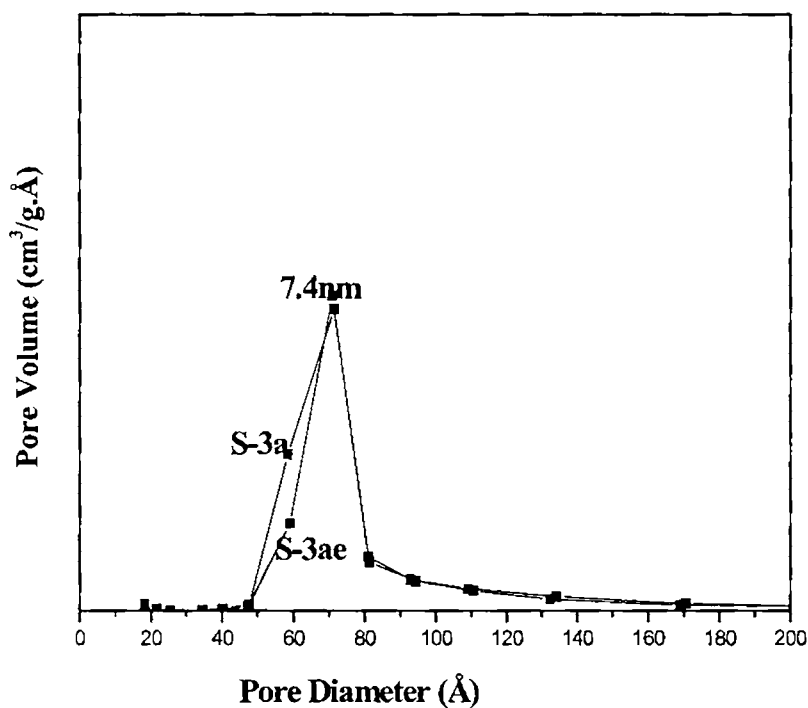by the propyl groups well within the pore. After enzyme immobilization the pore size distribution does not change much. (Fig.5.5)
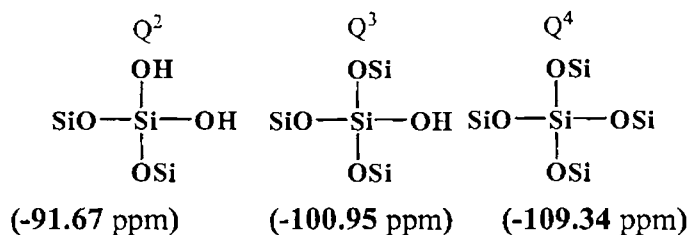
Comparing the XRD results with nitrogen adsorption studies, the XRD results reveal that the ordered structure is maintained only at the APTES concentration of 2.2 mmol and further increasing to higher concentration (6.6mmol) the peaks at higher 2θ values completely disappeared But from the adsorption studies it was evident that the pore structure is not completely destructed with functionalization but the broadening of PSD's indicated decrease in degree of order. This indicated that the incorporated aminopropyl groups are located inside the mesoporous channels, and hence reduce the pore dimension of the parent SBA-15 silica material [22-24].

As the ordered structure was important for the entrapment for biomolecules we have chosen 2.2 mmol of APTS /g of mesoporous silica, as the optimum concentration for the functionalization of silica. We did not mean to fill the pore with functional groups, instead to make a favorable environment in each pore that attracts the enzyme molecule to move into the unoccupied pore. This new environment stabilizes and increases the chemical reactivity of the enzyme.

5.2.3 [29] Si MAS spectroscopy

Fig. 5.6 shows the typical ^{29}Si CP/MAS NMR spectra for the siliceous SBA-15 samples with and without surface attachments of APTES groups, also with the chemical shift assignments for the observable resonance.

The broad resonance peaks of calcined samples from -90 to -110 ppm are typical for a range of Si–O–Si bond angles and the formation of more tetrahedral silicon environments. Three resonances at -109.34, -100.95 and -91.67 ppm which were assigned to the Si sites of Q^4, Q^3, and Q^2, respectively, could be observed on the template-extracted calcined SBA-15 (Scheme5.2). The intense Q^3 sites were associated with the isolated Si-OH groups (i.e., free and hydrogen-bonded) and the Q^2 sites corresponded to the geminal silanols. There were abundant silanol groups on the internal surface of the parent SBA-15 silica which essentially lined the tubular channels and served as sites for incorporation of the aminopropyl groups. The Q^4 structural units represented interlinked SiO_4 tetrahedrons in the interior of the mesopore walls, while Q^3 and Q^2 structural units are present on the wall surface associated with silanol group [24-29].

$$
\begin{array}{ccc}
Q^2 & Q^3 & Q^4 \\
\overset{\displaystyle OH}{\underset{\displaystyle OSi}{SiO-Si-OH}} & \overset{\displaystyle OSi}{\underset{\displaystyle OSi}{SiO-Si-OH}} & \overset{\displaystyle OSi}{\underset{\displaystyle OSi}{SiO-Si-OSi}} \\
\text{(-91.67 ppm)} & \text{(-100.95 ppm)} & \text{(-109.34 ppm)}
\end{array}
$$

Scheme 5.2 The structural units in silica corresponding to Q^2, Q3, Q4.

In contrast to the parent SBA-15 silica, the ^{29}Si CP MAS NMR spectra of modified SBA-15 materials showed a broad line centered at -110.6 ppm due to Q^4 structural units, and the lines at -92 due to Q^3 were not seen. While Q^2 structural units had considerably reduced in intensity and quite broadened (Fig. 5.6), demonstrating that the silylating agents effectively consumed the geminal as well as the free silanol sites.
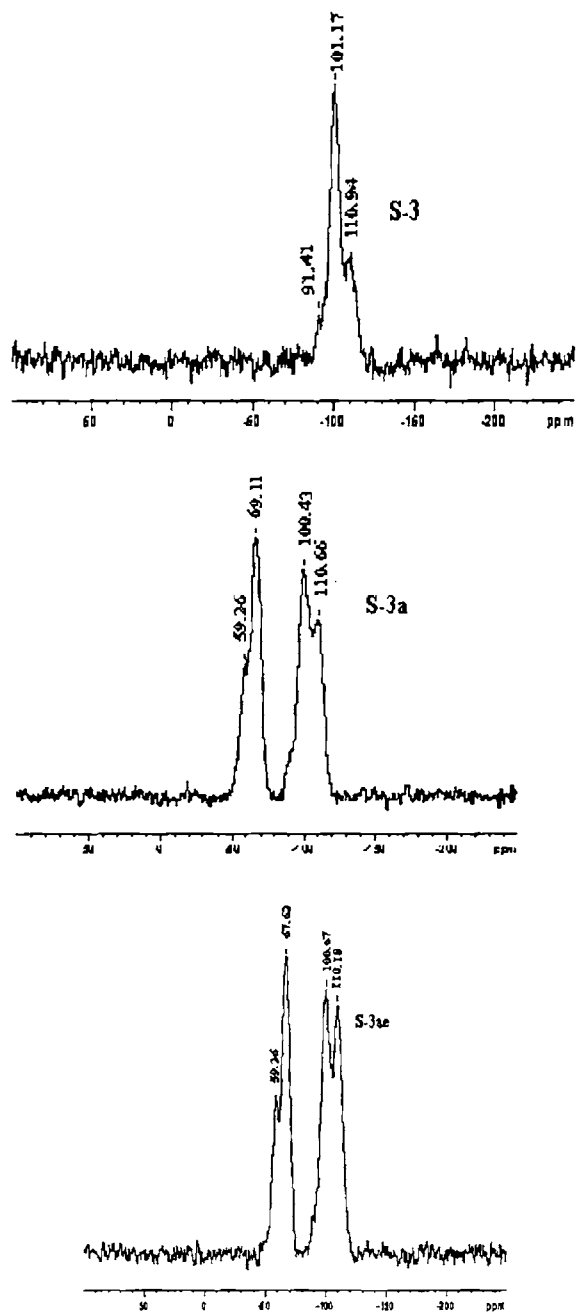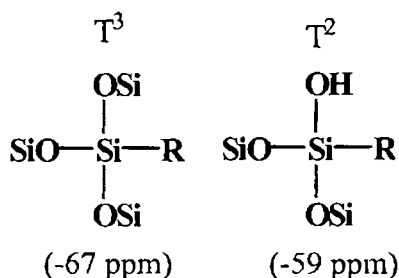
Fig. 5.6 CP MAS ^{29}Si NMR spectrum of pure, functionalized,enzyme bound sample

In addition, another two resonances at -59.2 and -67.1 ppm were observed upon incorporation of aminopropyl groups, and are greatly enhanced in intensity by ^{1}H cross-polarization. No line appeared at -45 ppm corresponding to the chemical shift of Si in liquid (3-aminopropyl)trialkoxysilane, indicating the absence of free silane molecules physically adsorbed on the SBA-15 silica surface. The additional peaks were assigned to the T^3 and T^2 sites, respectively [29].

$$T^3 \qquad\qquad T^2$$

$$
\begin{array}{cc}
\text{OSi} & \text{OH} \\
| & | \\
\text{SiO---Si---R} & \text{SiO---Si---R} \\
| & | \\
\text{OSi} & \text{OSi} \\
(\text{-67 ppm}) & (\text{-59 ppm})
\end{array}
$$

Scheme 5.3 The structural units in silica corresponding to T^3, T^2 The line at - 67 ppm is associated with aminopropylsilane Si attached via three siloxane bonds, (–O–)$_3$ Si CH$_2$CH$_2$CH$_2$NH$_2$ (T^3) while the line at -57 ppm is via two siloxane bonds, (–O–)$_2$ Si- CH$_2$CH$_2$CH$_2$NH$_2$ (T^2)

The observation of the lines at -59 and -67 ppm indicated formation of new siloxane linkages (Si–O–Si) of aminopropylsilane silicon to the surface silicon atoms of the SBA-15 silica (Scheme5.3). The relative high intensity of the line at -67 ppm indicates that the incorporated aminopropyl groups were closely packed on the internal surface of the SBA-15 materials [30]. The results suggested that the surface silanol groups, which were associated with Q^3 and Q^2 structural units of the parent SBA-15 silica, were consumed and attached with aminopropylsilane.

5.2.4 ^{13}C spectroscopy
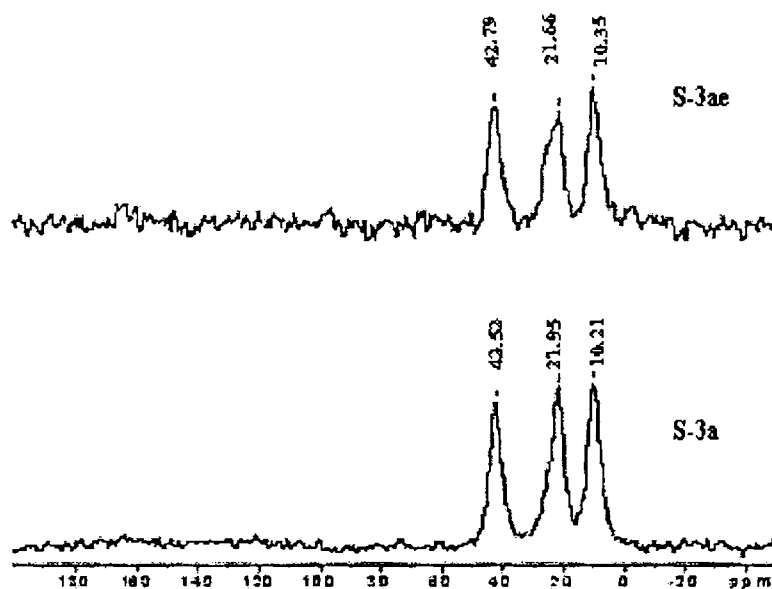
Fig.5.7 ^{13}C NMR spectra of APTES-anchored mesoporous materials before and after immobilization.

The ^{13}C NMR spectra of APTES-anchored mesoporous materials (Fig. 5.7) exhibited sharp, distinct resonance peaks at 10.34 and 21.2 ppm for the carbon atom (C1) adjacent to the amine moiety and to the central (C2) carbon atom, whereas the carbon atom (C3) bonded to the silicon shows a band at 42.8 ppm [29]. The three different carbon chemical environments of the sample were evident from the three distinct peaks. After immobilization the ^{13}C NMR exhibited a slight chemical shift only but the peaks were broadened which might be due the anchoring of protein molecules with the NH$_2$ moeities of silane.

5.2.5 FTIR Spectra

FTIR spectroscopy has been extensively used to study the surface properties of silica samples; in particular, the stretching vibrations of surface silanols (vOH) are very informative. The results are in Fig. 5.8.

The absence of strong absorption in the range of 2700–3000 cm^{-1} for the calcined SBA-15 sample clearly indicated the removal of surfactants. There was an abundance of silanol groups present in the parent SBA-15 silica that essentially lined the interior surface of the mesoporous channels. The vOH stretching vibrations observed in the 3600-3200 cm^{-1} region were attributed to the hydrogen-bonded silanol groups, and the sharp bands at 3740 cm^{-1} were attributed to the symmetrical stretching vibration mode of O–H from isolated terminal silanol. Stretching vibrations of geminal silanols are also observed in the same region of isolated silanols; hence distinguishing these in the IR spectral patterns was very difficult. The IR spectrum of SBA-15 samples was dominated by the asymmetric Si-O-Si stretching vibration at 1085 cm^{-1}. The band at 1640 cm^{-1} was assigned to O-H bending vibration of adsorbed water molecules. The symmetric Si-O-Si stretching vibration occured at 809 cm^{-1} whereas Si-O-Si bending mode was centered at 462 cm^{-1}. The band at 970 cm^{-1} corresponded to Si-OH vibration generated by the presence of defect sites, which was characrteristic of mesoporous silica [31, 32].
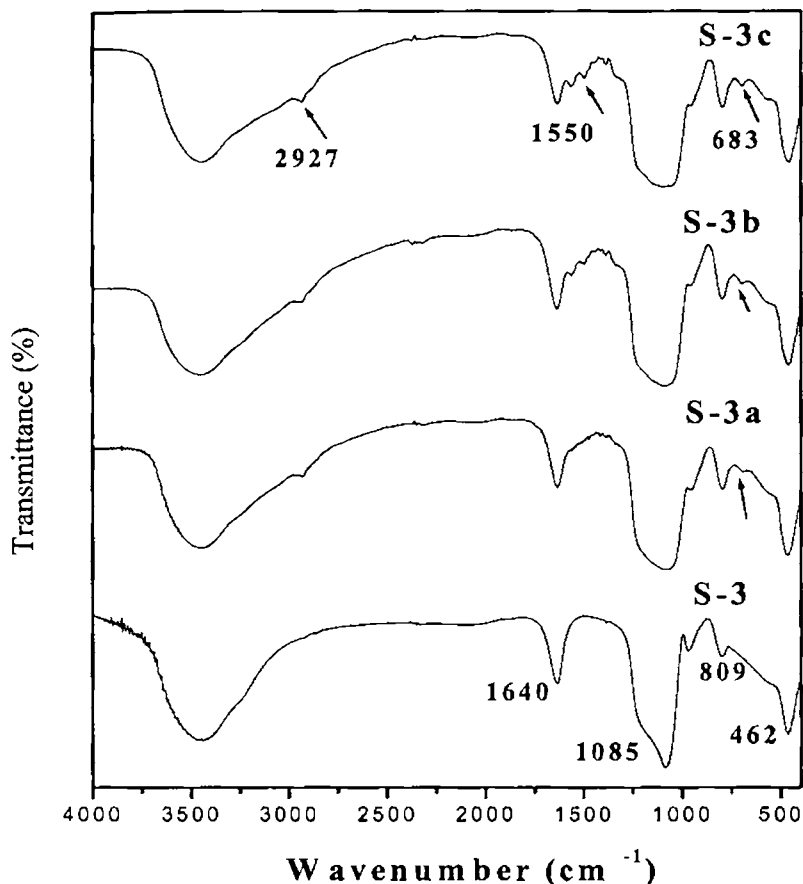
Fig. 5.8 FTIR spectra of pure and functionalized (at different APTES concentrations) samples

Generally, the free and geminal silanol sites are the active silanol sites participating in the condensation reactions with the silylating agents, whereas the hydrogen-bonded silanol groups do not actively participate due to the efficient hydrophilic networks formed among them (Scheme 5.4). However, the present results imply that the hydrogen-bonded silanol groups are also vulnerable in the reaction with aminopropyl groups.
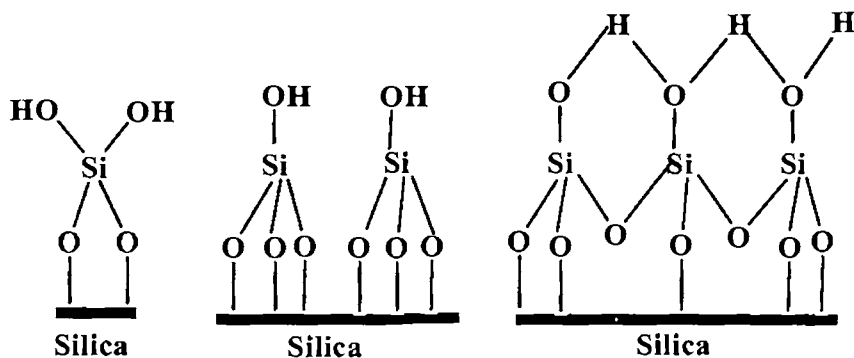
Geminal silanols   free silanols   Vicinal silanols hydrogen bonded

Scheme 5.4. Schematic representation of the silanol groups in silica surfaces.

In the present analysis, after APTES functionalization, complete disappearance of the isolated peak at 3740 cm^{-1} and the reduction of peak intensity at 3600-3200 cm^{-1},(Fig. 5.9) demonstrated the role of surface silanols in modifications.The width of this broad peak at 3500 cm^{-1} for APTES-functionalized sample slightly increased.This widening of the peak was due to the symmetric stretching of N-H. The N-H stretching was reported around 3346 cm^{-1} for free amine and around 3305 cm^{-1} for terminal amine groups, respectively, which were cross-linked with the silanol group. At 673 cm^{-1}, a weak peak was seen which was due to the wagging and twisting of N-H bonds, The structure of functionalized silica sample is shown in Scheme 5.5.
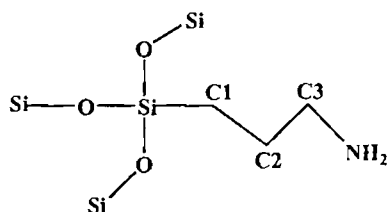
Scheme 5.5 Structure of functionalized silica sample.
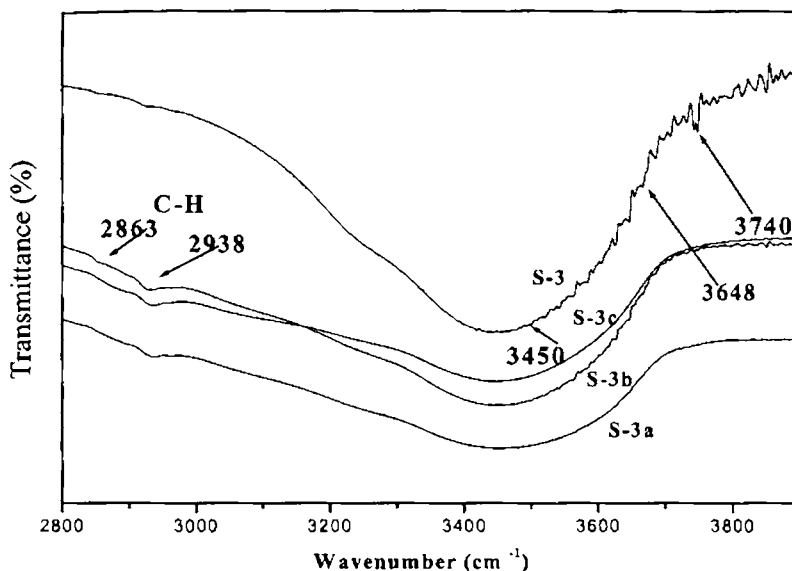
Fig. 5.9 FTIR spectra confirming the participation of silanol group for functionalization

The C-N stretching vibration is normally observed in the wavenumber range 1000-1200 cm^{-1}. However, this peak was not resolved due to the overlay with the IR absorptions of Si-O-Si in the range 1130-1000 cm^{-1}. Nevertheless, the peak in this region for the APTES-modified SBA-15 sample is broader indicating possible overlap of peaks. The presence of aminopropyl groups is confirmed by the appearance of C–H asymmetric stretching, C-H symmetric stretching at 2927 and 2857 cm^{-1} respectively [30], which increase in intensity with increasing loading of aminopropyl groups.
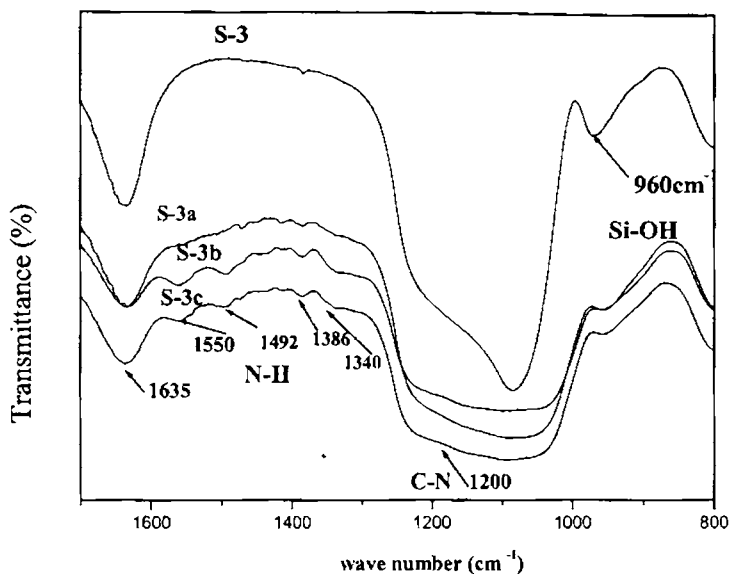
Fig. 5.10 FTIR spectra confirming the attachment of functional group to silica

Bands at 1635, 1550, 1492, 1386, and 1340cm^{-1} were observed in the spectrum after grafting, which are attributed to NH_2 scissor, N-H bending, CH_2 scissoring, CH_2 wagging, CH_2 twisting respectively (Fig. 5.10)[33-34]. These results confirmed the attachment of amino propyl groups on the solid supports. The spectra of enzyme loaded sample did not indicate any difference because of the poor loading, hence not shown.

5.2.6 CHN Analysis

Table 5.4 lists the chemical compositions of the APTES functionalized samples analyzed by using CHN element analysis. It was seen that reasonable amounts of both carbon and nitrogen were present in the samples. The increment of C and N was proportional to the amount of APTES added during synthesis. This data along with FTIR confirmed the loading of APTES with increase in concentration

Table 5.4 % of C,H,N after functionalization with APTES

Sample	Composition (%)		
	C	**H**	**N**
S-3a	6.32	2.66	1.88
S-3b	7.00	3.68	2.18
S-3c	7.99	4.07	2.42

5.2.7 Thermogravimetric analysis

The thermal stability of the incorporated functional groups was studied by using TGA (Fig. 5.11).The weight loss was below 120 $^{\circ}$C was due to physically adsorbed water or other gases. This peak was much lower in intensity compared to pure SBA-15 suggesting that amount of physisorbed water molecules was quite diminished after functionalization. The parent SBA-15 silica showed a constant but slight weight loss with increasing temperature which is apparently due to surface dehydration and/or dehydroxylation. There was no major weight loss at higher temperatures; this indicated the complete removal of surfactant. In contrast, modified SBA-15 materials with aminopropyl groups showed a small weight loss at about 300°C and a major weight loss at about 550 $^{\circ}$C. The first weight loss could be attributed to surface dehydration or structural rearrangement of the incorporated aminopropyl groups. The latter weight loss was due to decomposition and total loss of the aminopropyl groups from the materials, based on the fact that there was almost no significant weight loss in the parent SBA-15 silica over this same temperature range. However, such a decomposition temperature for incorporated aminopropyl groups was 300°C

higher than the boiling point of the liquid (3- aminopropyl)triethoxysilane, further confirming that the aminopropyl groups are chemically bonded to the internal surface of the SBA-15 materials and are relatively thermally stable [19].The TG curve for immobilized α-amylase demonstrates weight loss in several regions which was attributed to the enzyme decomposition.
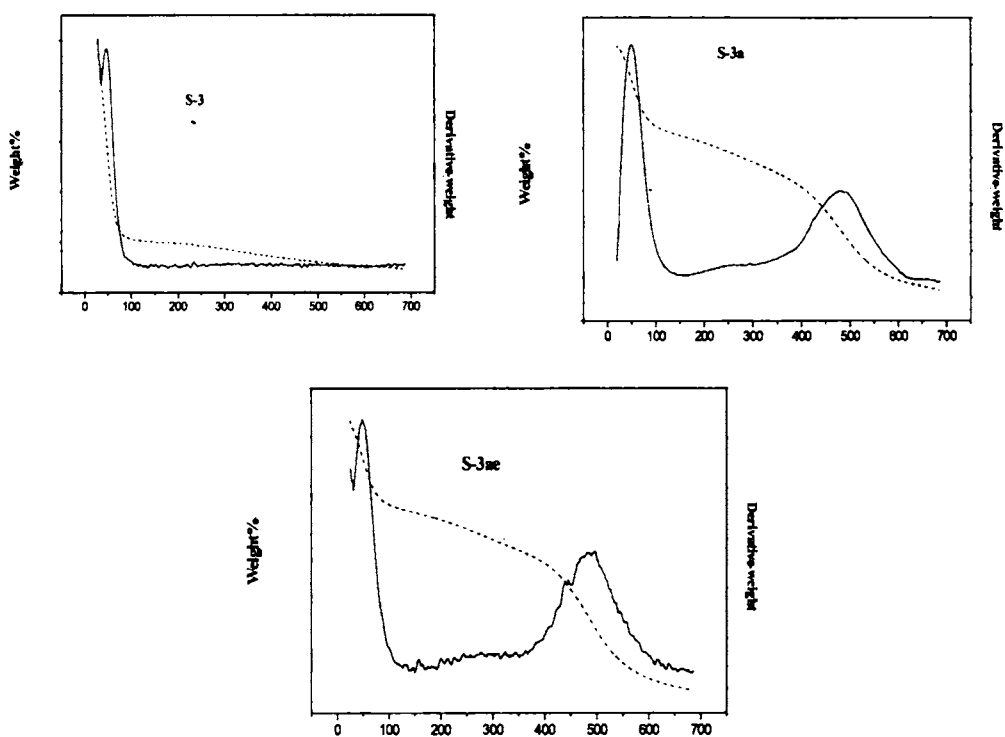

Fig. 5.11 TGA profiles of pure, functionalized and enzyme bound samples

5.3 Conclusions

The important conclusions deduced from these studies are

- Aminopropyl functional groups were successfully incorporated into the channels of the mesoporous SBA-15 silica molecular sieve

- The modified materials still possessed well-defined mesoporous structure with decreased pore dimensions ~10Å, due to the presence of surface aminopropyl groups. The low angle XRD remained intact for a very low concentration of APTES i.e 2.2 mmol per gram of mesoporous silica

- The free and germinal silanol groups over SBA-15 surfaces were responsible for such amine binding. This was evident from the FTIR and ^{29}Si NMR studies

- CHN analysis confirmed that the content of C and N was proportional to the amount of APTES added during synthesis

- Nitrogen adsorption isotherms confirm that the enzyme molecules were entrapped on the external surface of the pore. This might be due to the steric hindrance offered by amino propyl groups within the pore.

- Thermal stability of synthesized samples was evident from the thermograms

References

[1]   R.F. Talyor (Ed.), Protein Immobilization: Fundamentals and Applications, Marcel Dekker, New York, 1991.

[2]   A. Subramanian, S.J. Kennel, P.I. Oden, Enzyme Microb. Technol., 24 (1999) 26.

[3]   X.S. Zhao, G.Q. Lu, J. Phys. Chem. B., 102 (1998) 1556.

[4]   W. Tisher, F. Wedekind, Topics in Current Chemistry-Immobilized Enzymes: Method and Application, vol. 200, Springer-Verlag, Berlin, 1999.

[5]   F. De Juan, E. Ruiz-Hitzky, Adv. Mater., 12 (2000) 430.

[6]   R. Anwander, I. Nagl, M. Widenmeyer, G. Engelhardt, O Groeger, C. Palm, T. Röser, J. Phys. Chem. B., 104 (2000) 3532.

[7]   K. Moller, T. Bein, Stud. Surf. Sci. Catal., 117 (1998) 53.

[8]   D. Brunel, A. Caubel, F. Fajula, F. DiRenzo, in: L. Bonneviot, S. Kaliaguine (Eds.), Zeolites: A Refined Tool for Designing Catalytic Sites, Elsevier, Amsterdam, 1995 p. 173.

[9]   H. H. P. Yiua and P. A. Wright   J. Mater. Chem., 2005, 15, 3690

[10]   C. Yoshina-Ishii, T. Asefa, N. Coombs, M.J. MacLachlan, G.A. Ozin, J. Chem. Soc. Chem. Commun., (1999) 2539.

[11]   D.S. Shephard, W. Zhou, T. Maschmeyer, J.M. Matters, C.L. Roper, S. Parsons, B.F.G. Johnson, M.J. Ducr, Angew. Chem., Int. Ed., 37 (1998) 2179.

[12]   X.S. Zhao, G.Q. Lu, J. Phys. Chem. B., 102 (1998) 1556.

[13]   X.S. Zhao, G.Q. Lu, A.J. Whittaker, G.J. Miller, H.Y. Zhu, J. Phys. Chem. B., 101 (1997) 6525.

[14]   J.Y. Wing, C.P. Mehnert, M.S. Wong, Angew. Chem. Int. Ed., 38 (1999) 56.

[15]   A. Stein, B.J. Melde, R.C. Schroden, Adv. Mater., 12 (2000) 1403.

[16]   D. Brunel, Microporous Mesoporous Mater., 27 (1999) 329.

[17]   A.Vinu, K.Z.Hossain, K.Ariga, J. Nano. Sci. Technol., 5(2005)347.

[18]   C.Lei, Y.Shin,J, Liu, E. J. Ackerman, J.Am. Soc.,124(2002) 11242.

[19]   Z. Luan, Jay A Fournier, Jan B. Wooten, Donald E. Miser, Microporous Mesoporous Mater., 83 (2005) 150.

[20]   H.H. P. Yiu, P.A. Wright, N. P. Botting, J. Mol. Catal. B: Enzym., 15(2001) 81.

[21]   A.M. Liu, K. Hidajat, S. Kawi, D.Y. Zhao, J. Chem. Soc.Chem. Commun., (2000) 1145.

[22]   P.M. Price, J.H. Clark, D.J. Macquarrie, J. Chem. Soc., Dalton Trans., (2000) 101.

[23]   H. Yoshitake, T. Yokoi, T. Tatsumi,Chem. Mater., 14 (2002) 4603.

[24]   A.S. M. Chong, X.S. Zhao, Angeline T. Kustedjo, S.Z. Qiao, Microporous Mesoporous Mater., 72 (2004) 33

[25]   J. H.Y. Xu, H. M. Q.Zhang, D.G. Evans, X. Duan, J. Colloid Interface Sci., 298 (2006) 780.

[26]   A. Matsumoto, K. Tsutsumi,K. Schumacher, K. K. Unger, Langmuir, 18 (2002)4014.

[27]   A.S.M. Chong, X.S. Zhao, J. Phys. Chem. B, 107 (2003) 12650.

[28]   A. Stein, B.J. Melde, R.C. Schroden, Adv. Mater., 12 (2000) 1403.

[29]   S. Shylesh, A.P. Singh, J. Catal., 244 (2006) 52

[30]   P. Mukherjee, S. Laha, D. Mandal, R. Kumar, in: A. Sayari, M. Jaroniec, T.J. Pinnavaia, Stud. Surf. Sci. Catal., 129 (2000)283

[31]   G.S. Caravajal, D.E. Leyden, G.R. Quinting, G.E. Maciel, Anal. Chem., 60 (1988) 1776.

[32]   J. Y. Bae, S.H. Choi, B.S. Bae, Bull. Korean Chem. Soc., 27(2006)10.

[33]   B. H. Stuart, Infra red Spectroscopy: Fundamentals and Applications, John Wiley and Sons, 2004.

[34]   H. Yoshitake, T. Yokoi, T. Tatsumi, Chem. Mater., 14 (2002) 4603.

Adsorption and Activity Studies of Immobilized α- amylase

The structure–function relationship of a specific protein strongly depends on the interactions between the bio-molecule and the surrounding environment. The balance of intra- and intermolecular interactions between different amino acids residues, the supports and the ˙environment surrounding the protein determines its chemical and biochemical functionalities. Mesoporous materials provide well-defined nanostructures, which bare resemblances to the nanospaces found in biological systems in their size and accuracy. Therefore, dense assembling of biological components in mesopores could mimic structures and functions of rather complicated biomaterials. Pore geometries (pore diameter and volume) of mesoporous materials are the crucial factors for the size selective adsorption of biomaterials, especially proteins, which often have a size comparable to pore dimension. Studies on assemblies of biomaterials in mesoporous media are still in initial stage, but the development of appropriately designed mesoporous materials would powerfully promote researches in these fascinating unexplored field. In this chapter we have discussed the factors affecting the rate of adsorption of proteins on mesoporous materials. The dependence of enzyme activity and stability on pH, temperature, various parameters including kinetics for the free, adsorbed and covalently attached samples were also determined.

6.1 Introduction

In protein-surface interactions, the governing factors are determined both by the physical state of the material and protein surface and the intimate solution environment. Factors including solution pH, surface charge, pore size, surface elemental composition and surface energetics, etc., have to be considered in defining the role of the solid-solution interface.

Siliceous SBA-15 adsorbents can have a very high affinity and capacity for proteins [1]. The adsorption of enzymes on mesoporous silica is determined by several factors. The influencing factors may include the experimental conditions such as the temperature, pH of the buffer solutions and the material properties such as the size of enzymes and nanopores, the composition, mesostructure and morphology of mesoporous materials. The optimized pore conditions of the support suited for an enzyme is very important in improving the support efficiency [2, 3]. This was attained as discussed in the chapter 3.

Several reports describe the use of mesoporous molecular sieves to immobilize proteins[4]. Balkus et al. have studied the immobilization of enzymes with different sizes on MCM-41, MCM-48 and SBA-15 [5]. They suggested that the loading efficiency depends on the size of the enzyme and the pore size of the adsorbent, and indicated that the immobilization process takes place in the mesopores. Furthermore, they have found that the proteins retain their activity after adsorption. Takahashi et al. studied the adsorption of horseradish peroxidase and subtilisin on FSM-16, MCM-41 and SBA-15 and found that the amount of adsorption on MCM-41 and FSM-16 was higher compared to SBA-15 [6]. In contrast, Yiu et al. have studied the immobilization

of trypsin on MCM-41, MCM-48 and SBA-15, and reported that the amount of trypsin adsorbed depends on the pore diameter of the adsorbent and that SBA-15 showed the maximum amount of trypsin adsorption [7]. Most of the authors have compared the effect of pore size with different silica materials like MCM-41 and SBA-15. The effect of pore size on the rate of adsorption can be compared only if the same material with different pore sizes is taken. The adsorption property will differ with the structural framework of silica. Few authors have varied the pore size of SBA-15 using pore regulating agents like TMB (tri methyl benzene) and the effect of pore size on rate of adsorption of different proteins was studied. Katiyar et al. studied the adsorption of enzymes of various dimensions in SBA-15 materials of various pore sizes prepared using PST and TMB [8]. They have concluded that the adsorption capacity and rate of adsorption is dependant on the solution pH, protein and pore size.

Regulating the pore using TMB does not give well ordered structures. We have changed the pore sizes using the hydrothermal treatment, so the pores are well ordered and the silica material is of similar frame work. But raising the temperature to 130 °C has decreased the surface area considerably even though the pore size increased to 84 Å. From the adsorption studies it was evident that optimum pore size alone does not enhance adsorption rate. The morphology and particle size has a serious role for improving the adsorption properties of silica. This chapter covers the factors on which adsorption property depends. We have studied the rate of adsorption of α-amylase on SBA-15 silica of various pore dimensions and the rate of adsorption of three different enzymes on the same support of pore dimension suitable for enzyme chosen for detailed study.

α-amylase (EC3.2.1.1) (1,4-α-D-glucan glucanohydrolase; glycogenase) is a calcium metalloenzyme, completely unable to function in the absence of calcium. By acting at random locations along the starch chain, α-amylase breaks down long-chain carbohydrates, ultimately yielding maltotriose and maltose from amylose, or maltose, glucose and "limit dextrin" from amylopectin.

The enzyme, α-amylase which is mainly used as a thinning agent in starch hydrolysis, is widely applied in food, paper and textile industries. The traditional acid hydrolysis of starch was completely replaced by α-amylase and glucoamylase, which could convert starch with over 95%, yield to glucose. Starch industry became the second largest user of enzymes after detergent industry. Mainly two enzymes carry out conversion of starch to glucose: α-amylase cuts rapidly the large α-1, 4- linked glucose polymers into shorter oligomers in high temperature. This phase is called liquefaction and is carried out by bacterial enzymes. In the next phase called saccharification, glucoamylase hydrolyses the oligomers into glucose. This is done by fungal enzymes, which operate in lower pH and temperature than α-amylase. Sometimes additional debranching enzymes like pullulanase are added to improve the glucose yield. Currently high fructose corn syrup from starch is used for the manufacture of poly lactic acid which is a precursor for the biodegradable plastics [9-11].

6.2 Influence of various factors on rate of adsorption
6.2.1 Influence of pore diameter, Pore volume and Morphology

The kinetics of α-amylase adsorption on SBA-15 samples at pH 6 is shown in Fig.6.1. Since α-amylase has dimensions of 35×40×70Å it was expected that the protein had access to the pores of all samples prepared at 120 and 130 (°C).
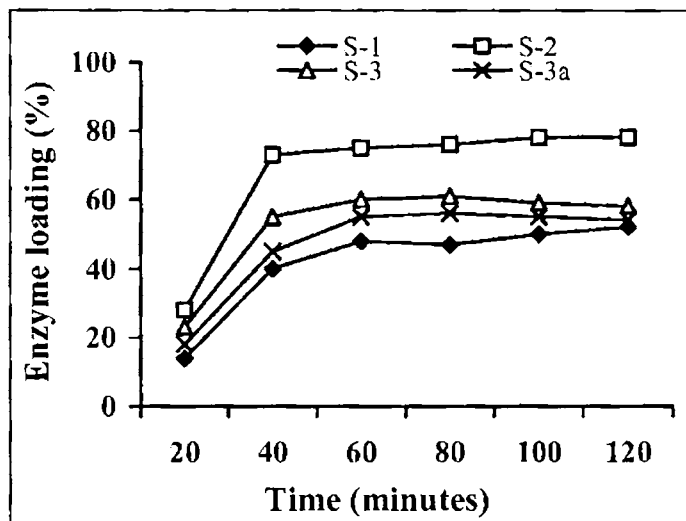
Fig.6.1 Rate of adsorption of enzymes on supports of various pore dimensions and functionalized material (Enzyme conc.3mg/mL, volume 20mL, 0.1 M Buffer, pH-6, Temp 303K, Silica support 0.1 mg)

High equilibrium capacity (> 220mg/g) in a short time of ~40 minutes indicated that the huge pore volume of S-2 with sufficient pore opening allows the complete penetration of enzyme molecules well within the pore. For S-1, the rise to saturation was much slower than for S-2 and S-3; for S-2 the rate curve was close to rectangular, indicating very good access to the pore. This might be due to the ordered nature of S-2 with optimum pore size. But from the adsorption studies it was evident that optimum pore size alone does not enhance adsorption rate. The loading with S-3 sample was low (< 165mg) even though the pore size was much larger 84Å. In SBA-15 type mesoporous silica the morphology and particle size played an important role in the immobilization ability [12]. Raising the temperature to 130°C had decreased the surface area considerably even though the pore size increased

to 84Å. At higher temperatures the slight coiling of silica rods blocked the free adsorption of biomolecules inside the channels.
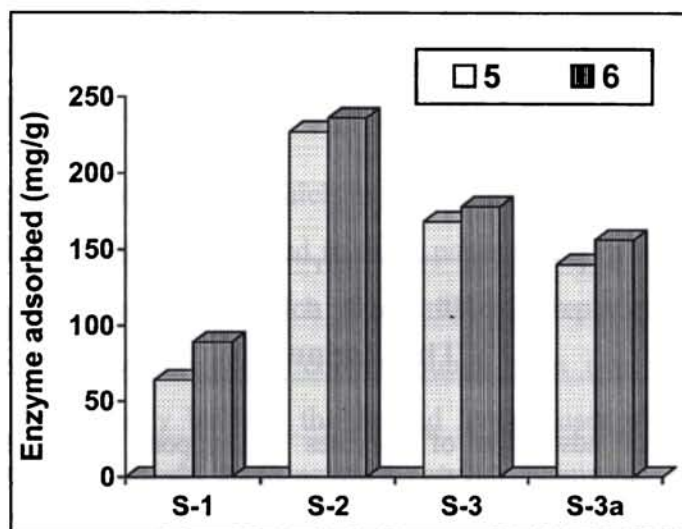

Fig. 6.2 Comparison of the amount of enzyme adsorbed for different SBA-15 materials at pH 5, 6 for a given time.

Zhao et al. had reported that rod-like SBA-15 with straight channels (1–2 μm in length) possesses the fastest adsorption rate reaching 200 mg/g within 10 minutes at 25°C and the largest immobilization amount of 500 mg/g among all reported mesoporous silica [13]. Comparison of the amount of enzyme adsorbed for different SBA-15 materials at pH5 and 6 for a given time is shown in Fig.6.2

By carefully controlling the morphology of mesoporous silica, it was revealed that silica with smaller particle sizes possessed more entrances to entrap enzymes than conventional mesoporous silica with larger particle sizes, which lead to much improved bioimmobilization abilities of mesoporous silica. So a control of morphology during the synthesis is

essential for good adsorption property. The accessible surface area for protein adsorption was not similar for the two materials S-2 and S-3 in spite of the higher pore diameter and hence the enzyme loading was also different. It was also noticed that the pore volume after immobilization decreased to 0.49 cm^3g^{-1} in the case of S-2 (62%) but the decrease was not sharp for S-3 (16%). Another reason for low loading was that the total pore volume decreased as the pore diameter increased, so that the surface area which could provide active sites for the enzyme immobilization also decreased. Vinu et al. had reported that the amount of adsorbed cytochrome c was dependant on pore volume which decreased with increase in pore diameter [14,15]. This result suggested that pore volume could be a more important parameter than pore diameter. To study the effect of pore structure we had also compared the enzyme loading on the cheap support natural rice husk silica with no regular pore structure. The acid leached rice husk silica had a surface area of 242 m^2/g and 27 % of the total surface area was occupied at equilibrium adsorption while it was 67 % for mesoporous silica with regular pore structure (S-2). The irregular pores with low dimension do not allow the enzyme molecules to penetrate in.

6.2.2 Effect of pH

Besides the pore size of the mesoporous silica, the solution pH was another important factor to be considered for enzyme immobilization. The forces binding proteins to hydrated silica surfaces included hydrogen bonding, hydrophobic interactions and electrostatic protein-surface interactions. The sign of the overall charge on a surface can readily be predicted on the basis of the isoelectric point pI (the pH at which the overall charge is zero). This pI value of a protein molecule depends on the balance of

surface functional groups which may have opposite charges. When the adsorption is performed at a pH lower than the pI of the enzyme (but higher than pI of the silica) the protein will be positively charged. The isoelectric point of the silica surface of mesoporous material is around 2 hence the adsorbent surface is negatively charged at pH above 2. The greater the positive charge on the enzyme, the stronger the attraction between protein and surface, but stronger the repulsion between adsorbed molecules. According to Su et al., surface adsorption capacities of proteins are found to vary with the pH of adsorption according to a bell-curve, the maximum of which occurs at the isoelectric point of protein [16, 17]. It therefore follows that by judicious variation of the pH, proteins could be selectively adsorbed and desorbed. Previous study on the adsorption of biomolecules on pure silica materials showed that strong electrostatic interactions between the surface silanol groups and the surface charge of protein molecules were a critical factor [18, 19]. According to Sakaguchi and coworkers the driving forces for the adsorption of Hb include hydrophobic interactions, electrostatic repulsion and attraction, the intramolecular cohesive attraction and repulsion [20]. Vinu et al. provide systematic researches on protein adsorption on mesoporous materials. The influence of the solution pH on the adsorption of cytochrome c and lysosome was studied by his group [21]. Typical results of adsorption of hen egg white lysozyme and horse heart cytochrome c onto three mesoporous silica materials obeyed Langmuir-type behavior.The results revealed that the adsorption of lysozyme was determined by electrostatic and hydrophobic interactions. The studies on the adsorption of biomaterials on the mesoporous carbon reveal that hydrophobic interaction between guest molecules

and surface of the mesoporous materials is an important parameter which controls the amount of biomaterials adsorption [22].

The effect of pH on adsorption was studied at room temperature by varying the pH in the range 4-8 on the size matching pore (Fig.6.3). It could be seen that the monolayer adsorption capacity of S-2 significantly changed depending on the solution pH. The isotherms measured in the pH range 4-6 showed a sharp initial rise, which suggested a high affinity between amylase and the adsorbent surface. Finally, the isotherms reached a plateau. The amount adsorbed increased from pH 4-6 and further decreased. At pH 8, adsorption was very low and it takes longer time to reach equilibrium. The maximum adsorption at pH 5-6 could be explained as follows; near the isoelectric point the net charge of the protein would be low and the coulombic repulsive force between the molecules would be minimal. Consequently a closer packing of the protein molecules was possible and the monolayer capacity increased. It was observed that there was a large reduction in the amount of α-amylase adsorbed on silica at pH below and above pI. At pH below the enzyme pI α-amylase assumed a positive charge and so the lateral repulsion between protein molecules increased. As a consequence, the protein molecule requires more space and the monolayer capacity decreased. When the solution pH was increased to 8 the surface of the α-amylase molecule became negatively charged and enhanced the electrostatic repulsion between protein molecules and the silica surface. The maximum adsorption occured at pH 6 which was close to the isoelectric point of α-amylase (5.5).
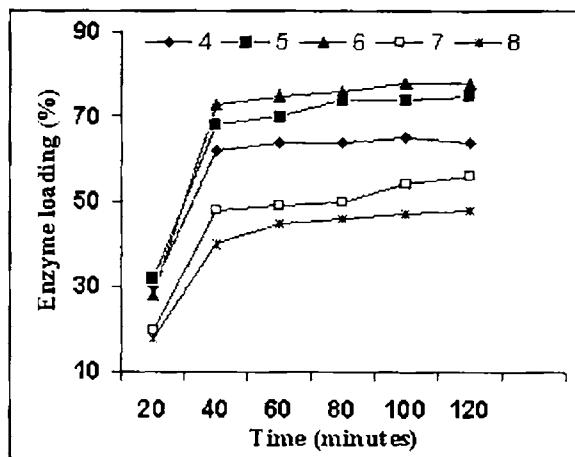
Fig. 6.3 Adsorption isotherms of α-amylase on SBA-15 of pore size 74Å at various pH.

6.2.3 Effect of enzyme size

Immobilzation of different enzymes in silica MCM-41 /40 was performed by Diaz and Balkus. They reported that due to the large size of the enzyme peroxidase (MW: 44000), only a small quantity of the enzyme was adsorbed, as compared to the smaller enzymes; e.g. trypsin (MW: 23400), papain (MW: 20700) and cytochrome (MW: 12300) [5]. A clear correlation between enzyme size and molar loading was reported. The dependence of the protein capacity of SBA-15 on the pore size was studied by measuring the adsorption isotherms of Lysozyme and BSA by Katyar et *al.* They concluded that the adsorption capacity of SBA-15 and rate of adsorption is dependent on the solution pH, due to the strong influence of electrostatic interactions, and protein and pore size [23].

We have also followed the adsorption properties of three different enzymes α-amylase, Lipase and Bovine serum albumin on the same SBA-15 material. All the three enzymes had pI in the similar range but with different molecular masses (as in Table 6.1) were adsorbed on SBA-15 silica with

same pore diameter 7.4nm at different pH6. The results showed a clear dependence on enzyme size (Fig.6.4). The rate of adsorption of different enzymes on the same support at the same pH 6 showed that the enzyme with higher molecular mass and large kinetic dimension takes more time for adsorption. The enzyme whose size matched with the size of the pore was adsorbed very fast than the enzyme with a different pore size. Compared to α-amylase, lipase has less affinity for SBA-15 silica.

Table 6.1 The molecular mass, pI and dimensions of three different proteins are summarized

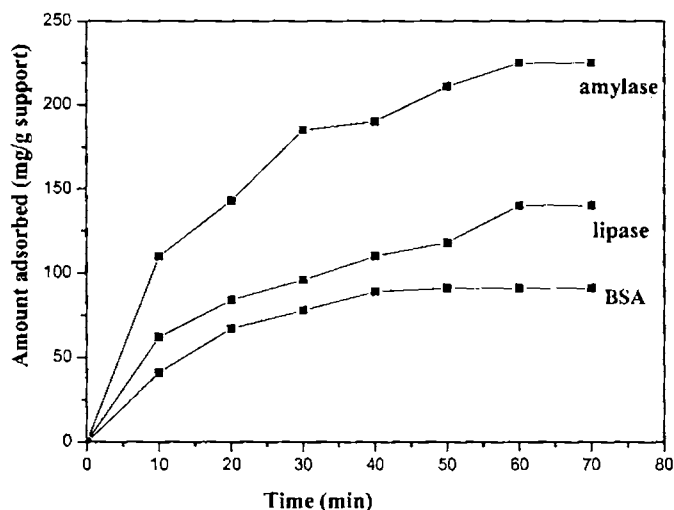| Protein	Mol.mass	Isoelectric point	Dimensions in Å
α-amylase	50,000-54,000	4.8-5.5	35×40×70
Lipase	45, 000–50, 000	4-5	35×40×50
Bovine serum albumin	66,400	4.7 -4.9	40×40×140

Fig. 6.4 Rate of adsorption of different enzymes on the same support S-2 of pore size 74Å at pH 6, enzyme conc. 3mg/ml, mass of support 0.1g, phthalate buffer(0.1 M)

6.3 Activity towards liquefaction of starch

In the design of enzyme support materials, enzyme activity after immobilization is one of the most important parameters for assessing the efficiency of the supported enzyme. Environmental parameters affect the activity of enzymes either in free or in immobilized forms. Immobilized enzymes were applied to the hydrolysis of starch, and their performance was compared with that of free enzymes. Studies were carried out at various pH, temperature and substrate concentrations in order to determine the optimum conditions for the reaction. The thermal, storage, pH stability studies were carried out. The reusability and operational stability of the immobilized catalyst was also evaluated.

6.3.1 Effect of pH

The activities of α-amylase immobilized on supports of various pore sizes and the amine functionalized surface measured as a function of pH is depicted in Fig. 6.5.

The activity increased with increase in pore size (S-3e>S2e>S-1e). The sample S-1 having pore size 63 Å does not allow the easy penetration of enzyme with molecular size 74Å. It is reported in the literature that BJH under estimate the pore size by ~10Å. So there is a chance for some of the molecules to enter the pore. The increase in activity with the pore size is definitely due to the easy diffusion of substrates and products inside and outside the pore. The enzymatic activity of HRP immobilized on mesoporous silica with various pore sizes was evaluated by the oxidative reaction of 1,2-diaminobenzene in an organic solvent by Takahashi *et al* [24]. A native HRP was used as the reference. The immobilized enzymes exhibited relatively high enzymatic activities compared with the native enzyme

activity. The authors also indicated that the immobilized enzyme in mesoporous silica, the pore size of which matched the enzyme kinetic diameter, exhibited the highest activity.
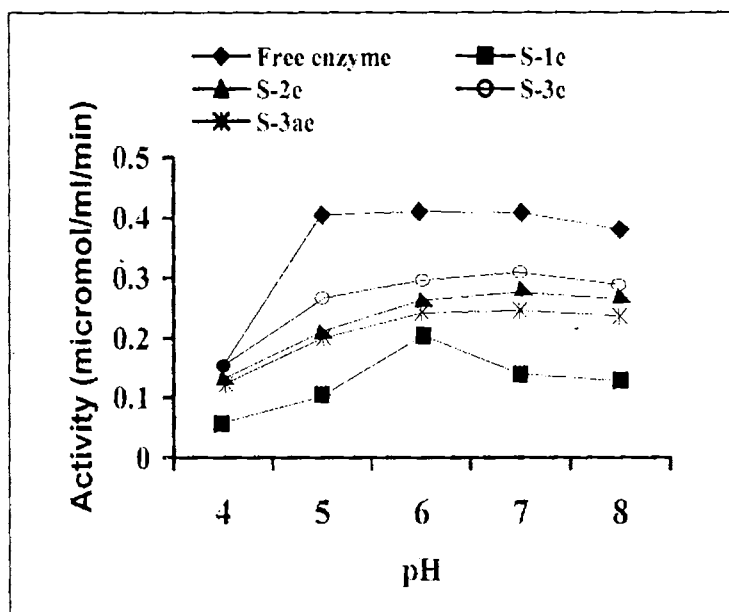

Fig.6.5 Effect of pH on activity of enzymes immobilized on various supports. (10mL-3%Starch, 10 mL-0.1 M Buffer, Temp 303K, Immobilized enzyme-100 mg.)

The enzyme immobilized in mesoporous silica and silica gel, which have pore sizes larger than that of the enzyme, showed however, medium activities. The lowest catalytic activity was observed for the enzyme immobilized on the outer surface. Trypsin has been immobilized onto pure siliceous MCM-41, MCM-48 and SBA-15 and the effect of pore size on the activity was studied [25, 26]. The hydrolysis of N-a-benzoyl-DL-arginine-4-nitroanilide (BAPNA) was used as a model reaction, by monitoring the formation of p-nitroaniline spectrophotometrically. The activity of the immobilized enzyme was found to

increase as the pore size increased probably due to the enhanced diffusion of the reactants and the products. However, leaching of enzymes is a major problem as the enzyme molecules are only loosely adsorbed onto the internal surface of the mesoporous silica carriers.

The enzyme immobilized on the amine functionalized surface also exhibited similar activity but lesser than the enzyme adsorbed on the size matching support. These studies also revealed that the activity of free and immobilized α-amylase in starch hydrolysis varied with the pH. Enzymes are amphoteric molecules containing a large number of acid and basic groups, mainly situated on its surface. The charges on these groups will vary, according to acid dissociation constants, with the pH of its environment. This will affect the total net charge of the enzymes and the distribution of charge on its exterior surfaces, in addition to the reactivity of the catalytically active groups. Taken together, the changes in charges with pH, affect the activity, structural stability and solubility of the enzyme. These effects are especially important in the neighborhood of the active sites. Each enzyme works within quite a small pH range. There is a pH at which its activity is greatest (the optimal pH). This is because changes in pH can make and break intra- and intermolecular bonds, changing the shape of the enzyme and, therefore, its effectiveness [27]. The maximum activity for free enzyme was observed at pH 6 and 7. After immobilization the net activity decreased but the maximum activity was at the same pH as the free enzyme. The reaction rate of enzyme bound on a porous particle could be affected by external or internal diffusion resistances, which corresponded to the transport of substrate and products

from the bulk solution to the outer surface of the enzyme particle, and to the internal transport of these species inside the porous system.

6.3.2 Effect of temperature

Temperature plays an important role in determining activity of enzyme. The effect of temperature studied towards activity of enzymes is shown in Fig.6.6.

There is a certain temperature at which an enzyme's catalytic activity is at its greatest. As the temperature rises, reacting molecules have more and more kinetic energy. This increases the chances of a successful collision and so the rate increases [28]. Above this temperature the enzyme structure begins to break down since at higher temperatures intra- and intermolecular bonds are broken as the enzyme molecules gain even more kinetic energy.
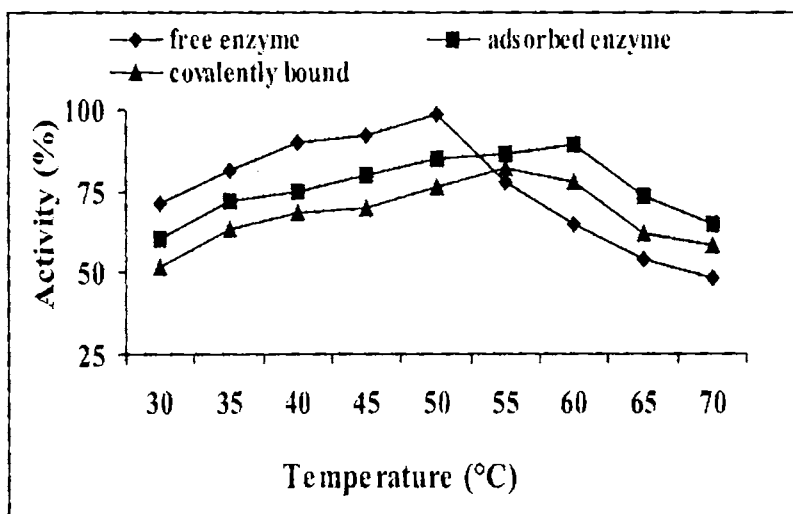

Fig.6.6 Effect of temperature on activity

The free enzyme exhibited an optimum temperature of 50°C, while the enzyme adsorbed in the size matching pore exhibited maximum

activity at 60°C. The one covalently bound exhibited maximum activity at 55°C. Immobilization could bring about a change in the optimum values.Tumturk et *al* was of the opinion that the increase in optimum temperature was caused by the changing physical and chemical properties of the enzyme. This could be explained by creation of conformational limitations on the enzyme movements as a result of hydrophobic interactions between the enzyme and the support [29]. S.Gopinath & S. Sugunan has suggested enzyme immobilization, retards the unfolding of protein, thereby maintaining activity [30].

A shift from 50°C to 70°C was reported for β-amylase immobilized on chitosan beads [29].On the other hand, a shift in optimum activity upon coupling of α-amylase in opposite direction, from 90°C to 80°C for Eudragit carriers, from 63°C to 41°C for zirconium dynamic membranes were also reported [31,32]

The higher thermal stability of the adsorbed enzyme in porous materials could be explained as follows. The adsorbed enzymes, being well within the pore were not in direct access to higher temperature of the bulk medium and they resisted the temperature to a higher extent. In the case of covalently bound enzymes they were not well trapped within the pore due to steric hindrance of the attached functional groups. Still binding the enzyme to a new environment has provided a better thermal resistance than the free enzyme.

6.3.3 Effect of substrate concentration

The rate of an enzyme reaction is decisively influenced by the concentration of its substrate. The substrate saturation curve obtained by plotting the velocity of

reaction against substrate concentration is given in Fig. 6.7. The kinetic parameters of the free and immobilized α-amylase were determined in a batch reactor.
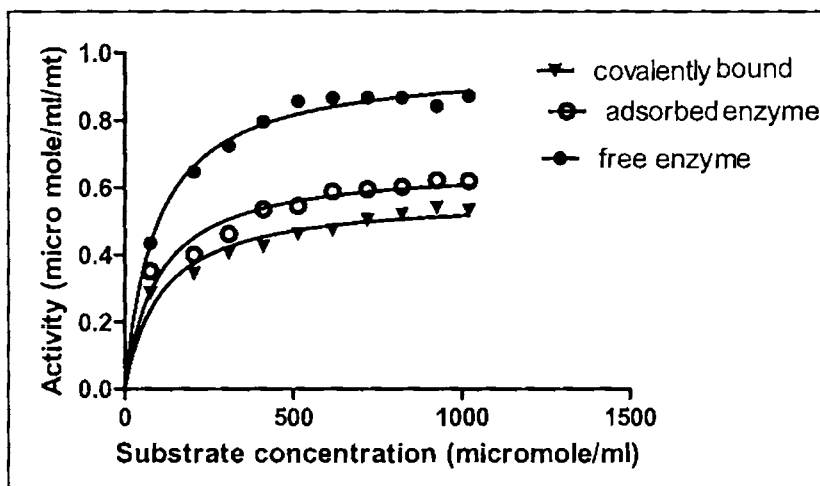

Fig. 6.7 Substrate saturation curve of an free and immobilized enzymes with Michaelis –Menten kinetics

The characteristic values of enzyme reactions, V_{max} and K_m were calculated using computer aided nonlinear regression curves. K_m is (roughly) an inverse measure of the strength of binding between the enzyme and its substrate. The immobilization of an enzyme often brings about a rise in the apparent K_m [33-34], a drop in the value of the constant is also not uncommon [35, 36]. In our case the calculated K_m values were higher than that of the free enzyme as shown in Table 6.2. The increase of K_m upon immobilization reflected a decreased affinity for the substrate. Silanol rich silica naturally should have a high affinity towards starch but the diffusion controlled mass transfer of substrate into the pore should have reduced the affinity.

Table 6.2 Kinetic parameters of free and immobilized enzymes.

Catalyst	Michealis constant Km (μmoles/mL)	V max (μ moles/mL/mt)	Effectiveness factor (η)
Free enzyme	130.9	1.02	
Adsorbed enzyme	147.8	0.71	0.70
Covalently bound enzyme	184.2	0.63	0.62

V_{max} measures the extent of activity of the enzyme. The reduction in V_{max} after immobilization could be explained as follows. Inside the pore, the concave surface gave a comfortable occupation of the biomolecule and the tertiary structure was conserved preventing unfolding. Still immobilization might block some of the active sites and only a fraction of the enzymes were oriented properly with their active sites exposed for the reactions to occur, which was one reason for the lower reactivity of the immobilized enzyme. The reaction rate of enzyme bound on a porous particle could be affected by external or internal diffusion resistances, which corresponded to the transport of substrate and products in and from the bulk solution to the outer surface of the enzyme particle, and to the internal transport of these species inside the porous system. So the loss in activity was essentially due to the diffusion effects i.e. internal mass transfer resistance arising when enzymes were entrapped in pores. In the case of covalently bound enzyme, decrease in activity was due to the conformational flexibility of the molecule due to multiple attachments. But these multiple attachments provided additional stability to covalently bound enzymes.

The effectiveness factor of the immobilized biocatalyst was defined as the ratio of the α-amylase activity of the immobilized system to that of the free enzymes. Effectiveness factor = V_{imm}/V_{free}. The effectiveness factor η provided information on the role of diffusion in the reaction. $\eta=1$ at conditions of complete diffusion i.e. in case of homogeneous reaction of the free enzyme. Immobilization reduces the effectiveness factor. In both the cases the effectiveness factor η was less than 1 and proved that the rate of reaction was diffusion controlled. The efficiency of immobilization, defined as the relative activity of enzyme after immobilization, was calculated as 100η. The efficiency of immobilization of adsorbed enzyme was found to be 70% and 62% for covalently bound form.

In the literature, there are various levels of activity retention for α-amylase immobilization. For example the preserved activities were reported as 7–40%, respectively, on polystyrene and silica based supports [32, 33] and 25–67%, respectively for dextran and cellulosic supports [27]

6.4 Thermal stability

In principle, the thermal stability of an immobilized enzyme can be enhanced, diminished or unchanged, relative to free counter parts and several examples of each kind have been previously reported [37]. Thermal stability experiments were performed with free and immobilized enzymes, which were incubated in the absence of substrate at higher temperatures i.e. 60°C in a batch reactor (Fig 6.8.).The activity of free enzyme reduced to 18% in 60 min. The adsorbed and covalently bound enzymes retained 75% and 48 % activity respectively in the same time.
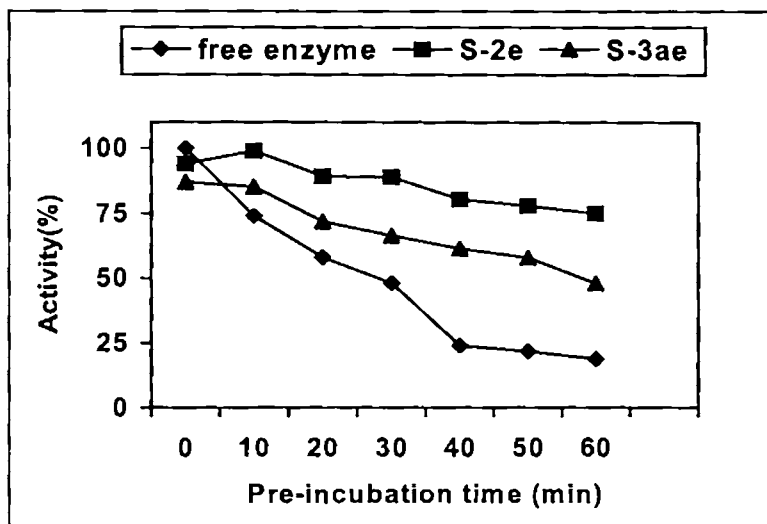
Fig.6.8 Thermal stability in a batch reactor

The experiments were repeated in a packed bed reactor at the same temperature (Fig.6.9). The adsorbed and covalently bound enzymes retained 72% and 58% activity respectively after 5h. The adsorbed enzyme exhibited better thermal stability than the covalently bound form, because in the case of adsorbed enzyme the pore size being large enough the enzymes are packed in the 1D channel was not subjected to the direct effect of environmental variations. In the covalently bound form the bulky functional groups does not allow the complete entrapment of enzymes, still the multiple attachment provide extra stability to the enzyme. On the basis of these results, we could confirm that the immobilization matrix increases the stability of enzyme against thermal denaturation.
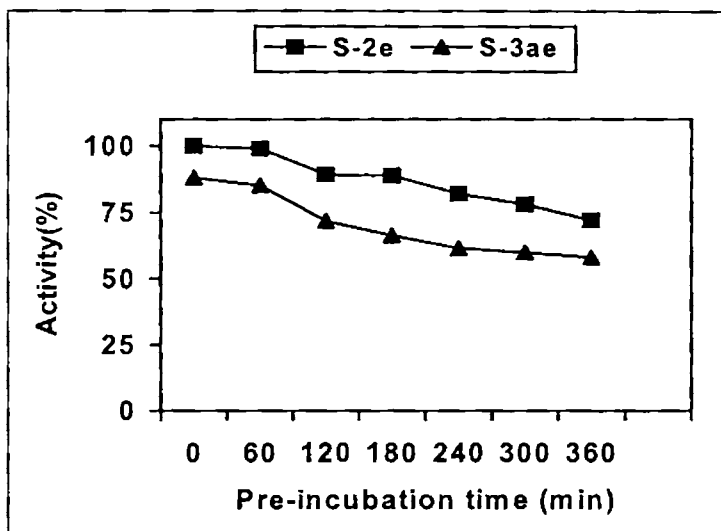
Fig. 6.9 Thermal stability in a packed bed reactor

6.5 Reusability

The application of an enzyme for a given reaction is often hampered by its reusability. Hence the idea of immobilizing the enzyme on a rigid solid support enabling easy separation and the possibility of operation in a packed-bed or batch reactor has been of great industrial interest for many years. The reusability studies were conducted using 50 mg of enzyme supported on 1 gm of support in a batch reactor. Adsorbed α-amylase and the covalently bound enzyme could be used without any loss in activity for 12 continuous cycles (Fig. 6.10). After 20 cycles, the adsorbed enzyme retained 83 % of its initial activity. For the covalently bound enzyme, at the end of 20 cycles, it retained 75 % of its initial activity. Immobilization of α-amylase on mesoporous silica has improved reusability of the enzyme. The loss in activity was due to the natural inactivation of enzyme as a result of time dependent denaturation of the enzyme
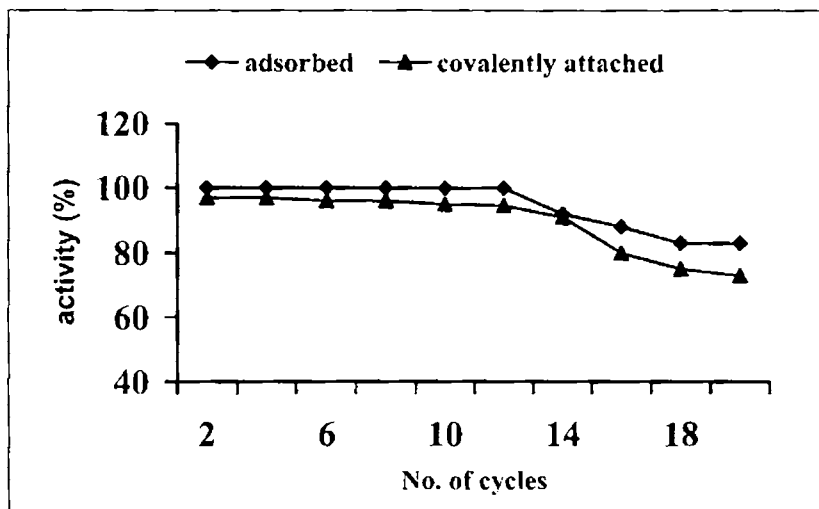
Fig. 6.10 Reusability in a batch reactor

Fig. 6.11 depicts the results of operational stability measurements on the immobilized enzymes. Employing a packed bed reactor facilitates the application of enzymes for continuous process for the mass production of the desired product. The performance of the catalyst was tested in a packed bed reactor. The process was continued for 4 days at a space velocity of $3.26h^{-1}$. The adsorbed α-amylase demonstrated 100 % initial activity for 48 hours after which it showed 28 % drop in activity at the end of 96 hours. While the activity of covalently bound form reduced to 60 % after 96 h. Ju et *al* have reported 65% retained activity after 30 cycles in case of α-amylase immobilized on hollow fibre reactor [38]. Tanyolac et *al* have reported complete reusability for α-amylase immobilized on nitrocellulose membrane up to 10 successive cycles followed by a 35% reduction in activity [39].
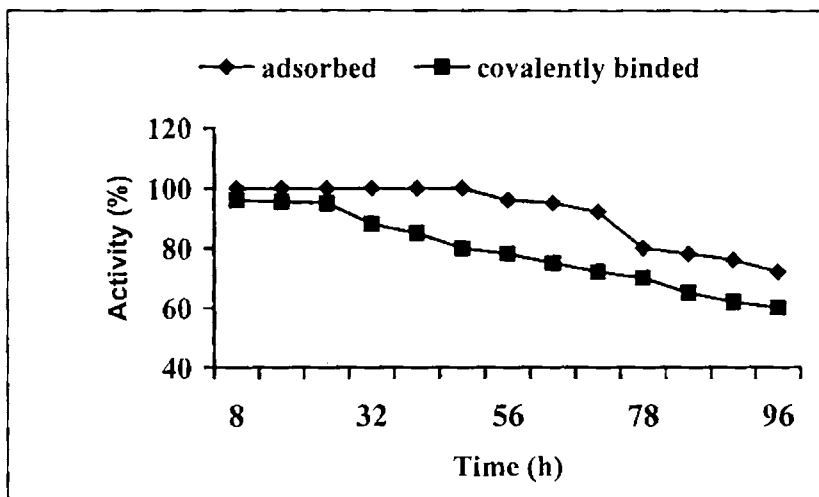
Fig. 6.11 Operational stability in a packed bed reactor

6.6 Storage stability

Enzymes are very delicate biocatalysts and lose their activity even during storage. Therefore, storage stability is a factor which should be examined. Storage stability measurements were conducted in the dry form at room temperature and in buffer solution of optimum pH at 4 °C. Free enzyme when kept at room temperature was melted and reduced all its activity on the second day itself, while the adsorbed amylase retained 75% activity, but the covalently bound form lost its activity. In this study, the activities of free and immobilized enzymes stored in buffer at 4°C were measured after certain periods of storage and the results are given in Fig. 6.12.The activity was reduced to 75% and 70% for adsorbed and covalently bound forms respectively after 21 days. When stored in 0.1 M buffer of optimum pH the free α-amylase lost all its activity within12 days.
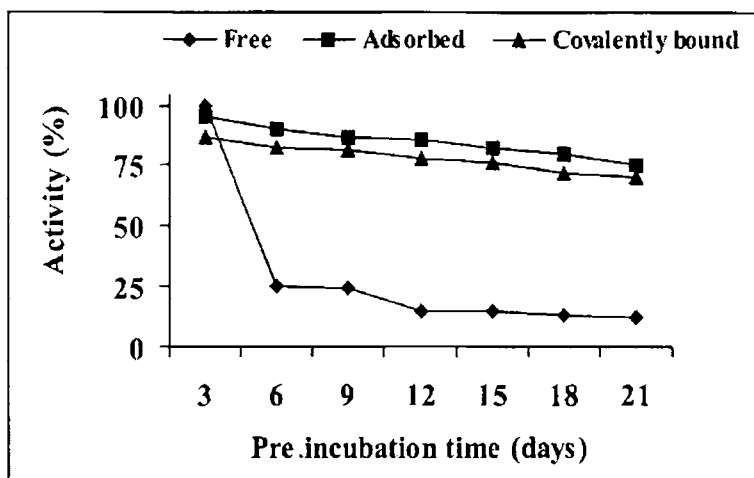
Fig. 6.12 Storage stability of immobilized enzymes.

It was also reported that α-amylase immobilized on silanized silica particles lost its activity at a rate of 10% every 12 days of storage over a period of 30 days[40].

6.7 Leaching studies

Table 6.3 shows the results of leaching studies at different enzyme loadings.

Table 6.3 Leaching studies at different enzyme loading

Enzyme loading(mg/g)	Enzyme retained (%) after shaking for 1h in buffer of pH 7 after 12 cycles.			
	S-1e	S-2e	S-3e	S-3ae
50	61	98	98	98
100	58	80	75	85
150	45	72	58	83

It can be seen that there was no leaching at lower loadings. As the loading increases leaching also increases. In all cases, the enzyme attached to

external surface leached (S-1e) faster whereas the one entrapped in the correct pore size (S-2e) resisted leaching to a considerable extent. The enzyme attached to the support of pore size slightly greater than the size of enzyme (S-3e) also showed considerable leaching compared to S-2e.

Diaz and Balkus also showed that the MCM-41/40 entrapped trypsin using 3-aminopropyltriethoxysilane (APTES) did not leak into solution when the material was immersed in pH 9.0 buffer, which would normally release ~ 90 % of the enzyme after 24 h [1]. The enzyme bound to functionalized silica S-3ae showed very low amount of leaching.
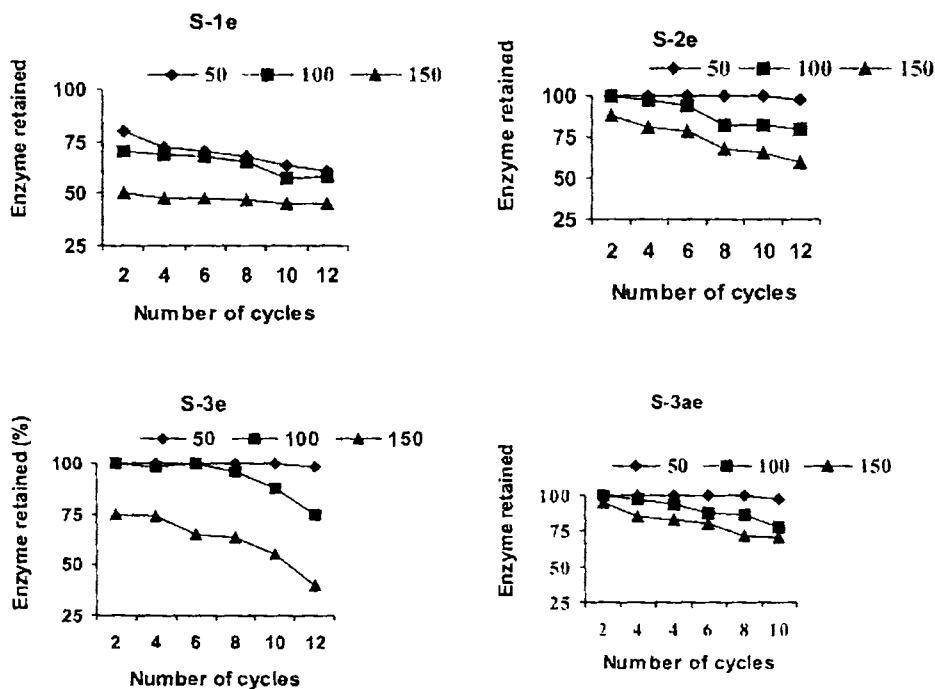

Fig. 6.13 Enzyme retained after continuous reuse at loadings of
(♦) 50, (■) 100 and (▲) 150 mg

6.8 Conclusions

The following conclusions can be derived from this chapter.

- For a given pore diameter the amount of enzyme adsorbed is a function of the polarity of the surface and maximum adsorption was around the isoelectric point of enzyme.

- For a given surface polarity the amount adsorbed increases with pore volume and for maximum adsorption optimum pore size with controlled morphology is essential.

- Each enzyme has different affinity for the support and the enzyme with higher molecular mass and large kinetic dimension takes more time for adsorption.

- The optimum pH for reaction does not change much after immobilization.

- The optimum temperature shifts to higher values after immobilization.

- Enzyme immobilized in a porous material exhibited lesser activity than the free enzyme due to the internal mass transfer resistances offered by the improper diffusion of substrate from bulk to enzyme surface.

- Reusability, operational stability, storage stability and thermal stability are the advantages of immobilization.

References

[1]   Y.J Han,G. D Stucky, A.Butler, J. Am. Chem. Soc., 121 (1999) 9897.

[2]   Y.J. Han, J.T. Watson, G.D. Stucky, A. Butler, J. Mol. Catal. B:Enzym., 17 (2002) 1.

[3]   J. Deere,E.Magner,J.G.Wall, B.K. Hodnett, J. Phys. Chem. B.,106(2002) 7340

[4]   M. Hartmann Chem. Mater., 17 (2005) 4577

[5]   J.F. Dýaz, K.J. Balkus Jr, J. Mol. Catal. B, 2 (1996) 115

[6]   H. Takahashi, B. Li, T. Sasaki, C. Miyazaki, T. Kajino, and S. Inagaki, Micropor. Mesopor. Mater., 44/45 (2001)755.

[7]   H.H.P. Yiu, P.A.Wright, N.P.Botting, Micropor. Mesopor. Mater., 44/45 (2001). 763

[8]   L. Ji, A. Katiyar, N.G. Pinto, M. Jaroniec, P.G. Smirnioti, Micropor. Mesopor. Mater., 75 (2004) 221

[9]   J.F. Kennedy, Handbook of Enzyme Biotechnology, Wiseman A, Ellis Horwood, London, 1995, Chapter 5.

[10]   N.W. Fadnavis, V. Bhaskar, M.L. Kantam, B.M. Choudary, Biotechnol. Prog., 19 (2003) 346

[11]   G. Alvaro, R. Fernandez-Lafuente, R.M. Blanco, J.M. Guisan, Appl. Biochem. Biotechnol., 26 (1990) 181

[12]   J. Fan, J. Lei, L. Wang, C. Yu, B. Tu, D. Zhao, Chem. Commun., (2003)2140

[13]   J. Lei, J. Fan, C. Yu, L. Zhang, S. Jiang, B. Tu,D. Zhao, Micropor. Mesopor. Mater., 73 (2004) 121

[14]   A. Vinu, V. Murugesan, M. Hartmann, J. Phys. Chem. B, 108 (2004) 7323

[15]   A. Vinu, V. Murugesan, W. Bo" hlmann, M. Hartmann, J. Phys. Chem. B, 108 (2004) 11496.

[16]   T.J. Su, J.R. Lu, R.K. Thomas, Z.F. Cui, J. Penfold, J. Colloid Interface Sci., 203(1998)419

[17]   T. J. Su, R. J. Green, Y. Wang, E. F. Murphy, J. R. Lu, R. Ivkov S. K. Satija, Langmuir, 16 (2000) 4999

[18]   J.M. Kisler, G.W. Stevens, A.J. O.Connor, Mater. Phys. Mech., 4(2001) 89.

[19]   S.Z. Qiao, C.Z. Yu, W. Xing, Q.H. Hu, H. Djojoputro, G.Q. Lu, Chem. Mater., 17(2005) 6172

[20] M. Matsui, Y. Kiyozumi, T. Yamamoto, Y. Mizushina, F. Mizukami, K. Sakaguchi, Chem. Eur. J., 7(2001) 1555

[21] Vinu, V. Murugesan, O. Tangermann, M. Hartmann, Chem. Mater., 16 (2004) 3056

[22] M. Hartmann, A. Vinu, G. Chandrasekar, Chem. Mater., 17(2005) 829

[23] A.Katiyar,L. Ji, P. Smirniotis, N. G. Pinto, J. Chromatogr. A, 1069 (2005) 119

[24] H .Takahashi, B. Li, T. Sasaki,C. Miyazak, T.Kajino, S. Inagaki, Chem. Mater.,12(2000)3001

[25] H. H. P.Yiu, P. A.Wright, N. P. Botting, J. Mol. Catal. B., (2001)15

[26] H. H. P. Yiu, P. A. Wright, J. Mater. Chem.,15(2005)3690

[27] Harttmeier W.,immobilized biocatalysts An Introduction, Springer − Verlag, Berlin (1988) p 1-80.

[28] Immobilized Biocatalysts, S.Pedersen, M.W Christensen Harwood Academic Publishers, Amsterdam , 2000

[29] H.Tumturk, S.Akshoy, N.Hasirci, Food Chem., 68 (2000)259

[30] S.Gopinath,S.Sugunan, Clays Clay Miner.,40(2005) 499

[31] T.Nodo, S.Furuta,I.Suda, Carbohydr.Polym.,44(2001)189.

[32] L.Cong, R.Kaul, U.Dissing.B.Mattiasson,J.Biotechnool.,42(1995)75

[33] A.R.Varalan,W.Sansen,A.V.Loey.M.Hendrickx,Biosens.Bioelect.,11(1996) 443

[34] R.Ulbrich,A.Schellenberger,W.Damerav, Biotechnol. Bioeng., 28 (1986) 511.

[35] G.I. Kvesitadze, M.S.H. Dvali, Biotechnol. Bioeng., 24(1982) 1765

[36] Y.Ohtuska,H.Kawaguchi,T.Yamamoto,J.Appl.Poly.Sci.,29(1984)3295

[37] N.Hasirci, H.Tumturk, S.Akshoy,React. Funct. Polym.,66(2006) 1546

[38] Y.H. Ju, W.J. Chen, C.K. Lee, Enzym. Microb. Technol.,17(1995) 685

[39] D.Tanyolac,I.Belma,I.Yürüksoy,A.R.Özdural,Biochem.Eng.J.,2(1998)179

[40] M. V. Kahraman,G. Bayramo lu ,N K.Apohan, A.Güngör, Food Chem., 104 (2007)1385

Tailoring materials for specific purposes and generating applications can bring better results. The current venture deals with the tuning of the pores of an ordered mesoporous material SBA-15 for the encapsulation of biocatalyst α-amylase. Synthesis of organic–inorganic hybrid materials for enzyme immobilization was the second phase of research. Characterization of materials prepared, and detailed activity and adsorption studies gave an insight into the complexities of immobilization process. This chapter deals with the summary of the present work and also the scope for further research in this field

7.1 Introduction

Although quite young, the field of mesoporous silicas doped with biologically interesting molecules has already exhibited its diversity and potential applications in many frontiers of modern materials science including biocatalysis, biosensing, drug release, and separation of biological molecules.

It has been shown that ordered mesoporous materials are useful for stable entrapment of biofunctions and the stabilization of biological interesting molecules under severe conditions. For example, enzymes immobilized on ordered mesoporous supports often show higher stability as compared to the free enzyme. In the present work the ordered pore structure of SBA-15 silica was tuned for the encapsulation of α-amylase of hydrodynamic radius 35×40×70(Å) using hydrothermal method at different temperatures and time. Further we have also undertaken an effort to incorporate organic components within an inorganic silica frame work to achieve symbiosis of the properties of both the components.The mesoporous silica and enzyme immobilized systems were characterized by various techniques and their activity studies were carried out. A detailed study into the adsorption properties of SBA-15 silica was also conducted. Chapter wise summary is given below

7.2 Summary

Chapter 1 deals with the general principles and mechanism for the synthesis of ordered mesoporous silicas. Literature covers the different

ordered mesoporous silicas synthesized and their application for the immobilization of enzymes.

Chapter 2 focuses on the materials and methods adopted for catalyst support preparation, physico chemical characterization, method adopted for the immobilization of proteins and catalytic activity measurements.

Chapter 3 focuses on the extraction of pure amorphous silica from a cheap source, rice husk and its characterization using various techniques XRD, SAXRD, Adsorption isotherms,[29] SiNMR, TG/DTG analysis, FTIR, DRIFT, SEM. Changes in the physico chemical properties of the materials after immobilization was also characterized.

An attempt to synthesize an ordered mesoporous material from rice husk silica with a large pore size was a failure. Further surface modification of rice husk silica to covalently bind the enzyme was discussed. The activity and stability studies of immobilized rice husk silica for the hydrolysis of starch are discussed in detail.

Chapter 4 deals with the tuning of the pores of ordered mesoporous materials SBA-15, for the encapsulation of α-amylase of hydrodynamic radius 35×40×70Å. Hydrothermal method was adopted to increase the pore size of SBA-15. Materials were characterized using SAXRD, Adsorption isotherms, SEM, HRTEM, ^{29}SiNMR, FTIR and TG/DTG analysis. Encapsulation of enzyme within the pore was evident from the adsorption isotherms

Chapter 5 deals with the optimization of APTES concentration required for the functionalization of mesoporous material SBA-15 without loss in ordered structure. The functionalized materials as well as counter parts

were characterized with various techniques like ^{13}C, ^{29}Si NMR, SAXRD, Adsorption isotherms, TG, FTIR and CHN analysis.

Chapter 6 deals with the various factors effecting adsorption of enzymes on mesoporous materials. Activity and stability studies of immobilized enzymes for the liquefaction of starch were also followed systematically.

Chapter 7 contains conclusions and future perspectives

However, the activity of immobilized enzymes is often found to be lower than that of the free enzyme. Leaching of the enzyme at high loading was the disadvantage of adsorption process. But with the functionalized material leaching could be controlled to a large extent. The decrease in activity was a major problem with the functionalized material. Reusability, storage stability, operational stability and thermal stability are the advantages of immobilization

7.3 Conclusions

- Hydrothermal synthesis at various temperatures can tailor the pore size of mesoporous materials with ordered structure.

- Selective adsorbents could be prepared from the ordered mesosporous silica by grafting chemical moieties that have specific affinity for the target molecules.

- The adsorption capacity and rate of adsorption of enzyme is dependant on the solution pH, protein size, pore size, pore volume and morphology of the material.

- For a given pore diameter the amount of enzyme adsorbed is a function of pH of the medium and maximum adsorption was around the isoelectric point of enzyme.

- For a given surface charge the amount adsorbed increases with pore volume and for maximum adsorption, optimum pore size with controlled morphology is essential.

- Enzyme confined within the pore exhibited greater activity. In a confined space or cage the unfolding of the protein is very much reduced.

- Leaching was controlled to a considerable extent by trapping enzyme within the pore and using functionalized mesoporous materials.

- The kinetic parameters V_{max} decreased and K_m increased with immobilization. The altered kinetic parameters are due to partitional effects combined with diffusional limitations and blocking of active sites during immobilization.

Future perspectives

Research on mesoporous silica phases and on hybrid materials is still in its early stages. A goal in the coming years will be to convert the acquired knowledge into technical applications. For industrial applications, particle size and morphology of the mesoporous support are important which include several critical points such as mechanical stability and shaping of (macroscopic) particles with well-defined properties. Moreover, the access of a substrate to the enzyme confined in a mesoporous host might be orientation selective resulting in a unique selectivity of a reaction. A detailed study into

the selectivity of products is to be conducted. Commercial issues such as cost of the adsorbent and scale up of the preparation of a biocatalyst or biosensor by immobilization of an enzyme have to be assessed in competition with existing materials.

A major issue in biocatalysis is the low space time yield in comparison to conventional "chemical routes". However, the high selectivity to the (enantiopure) target molecule might over compensate this drawback. In conclusion, the use of ordered mesoporous materials in biocatalysis, bioadasorption and biosensing is a young and growing but still challenging field with still high demand of new and improved materials. While potential applications such as biosensing and drug release are only sparsely addressed, the ability of mesoporous adsorbents to separate molecules by size exclusion has been demonstrated. Moreover, a possible reuse of these (at present, cost intensive) adsorbent/catalyst has to be investigated in detail.

RESEARCH PUBLICATIONS

- Tuning mesoporous molecular sieve SBA-15 for the immobilization of α-amylase. S.Ajitha & S. Sugunan, Journal of porous materials (Under revision)

PAPERS/POSTERS PRESENTED IN INTERNATIONAL/NATIONAL CONFERENCES

- **S.Ajitha** and **S.Sugunan**, Organic-inorganic hybrid molecular sieves for enzyme immobilization, **National** Seminar on Current trends in Chemistry, Cochin University of science and technology,18,19 January,2008-CTriC-2008

- **S.Ajitha& S.Sugunan** The effect of pore size on the rate of adsorption of Protein on Mesoporous Silicate SBA-15, **International** Conference on Advanced Materials and Composites (ICAMC-2007)organized by NIIST, Thiruvananthapuram

- **S.Ajitha& S.Sugunan**, Architecturing large pore SBA-15 for enzyme stabilization, **National** Conference on Smart Electroceramics (NCSE 2007) organized by C-MET during March 8-9, 2007.

- **S.Ajitha & S.Sugunan**, SBA-15 Mesoporous molecular Sieves with functionalized surfaces for enzyme immobilization, **International** Conference on Materials for the Millennium. Cochin University of science and technology on 1-3 March 2007.

- **S.Ajitha & S.Sugunan**, Nature's silica for nature's catalyst, **National** conference in chemistry-2006 Central College Campus, Bangalore University, Bangalore 27-29-September-2006

- **S.Ajitha& S.Sugunan**, Sol-gel Zirconia 'A novel Material to immobilize Biocatalyst α- amylase', **National** Seminar on Frontiers in Chemistry Cochin University of science and Technology on 24- 25 March 2005.

ACHIEVEMENTS

The best poster award was won for the paper entitled **S.Ajitha& S.Sugunan**, "Architecturing large pore SBA-15 for enzyme stabilization" at the National Conference on Smart Electroceramics (NCSE 2007) organized by C-MET during March 8-9, 2007

CURRICULUM VITAE

AJITHA.S.

Research Scholar   W/o Babu.S.V
Dept.of Applied Chemistry   Sasthamvalappil
Cochin University of Science and Technology   Amalanagar P. O
Cochin-22, Kerala, India.   Kerala, India.

Email: ajitha@cusat.ac.in   Email: ajithasnc@yahoo.co.in

EDUCATIONAL PROFILE

- **Doctor of Philosophy (Ph.D)** at Department of Applied Chemistry, Cochin University of Science and Technology, Cochin-22, Kerala, India from 2003 to at present. Topic of the work is "Ordered mesoporous silica as supports for immobilization of biocatalyst",under the Guidance of Dr. S. Sugunan, Department of applied Chemistry, Cochin University of science and Technology, Cochin-22, Kerala, India.

- **Master of Philosophy** (M. Phil) in Chemistry from Department of Applied Chemistry, Calicut University, Tenhipalam, Kerala, India in 2002.

- **Master of Science** (M. Sc) in Applied Chemistry from Department of Chemistry, Calicut University, Tenhipalam, Kerala, India in 1988

- **Bachelor of Science** (B. Sc) in Chemistry from Vimala College, Thrissur, Kerala, India in 1986

TEACHING EXPERIENCE

- 18 years teaching experience in various S.N. Colleges affliated to Calicut University.

PROJECTS

M. Phil Project

"Antimicrobial and Mass spectral studies of 1,2,4- Triazine derivatives", in the, Department of AppliedChemistry, Calicut University, Kerala., under the guidance of Dr. E.Purushothaman